SI Appendix for:

Reversible photoswitching of encapsulated azobenzenes in water

Dipak Samanta[a], Julius Gemen[a], Zonglin Chu[a], Yael Diskin-Posner[b], Linda J. W. Shimon[b], and Rafal Klajn[a]

[a] Department of Organic Chemistry, Weizmann Institute of Science, Rehovot 76100, Israel
[b] Department of Chemical Research Support, Weizmann Institute of Science, Rehovot 76100, Israel

Table of contents

1. General information

All commercial chemicals were used as received. Solvents were dried according to standard procedures (dichloromethane was dried over 4 Å molecular sieves). Cage **1** and guests **3**-**5** were prepared following the literature procedures. NMR spectra were recorded on a Bruker Avance III 400 MHz or on Bruker Avance III HD 500 MHz spectrometer. Chemical shifts (δ) are given in ppm relative to residual protio solvent resonances (2.51 ppm for $(CD_3)_2SO$ and 4.79 ppm for D_2O). 2D ^{1}H-DOSY NMR measurements were performed on a Bruker Avance III 400 MHz spectrometer with temperature and gradient calibration prior to the measurements. The diffusion coefficient of the solvent was used as a calibration standard. A constant temperature of 298 K was maintained during the measurements unless indicated otherwise. UV/Vis absorption spectra were recorded with a Shimadzu UV-2700 or a UV-3600 spectrophotometer. For photoirradiation experiments, we used a Prizmatix Mic-LED 365 nm light-emitting diode (LED) or a 4 W hand-held UV lamp (UVP, LLC; model number UVGL-25) as a UV light source, a 100-W UV lamp (UVP, LLC; model number B-100AP; light intensity ~10 $mW \cdot cm^{-2}$) as a high-intensity UV light source, a Prizmatix Mic-LED 420 nm LED as a blue light sources (Mic-LEDs had a collimated LED power of 400 mW), a Prizmatix 520 nm Ultra High Power (UHP) Mic-LED LED (collimated LED power of 900 mW) as a green light source, and a Prizmatix UHP White LED equipped with a bandpass filter of 580±25 nm as a yellow light source. For studying the photoisomerization reactions in-situ using NMR spectroscopy, the LEDs were equipped with a high numerical aperture polymer optical fiber (POF) (diameter 1 mm, length 5 m), which was inserted into the NMR spectrometer. The measurement was performed under a nitrogen flow (100 $mL \cdot min^{-1}$) at a heating rate of 10 $°C \cdot min^{-1}$. Elemental analysis was carried out on a FlashEA 1112 CHN analyzer (Thermo Fischer Scientific). Infrared (IR) spectra were recorded on a Thermo Scientific Nicolet 380 FT-IR spectrometer. The spectra were recorded in KBr pellets.

2. Synthesis of cage **1**

Cage **1** was synthesized according to a modified literature procedure (1). A solution of *cis*-[(tmen)Pd$(NO_3)_2$] (200 mg, 0.577 mmol) in water (25 mL) was added slowly to 1,3,5-tris(1-imidazolyl)benzene (106 mg, 0.384 mmol) and the resulting reaction mixture was stirred for 24 h at room temperature. Then, the mixture was centrifuged to remove any insoluble materials. The supernatant was collected and it was concentrated under reduced pressure. Cage **1** in the crystalline form was obtained by slow vapor diffusion of acetone. Isolated yield: 95%.

^{1}H NMR (500 MHz, D_2O): δ = 9.10 (s, 8H, $\mathbf{4_4}$), 8.82 (s, 4H, $\mathbf{4_1}$), 7.74 (s, 4H, $\mathbf{4_8}$), 7.71 (s, 4H, $\mathbf{4_3}$), 7.69 (s, 8H, $\mathbf{4_7}$), 7.64 (s, 8H, $\mathbf{4_6}$), 7.54 (s, 12H, $\mathbf{4_{2+5}}$), 3.11 (s, 24H, $\mathbf{4}_{CH2}$), 2.77–2.70 (m, 72H, $\mathbf{4}_{CH3}$). **^{13}C NMR** (100 MHz, D_2O): δ = 138.04 ($\mathbf{4_9}$), 137.75 ($\mathbf{4_{10}}$), 137.49 ($\mathbf{4_4}$), 137.25 ($\mathbf{4_1}$), 128.73 ($\mathbf{4_{2+5}}$), 120.74 ($\mathbf{4_6}$), 120.52 ($\mathbf{4_3}$), 114.79 ($\mathbf{4_8}$), 113.09 ($\mathbf{4_7}$), 62.52 ($\mathbf{4}_{CH2}$), 50.29 ($\mathbf{4}_{CH3}$), 50.24 ($\mathbf{4}_{CH3}$), 50.02 ($\mathbf{4}_{CH3}$).

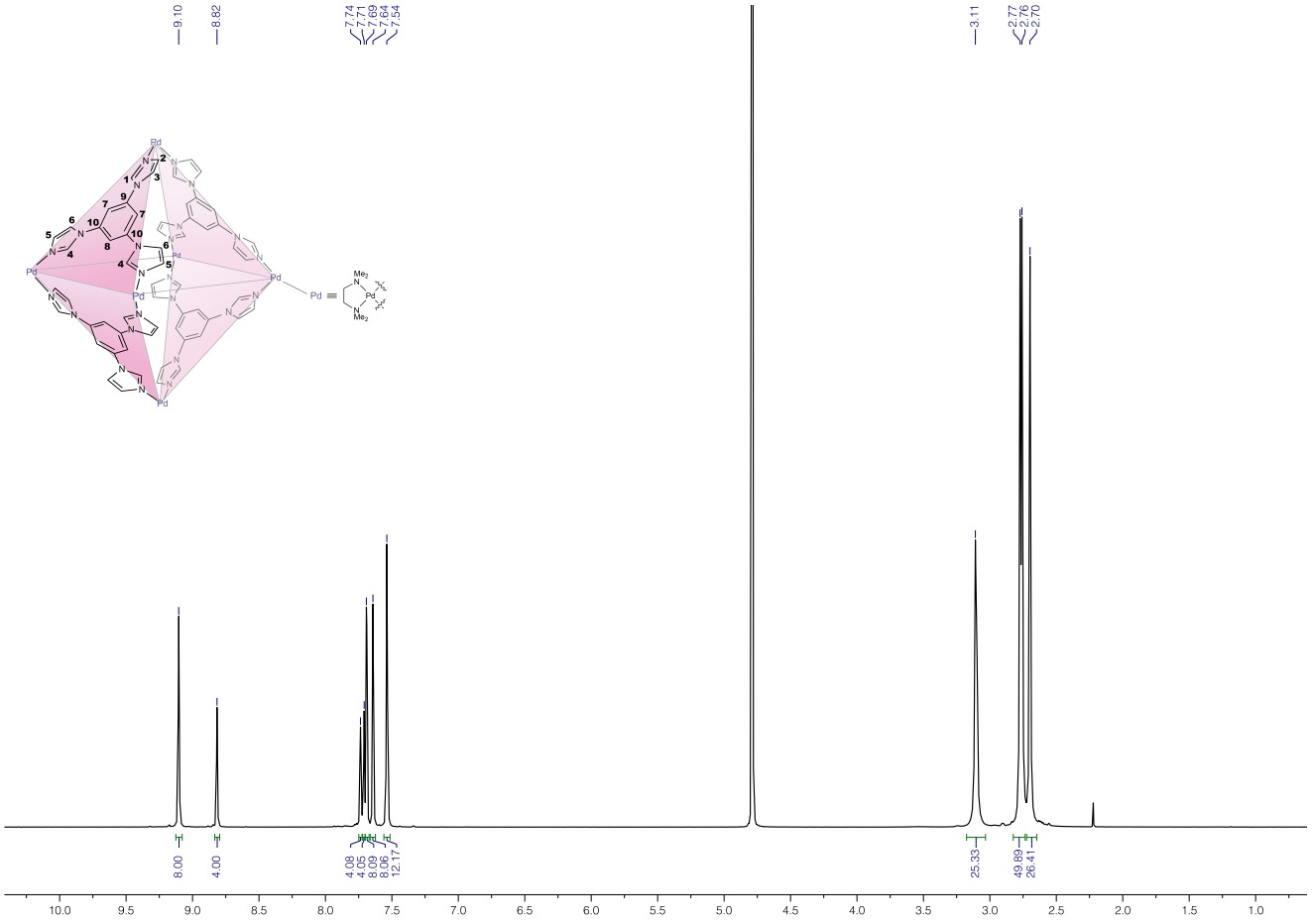

Fig. S1. ^{1}H NMR spectrum of **1** (500 MHz, D_2O, 298 K).

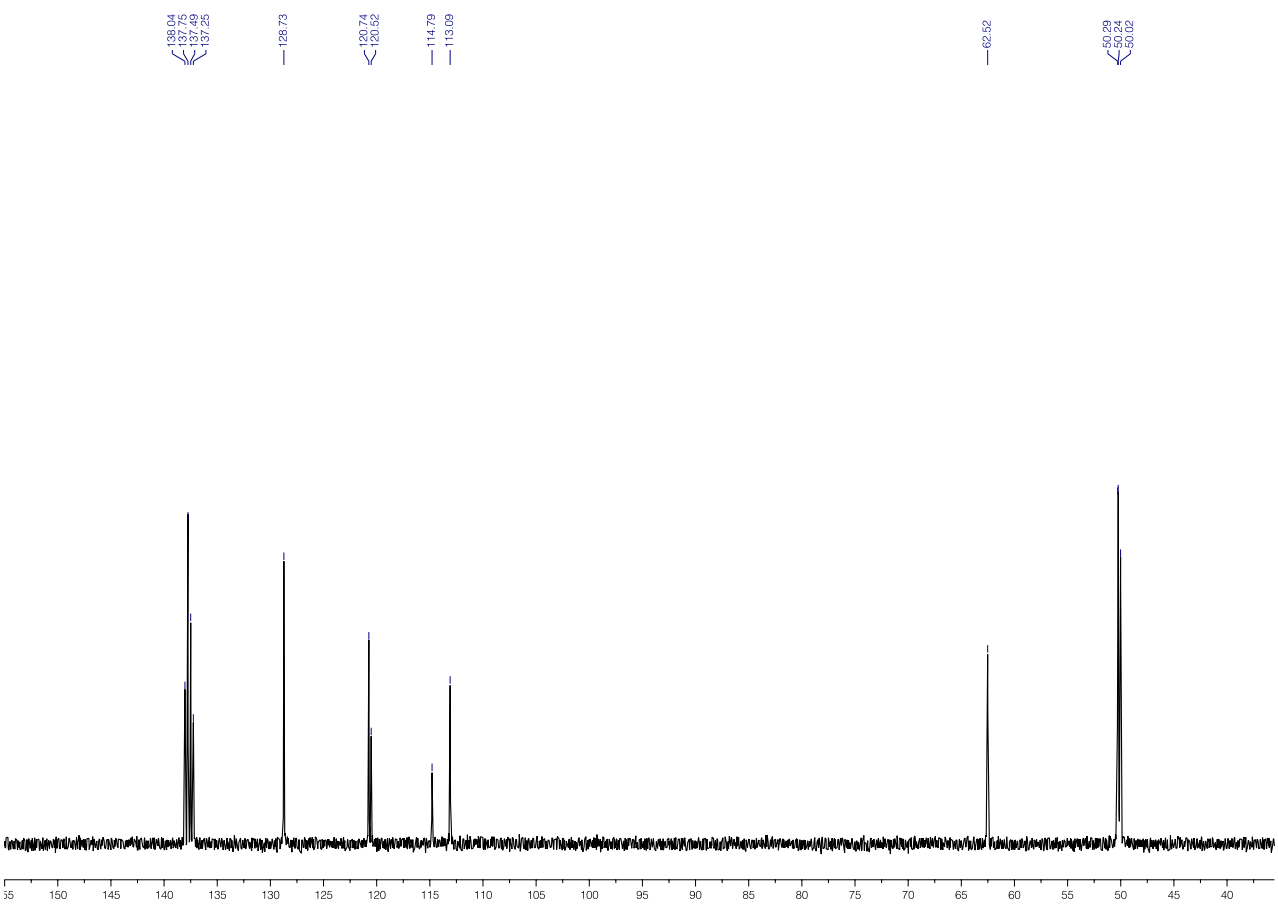

Fig. S2. ^{13}C NMR spectrum of **1** (125 MHz, D_2O, 298 K).

3. Synthesis of guest molecules

- Guest **2** (azobenzene) was used as received (Aldrich).
- Guest **3** (*p*-allyloxyazobenzene) was synthesized based on a reported literature procedure (2).
- Guest **4** (tetra-*o*-methoxyazobenzene) was synthesized based on a reported literature procedure (3). This procedure afforded a mixture of ~90% *cis*-**4** and ~10% *trans*-**4**. Pure *trans*-**4** was obtained by irradiating a solution of **4** in DCM with 420 nm light for 2 h followed by removing the solvent *in vacuo* and washing the residue with diethyl ether (once) and *n*-hexane (once).
- Guest **5** (tetra-*o*-fluoroazobenzene) was synthesized based on a reported literature procedure (4).

4. Encapsulation of guests inside cage **1**

General procedure for encapsulation: solid **2** (3.7 mg; 0.02 mmol), **3** (4.8 mg; 0.02 mmol), *cis*-**4** (6.1 mg; 0.02 mmol), *trans*-**4** (6.1 mg; 0.02 mmol), or **5** (5.1 mg; 0.02 mmol) was added to an aqueous (H_2O or D_2O) solution of cage **1** (15 mg = 0.005 mmol) in 1 mL of water. The mixture was stirred for 24 h at room temperature. Encapsulation entailed solubilization of the guest in water. The resulting milky suspension was filtered through glass wool and centrifuged several times at 5,000 rpm to yield a clear solution. The encapsulation yield was determined by ^{1}H NMR spectroscopy by comparing the intensity of the signals due to the encapsulated guests' aromatic protons to the intensity of **1**'s imidazole protons. We verified that stirring times longer than 24 h did not increase the encapsulation yield. In addition, we found that the encapsulation yield did not increase by ultrasonication or heating to 60 °C.

The high molar absorption coefficients of azobenzene dyes allowed us to follow the encapsulation kinetics by UV/Vis absorption spectroscopy. In a typical experiment, an aqueous solution of **1** (c = 1.73 mg/mL) was stirred with solid azobenzene **2**, **3**, *cis*-**4**, *trans*-**4**, or **5** for a given amount of time, after which an aliquot was removed from the mixture and centrifuged for 5 min to remove the excess of azobenzene. Then, 20 µL of the supernatant was diluted with 600 µL of distilled water and a UV/Vis absorption spectrum was recorded. Representative spectra (for azobenzene **2**) are shown Fig. S3. From these spectra, we can conclude that the encapsulation is practically complete within 4.5 h.

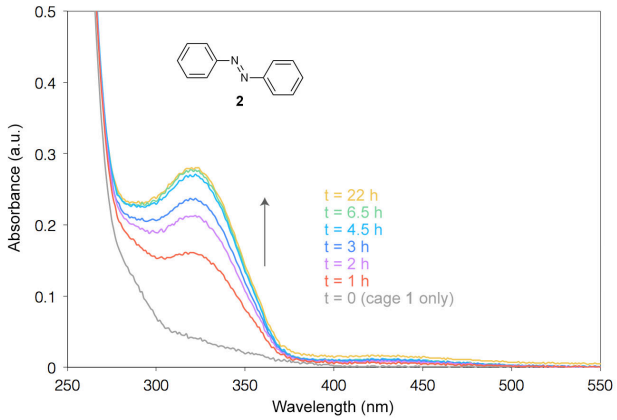

Fig. S3. Following the uptake of azobenzene **2** by cage **1** using UV/Vis absorption spectroscopy.

Similarly, we collected sets of absorption spectra for azobenzenes **3**-**5** and plotted the absorption maxima as a function of time (Fig. S4). Interestingly, these results show that both isomers of **4** (which form 1:1 complexes with 1) are solubilized significantly slower than azobenzenes **2**, **3**, and **5** (all of which form 2:1 complexes), which suggests a cooperative mechanism of encapsulation of **2**, **3**, and **5**.

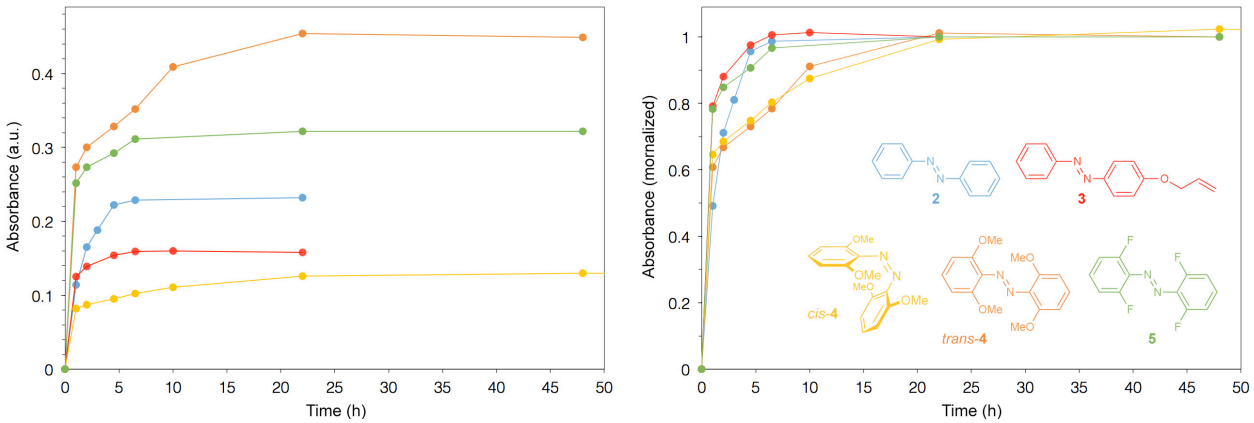

Fig. S4. Uptake profiles of azobenzenes **2**-**5** by cage **1** before (left) and after (right) normalization. Absorption maxima: 317 nm (**2**), 352 nm (**3**), 435 nm (*cis*-**4**), 327 nm (*trans*-**4**), and 313 nm (**5**).

5. Photoisomerization of **1**-encapsulated azobenzenes **2**-**5**

- To isomerize **2** within (*trans*-**2**)$_2$⊂**1**, we used a 365 nm LED. 10 min of irradiation was needed to reach a photostationary state. For back-isomerization, we used a 420 nm LED; photostationary state was reached after 8 min.
- To isomerize **3** within (*trans*-**3**)$_2$⊂**1**, we used a 365 nm LED. 4 min of irradiation was needed to reach a photostationary state. For back-isomerization, we used a 420 nm LED. A photostationary state was reached after 4 min.
- To isomerize **4** within *cis*-**4**⊂**1**, we used a 420 nm LED. 5 min of irradiation was needed to reach a photostationary state.
- To isomerize **4** within *trans*-**4**⊂**1**, we used a 580 nm LED. 90 min of irradiation was needed to reach a photostationary state.
- To isomerize **5** within (*trans*-**5**)$_2$⊂**1**, we used a 520 nm LED. 4 min of irradiation was needed to reach a photostationary state. For back-isomerization, we used a 420 nm LED. A photostationary state was reached after 4 min.

In all cases, the concentration of the complex was ~0.05 mM.

6. Characterization of inclusion complex (*trans*-**2**)$_2$⊂**1**

Inclusion complex (*trans*-**2**)$_2$⊂**1** was obtained in ~60% yield (i.e., treating **1** with excess of *trans*-**2** resulted in filling of ~60% of the cages).

^{1}H NMR (500 MHz, D_2O, 298 K): δ = 9.15 (br, 4H, **1**$_1$), 9.06 (br, 8H, **1**$_4$), 7.70 (m, 8H, **1**$_{2+3}$), 7.51 (m, 24H, **1**$_{5+7+8}$), 7.28 (br, 6H, **1**$_6$), 7.03 (t, ^3J = 7.3 Hz, 4H, *trans*-**2**$_a$), 6.71 (t, ^3J = 7.6 Hz, 8H, *trans*-**2**$_b$), 6.19 (d, ^3J = 7.6 Hz, 8H, *trans*-**2**$_c$), 3.14–3.07 (m, 24H, **1**$_{CH2}$), 2.79–2.61 (m, 72H, **1**$_{CH3}$). **^{13}C NMR** (100 MHz, D_2O, 298 K): δ = 150.34 (*trans*-**2**$_d$), 137.96 (**1**$_9$), 137.63 (**1**$_{10}$), 137.44 (**1**$_4$), 137.01 (**1**$_1$), 131.71 (*trans*-**2**$_a$), 129.29 (**1**$_2$), 129.06 (*trans*-**2**$_b$), 128.86 (**1**$_5$), 121.08 (*trans*-**2**$_c$), 120.75 (**1**$_3$), 120.42 (**1**$_6$), 113.65 (**1**$_8$), 112.40 (**1**$_7$), 62.64 (**1**$_{CH2}$), 62.54 (**1**$_{CH2}$), 62.12 (**1**$_{CH2}$), 50.30 (**1**$_{CH3}$), 50.28 (**1**$_{CH3}$), 50.02 (**1**$_{CH3}$), 49.80 (**1**$_{CH3}$). **^{1}H-DOSY NMR** (D_2O, 298 K): D = 0.19 (± 0.01) × 10^{-5} cm^2/s. **Elemental analysis**: calcd: C, 38.96; H, 4.62; N, 20.74; found: 38.86; H, 4.52; N, 20.74.

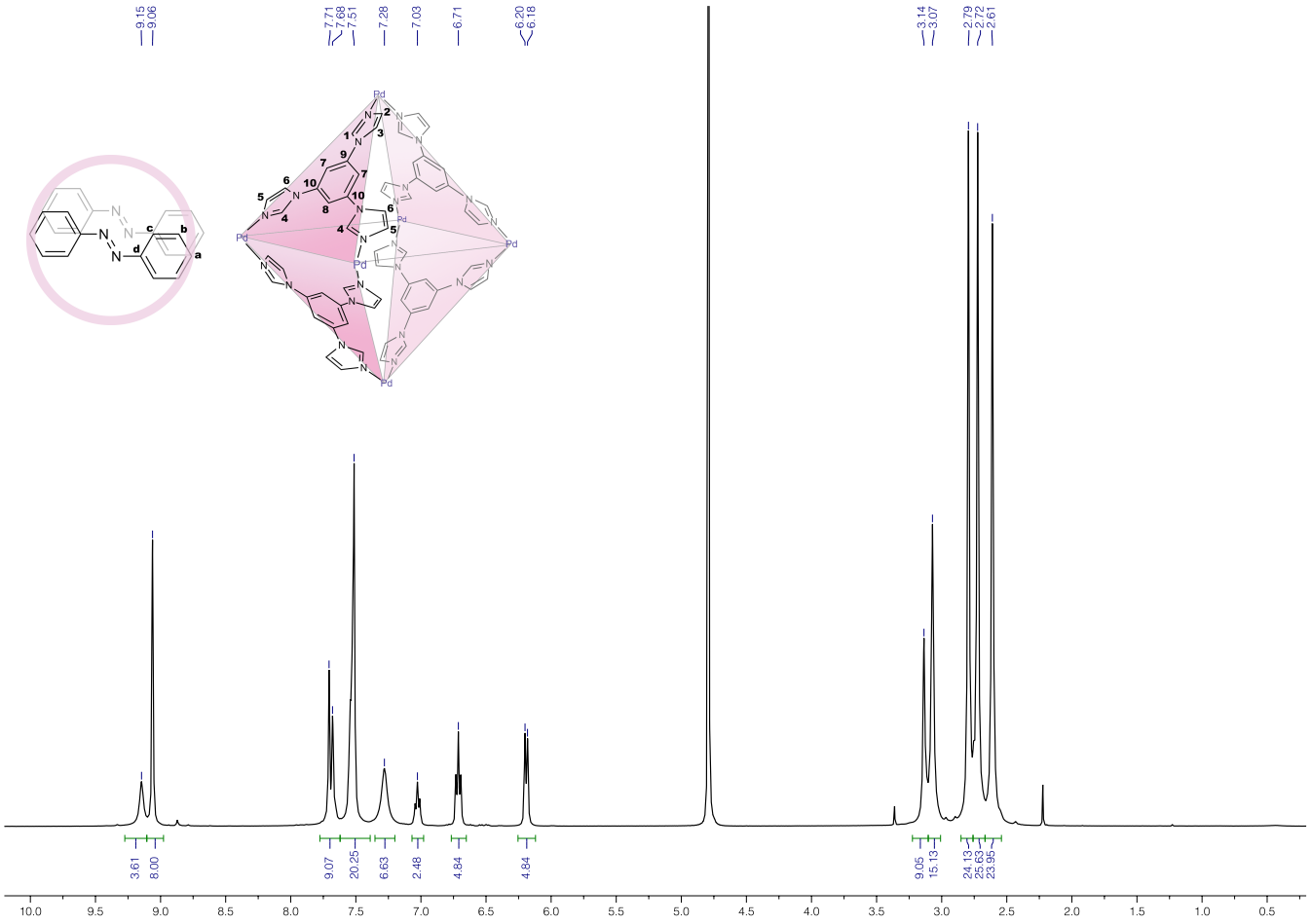

Fig. S5. ^{1}H NMR spectrum of (*trans*-**2**)$_2$⊂**1** (500 MHz, D_2O, 298 K). For signal assignment, see p. 7, above.

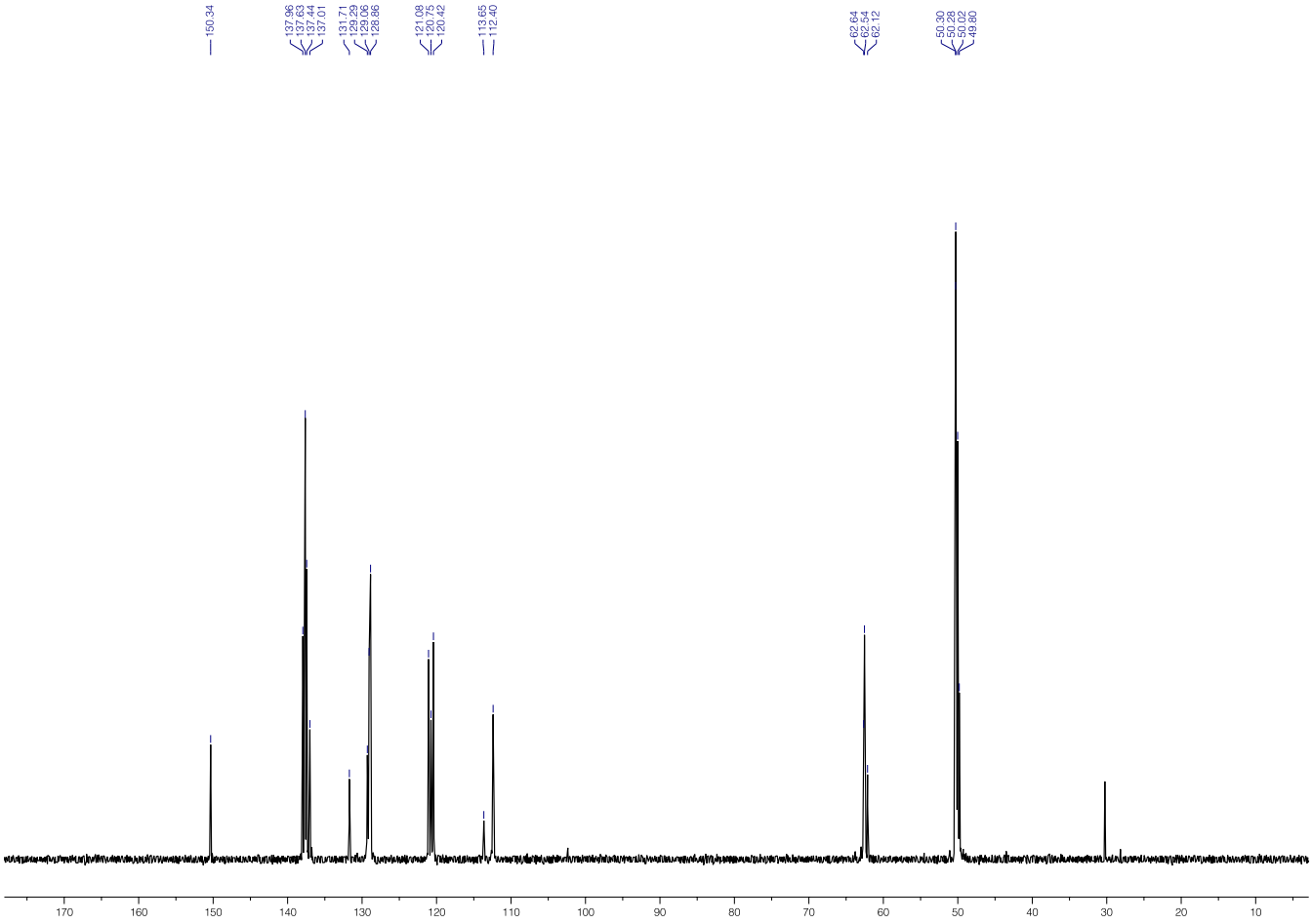

Fig. S6. ^{13}C NMR spectrum of (*trans*-**2**)$_2$⊂**1** (100 MHz, D_2O, 298 K).

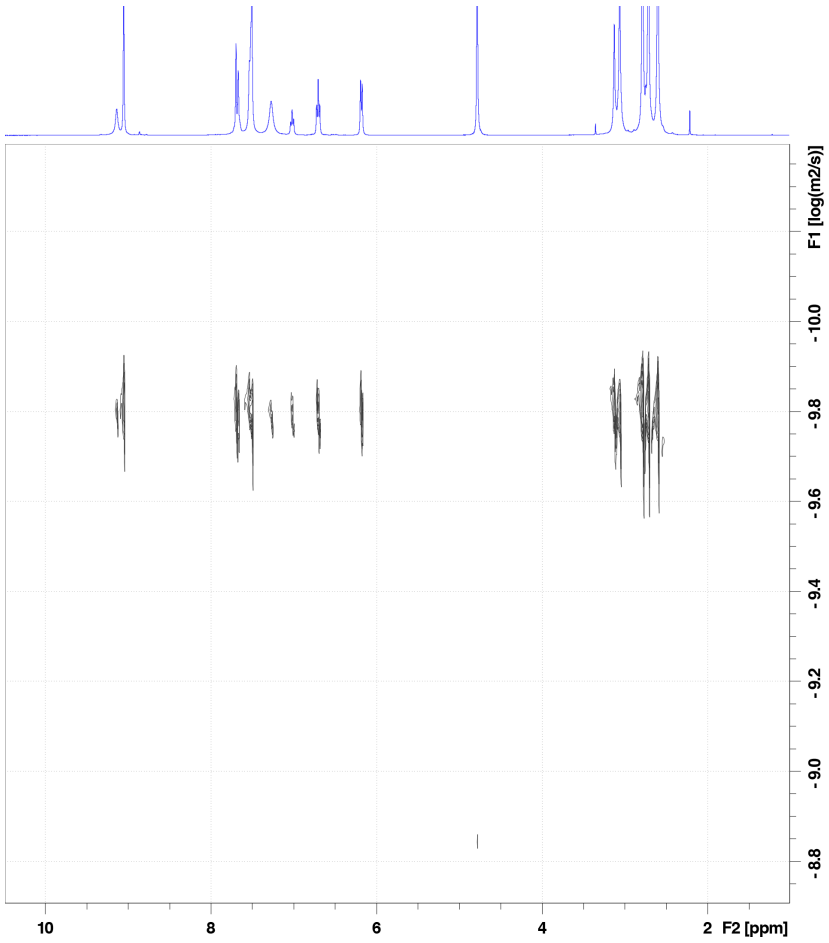

Fig. S7. ^{1}H DOSY NMR spectrum of (*trans*-**2**)$_2$⊂**1** (400 MHz, D_2O, 298 K). The spectrum reveals that all the resonances belong to a single chemical species.

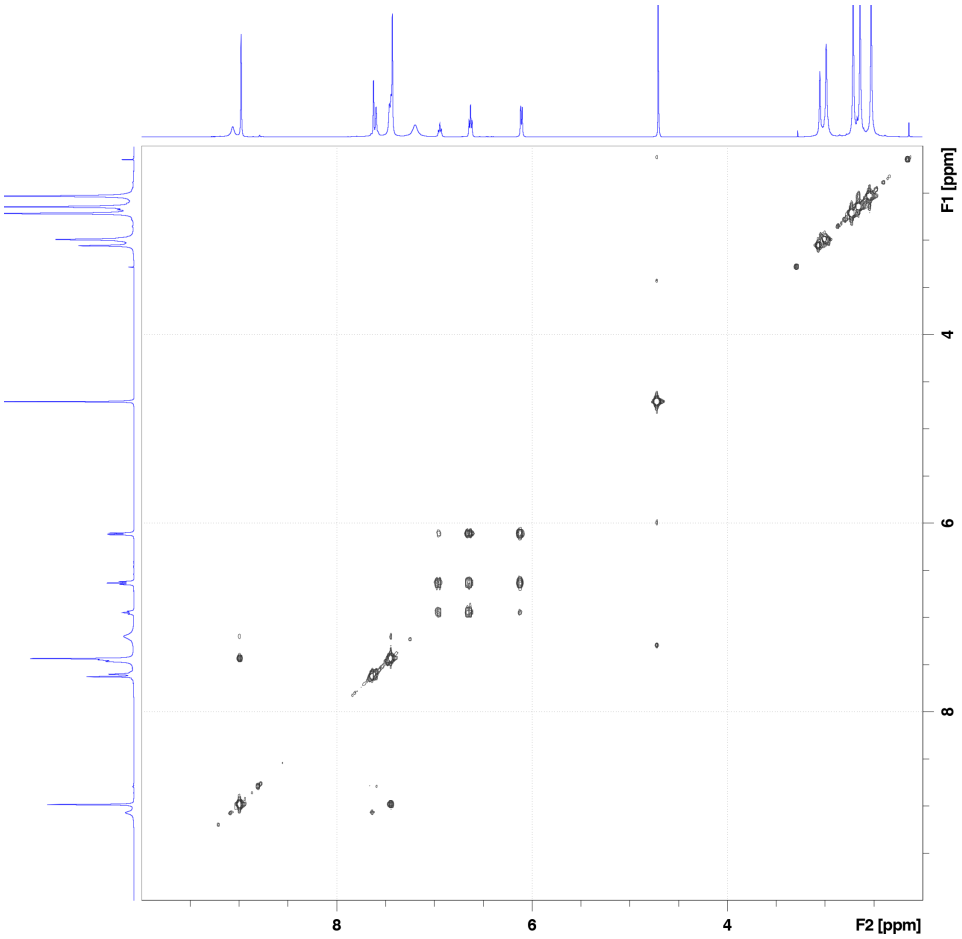

Fig. S8. ^{1}H-^{1}H COSY NMR spectrum of (*trans*-**2**)$_2$⊂**1** (500 MHz, D_2O, 298 K).

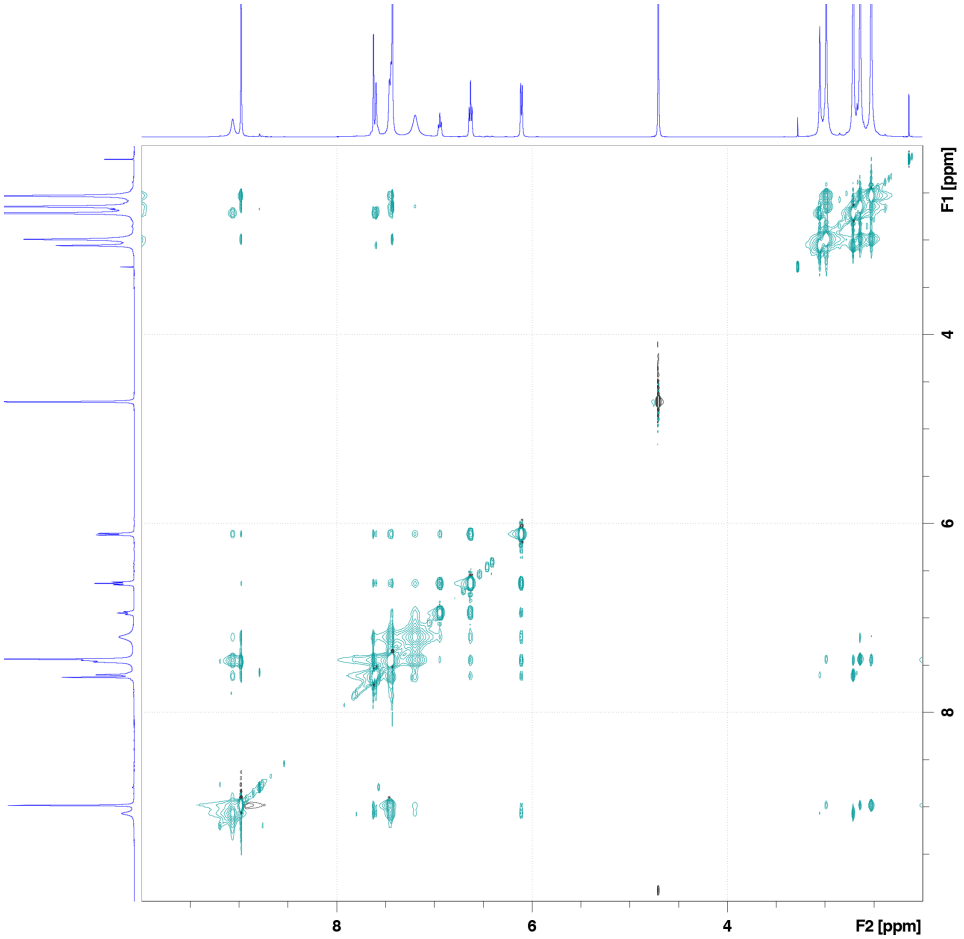

Fig. S9. ^{1}H-^{1}H NOESY NMR spectrum of (*trans*-**2**)$_2$⊂**1** (500 MHz, D_2O, 298 K).

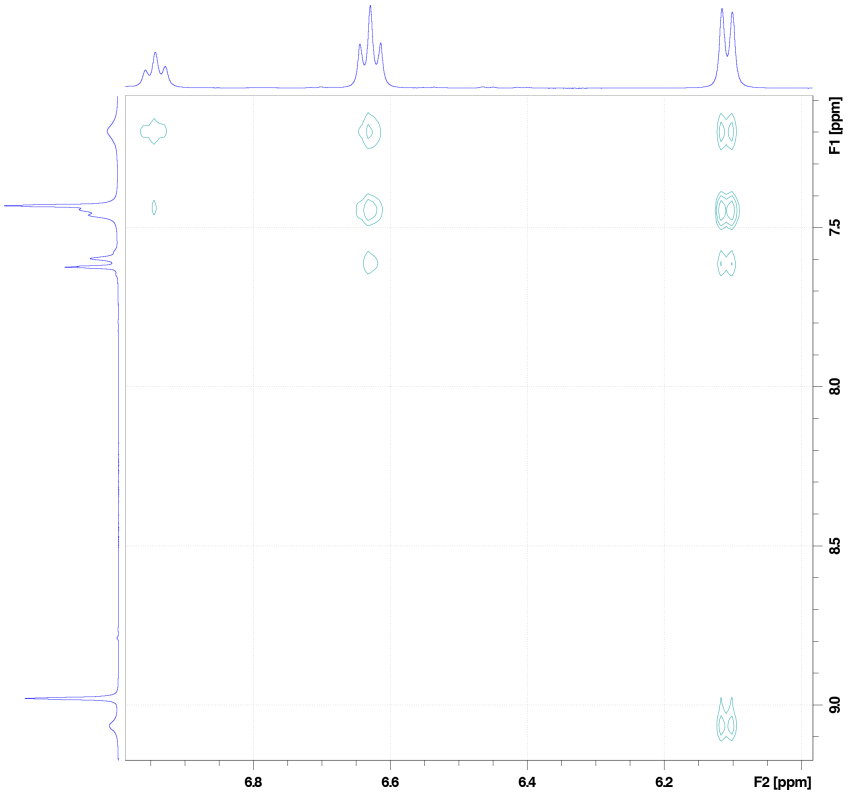

Fig. S10. Partial ^{1}H-^{1}H NOESY NMR spectrum of (*trans*-**2**)$_2$⊂**1** showing nuclear Overhauser (nOe) correlations between the host and the guests (500 MHz, D_2O, 298 K) (the corresponding full-range spectrum is shown in Fig. S9).

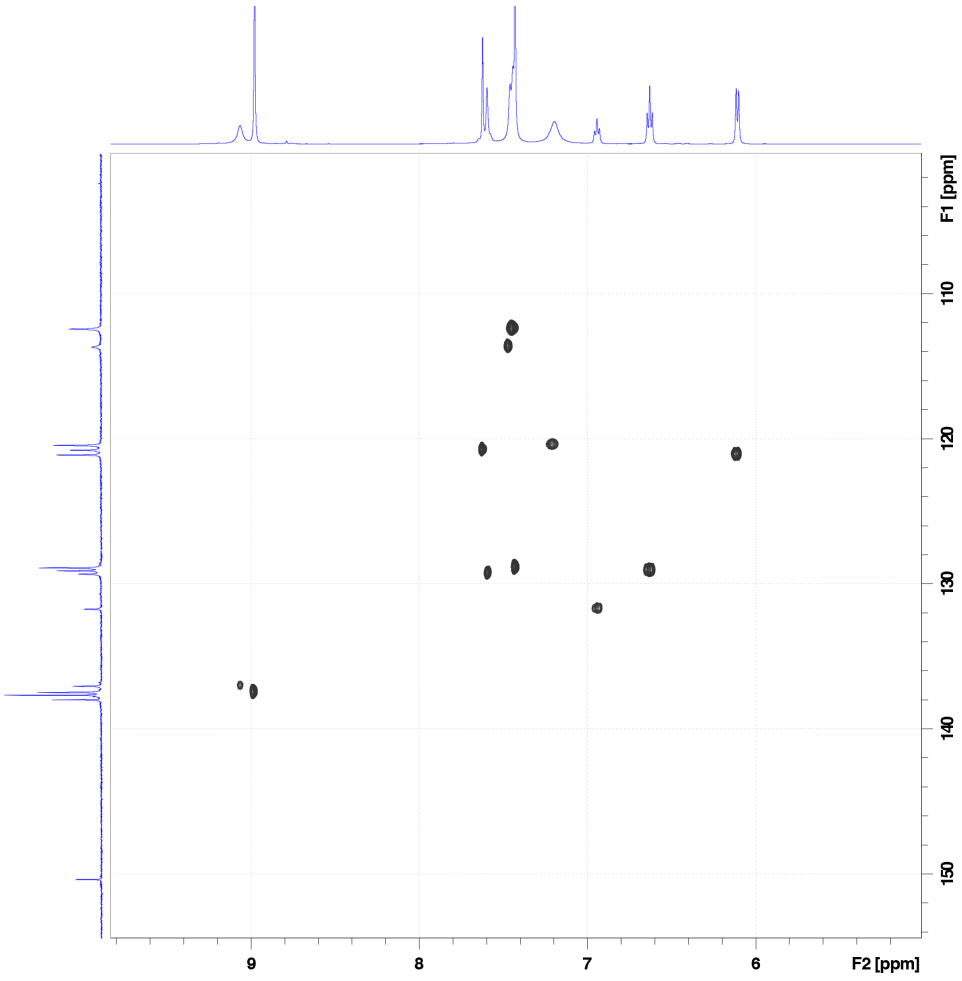

Fig. S11. ^{1}H-^{13}C HSQC NMR spectrum of (*trans*-**2**)$_2$⊂**1** (400 MHz, D_2O, 298 K).

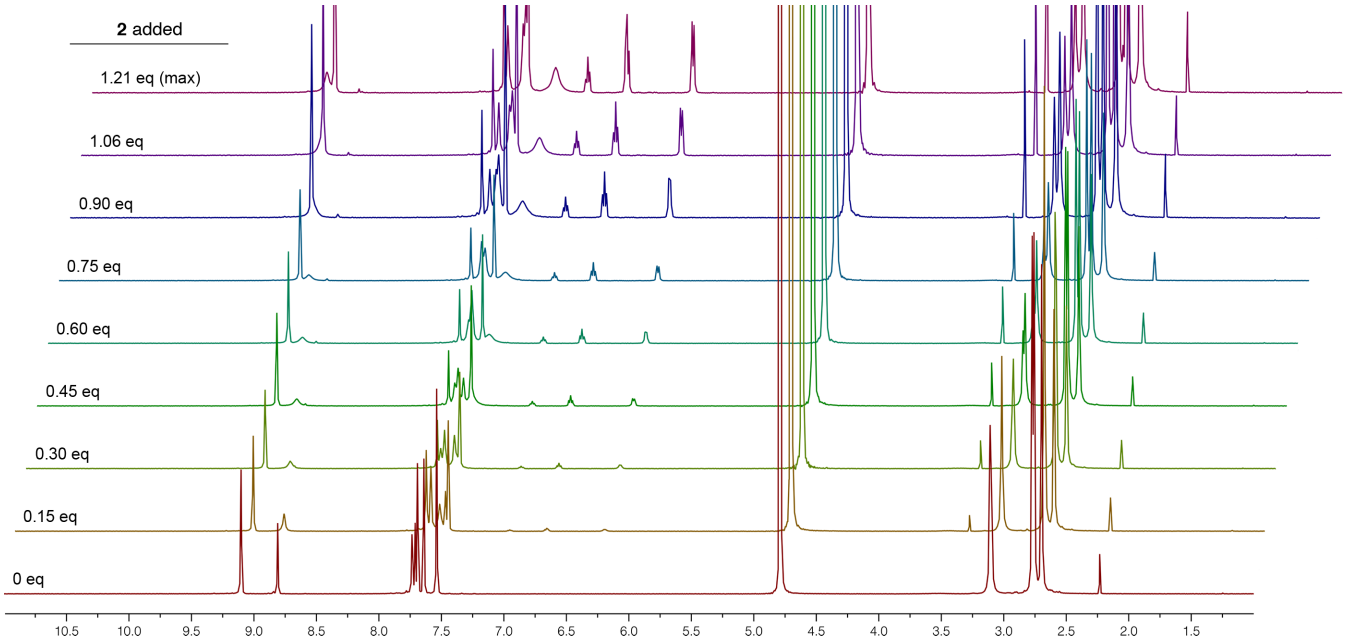

Fig. S12. Changes in the ^{1}H NMR spectra of **1** during the gradual addition of **2** (500 MHz, D_2O, 298 K).

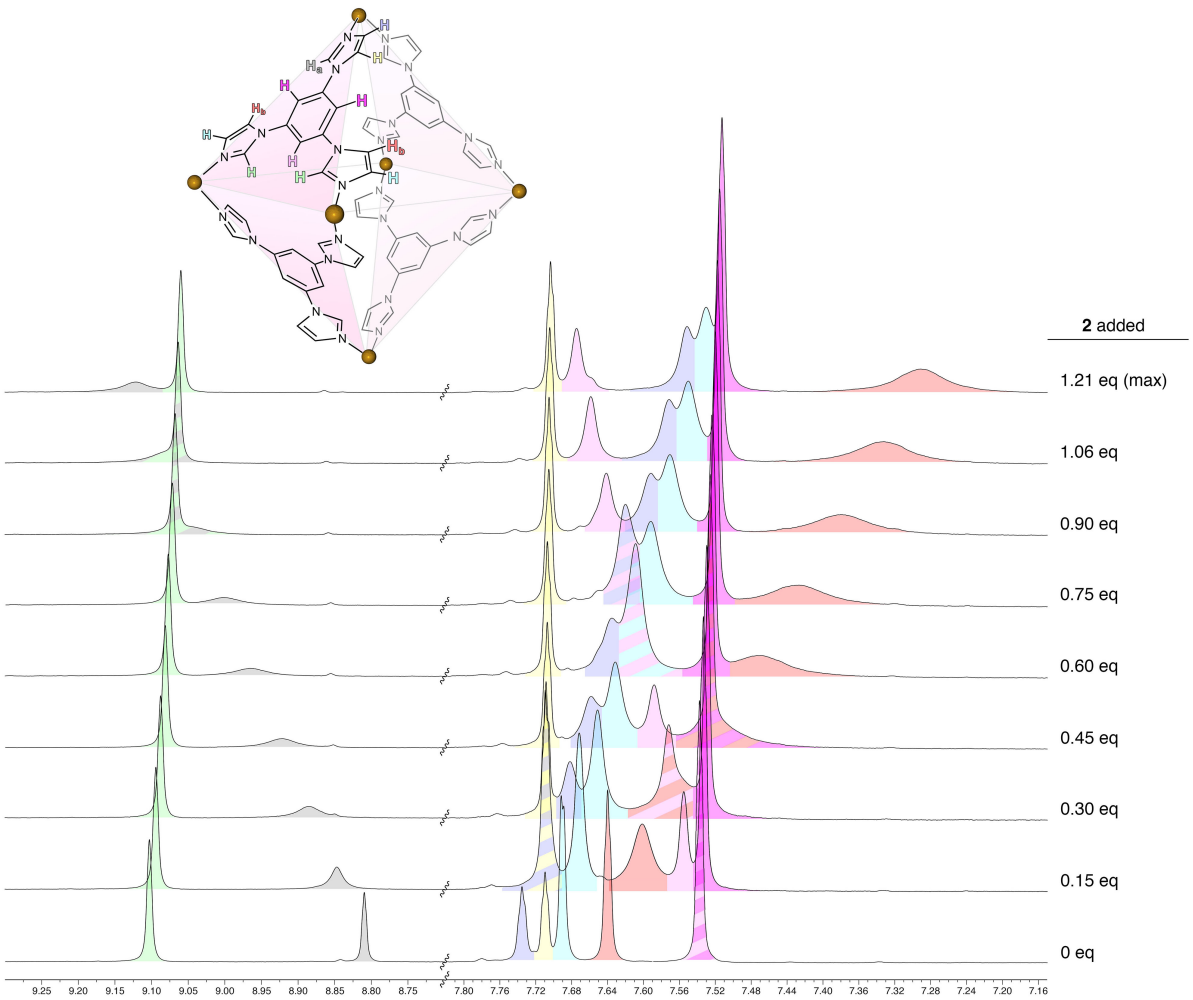

Fig. S13. Changes in the partial ^{1}H NMR spectra of **1** (focusing on **1**'s aromatic protons) during the gradual addition of **2** (500 MHz, D_2O, 298 K) (the corresponding full-range spectra are shown in Fig. S12).

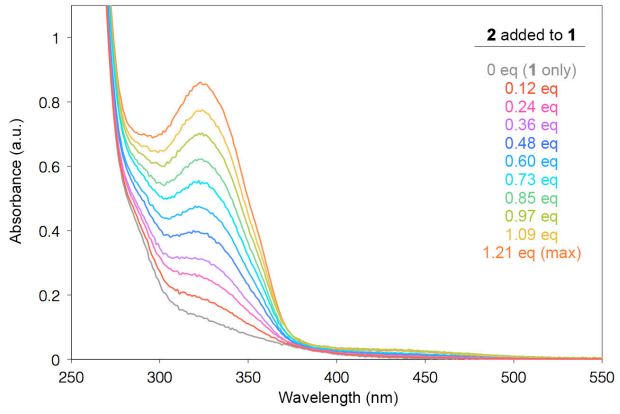

Fig. S14. Changes in the UV/Vis spectra of **1** in the presence of increasing amounts of **2**.

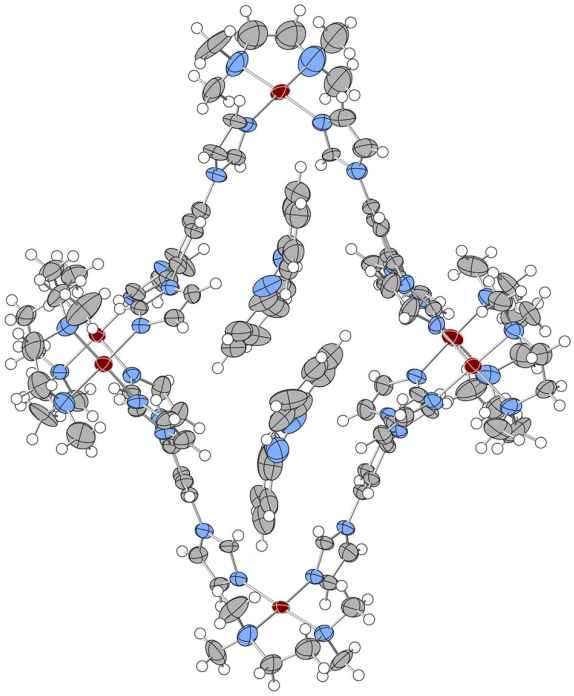

Fig. S15. ORTEP representation of the X-ray structure of inclusion complex (*trans*-**2**)$_2$⊂**1** (thermal ellipsoids at a 50% probability level). Anions and solvent molecules were eliminated for clarity. Pd, brown; C gray; N, blue; H, white.

Analysis of intermolecular interactions within inclusion complex (*trans*-**2**)$_2$⊂**1**

Analysis was performed with PLATON on the cif file deposited in CCDC (accession number 1551435).

Host-guest interactions

Cage **1** contains four benzene rings: Ring19 (C10-C15); Ring20 (C34-C39); Ring21 (C52-C57); Ring22 (C70-C75). Encapsulated azobenzenes **2** contain four benzene rings: Ring23 (C100-C105); Ring24 (C106-C111); Ring25 (C200-C205); Ring26 (C206-C211).

The table below lists distances between the center of gravity of a given ring to the plane of the neighboring ring (in blue); distances between the center of gravity of the neighboring ring to the plane of the given ring (in red); and dihedral angles between the planes of the two rings (in green).

	Ring23	Ring24	Ring25	Ring26
Ring19	3.23 Å / 3.69 Å 20.1°	3.60 Å / 3.13 Å 18.4°		
Ring20			3.76 Å / 2.87 Å 27.6°	
Ring21			3.51 Å / 2.93 Å 17.0°	3.25 Å / 3.62 Å 20.8°
Ring22		3.65 Å / 3.12 Å 27.6°		

In addition, the following edge-to-face interactions are present:

C111 to the imidazole ring (N31N32C79C80C81), distance = 3.65 Å
C202 to the imidazole ring (N15N16C40C41C42), distance = 3.43 Å

Guest-guest interactions

The distance between the center of gravity of azobenzene's Ring23 to the plane of the neighboring azobenzene's Ring26 is 3.34 Å. The distance between the center of gravity of azobenzene's Ring26 to the plane of the neighboring azobenzene's Ring23 is 3.42 Å. The dihedral angle between the planes of the benzene rings is 1.5°.

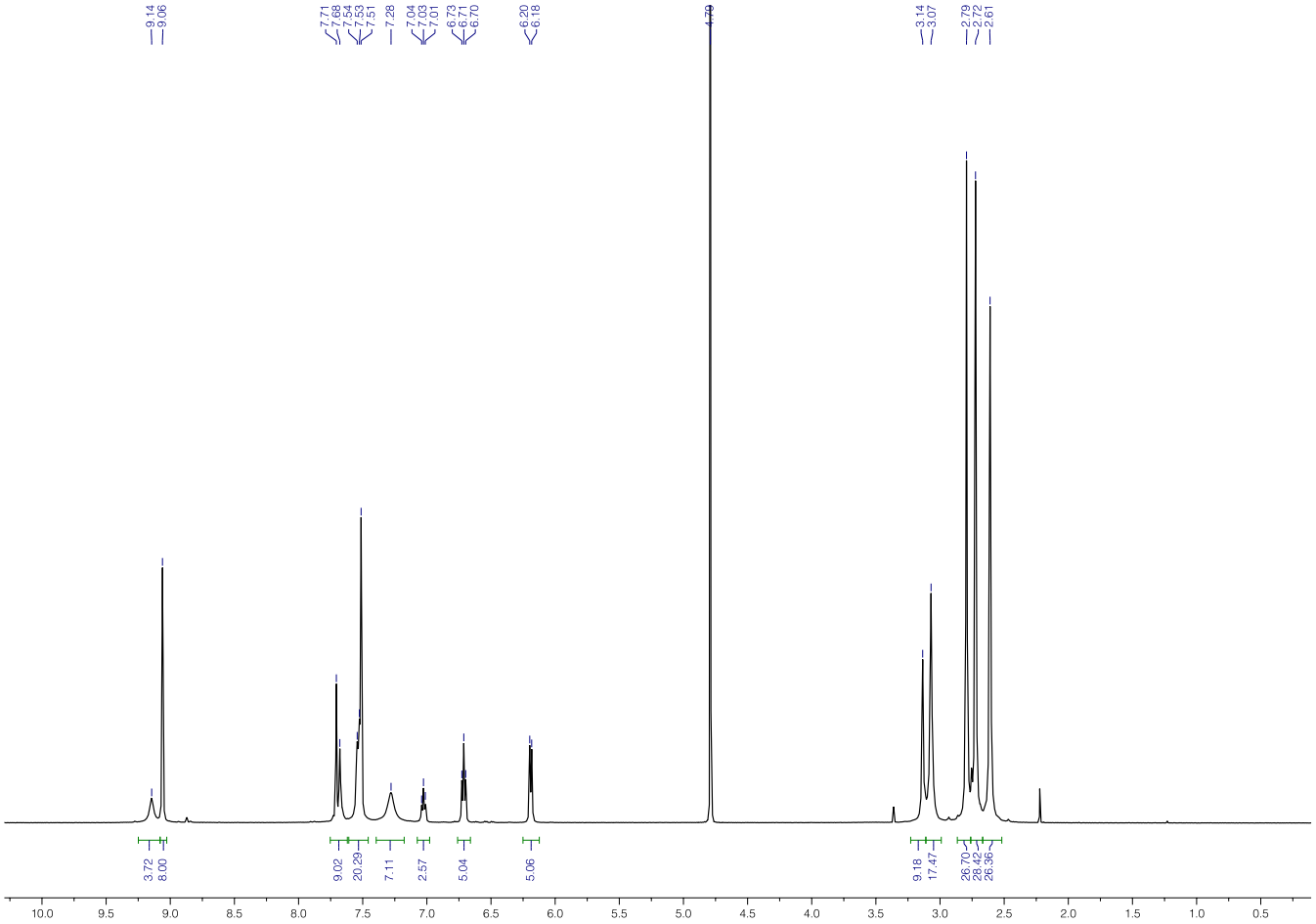

Fig. S16. ^{1}H NMR spectrum obtained by dissolving crystalline (*trans*-**2**)$_2$⊂**1** in water (500 MHz, D_2O, 298 K). Integration reveals that 63% of the cages are filled, compared to 61% in the sample obtained by saturating a solution of **1** with *trans*-**2** (Fig. S5). Initially, (*trans*-**2**)$_2$⊂**1** formed a clear solution in water. Within ~10 min, the solution became hazy, followed by precipitation of a yellow solid (*trans*-**2**). The solid was discarded and the resulting yellow solution was analyzed by NMR.

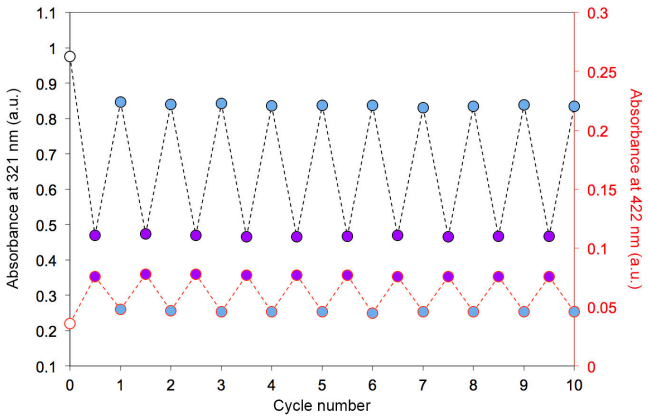

Fig. S17. Reversible photoisomerization of $\mathbf{2}_2\subset\mathbf{1}$. Purple markers correspond to the absorbance of solutions exposed to a 365 nm LED until no further changes in the spectra were seen (a photostationary state reached after 10 min). Blue markers correspond to the absorbance of solutions exposed to a 420 nm LED until no further changes in the spectra were seen (a photostationary state achieved after 8 min).

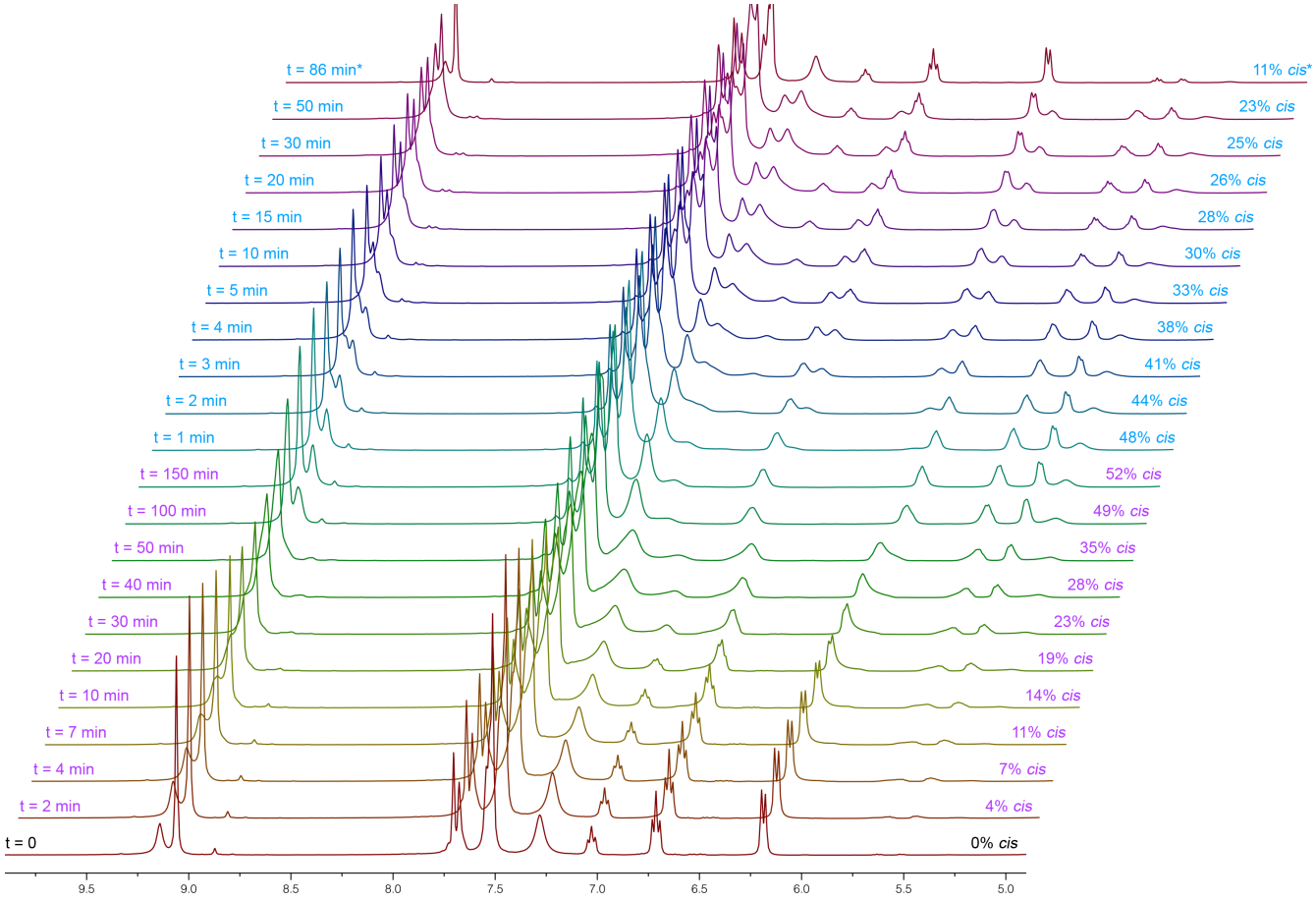

Fig. S18. A series of partial ^{1}H NMR spectra (400 MHz, D_2O, 298 K) of $\mathbf{2}_2\subset\mathbf{1}$ at a concentration of ~15 mg/mL following exposure to UV light (λ = 365 nm) inside the NMR spectrometer (using an optical fiber) for different periods of time (indicated in purple font) for up to 150 min and after a subsequent exposure to blue light (blue font) for up to 50 min. The top spectrum, marked with an asterisk (*), was recorded following 56 min of exposure to blue light inside the spectrometer, followed by 30 min of direct exposure to blue light outside of the spectrometer.

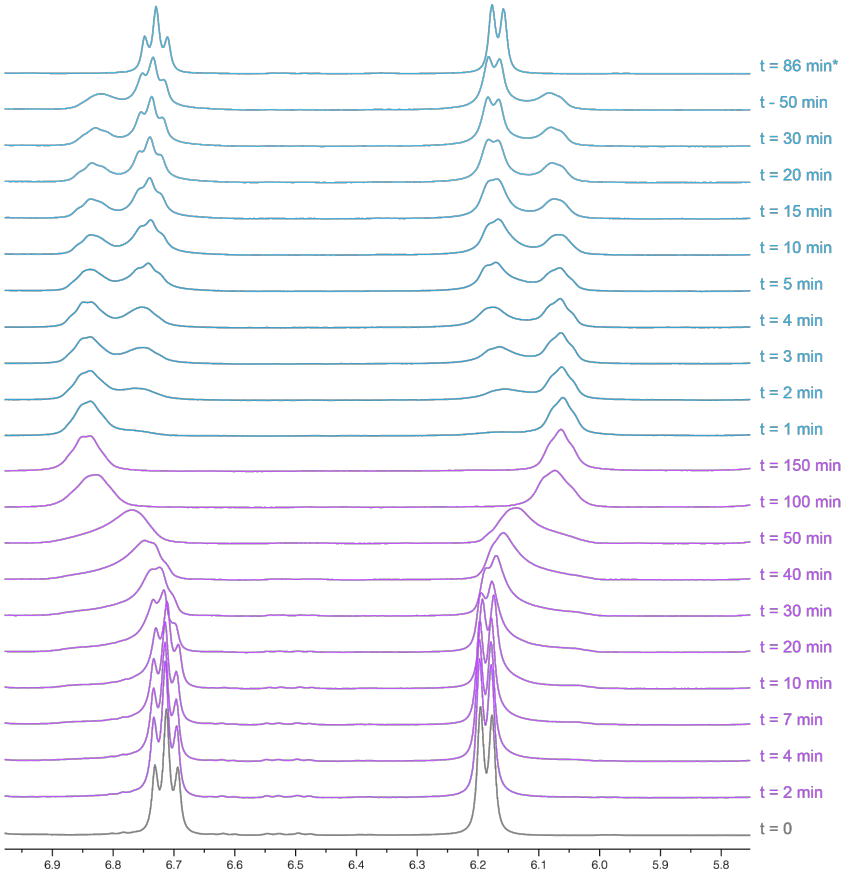

Fig. S19. A series of partial ^{1}H NMR spectra (replotted from Fig. S18) of $\mathbf{2}_2\subset\mathbf{1}$ following exposure to UV light (λ = 365 nm) inside the NMR spectrometer (using an optical fiber) for different periods (indicated in purple font) for up to 150 min and after a subsequent exposure to blue light (blue font) for up to 50 min. The top spectrum, marked with an asterisk (*), was recorded following 56 min of exposure to blue light inside the spectrometer, followed by 30 min of direct exposure to blue light outside of the spectrometer.

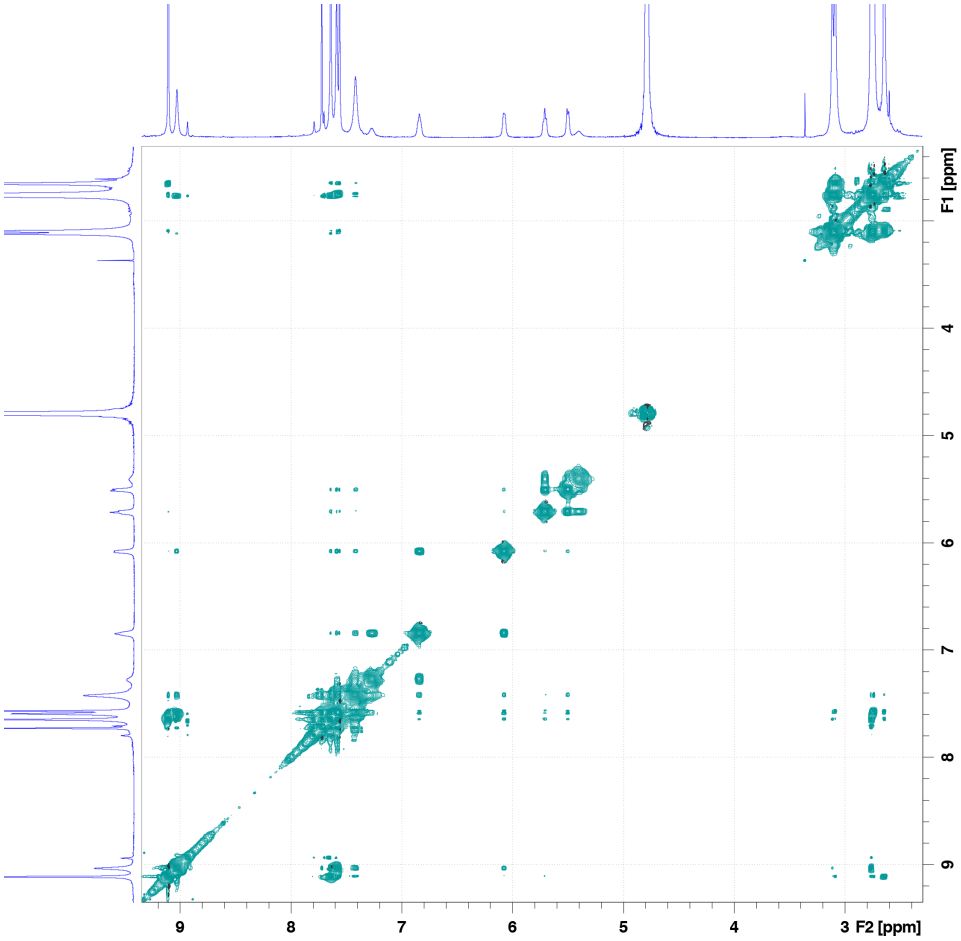

Fig. S20. ^{1}H-^{1}H NOESY NMR spectrum of $\mathbf{2}_2\subset\mathbf{1}$ subjected to partial isomerization and consisting of a ~1:1 mixture of *trans*-**2** and *cis*-**2** (500 MHz, D_2O, 298 K).

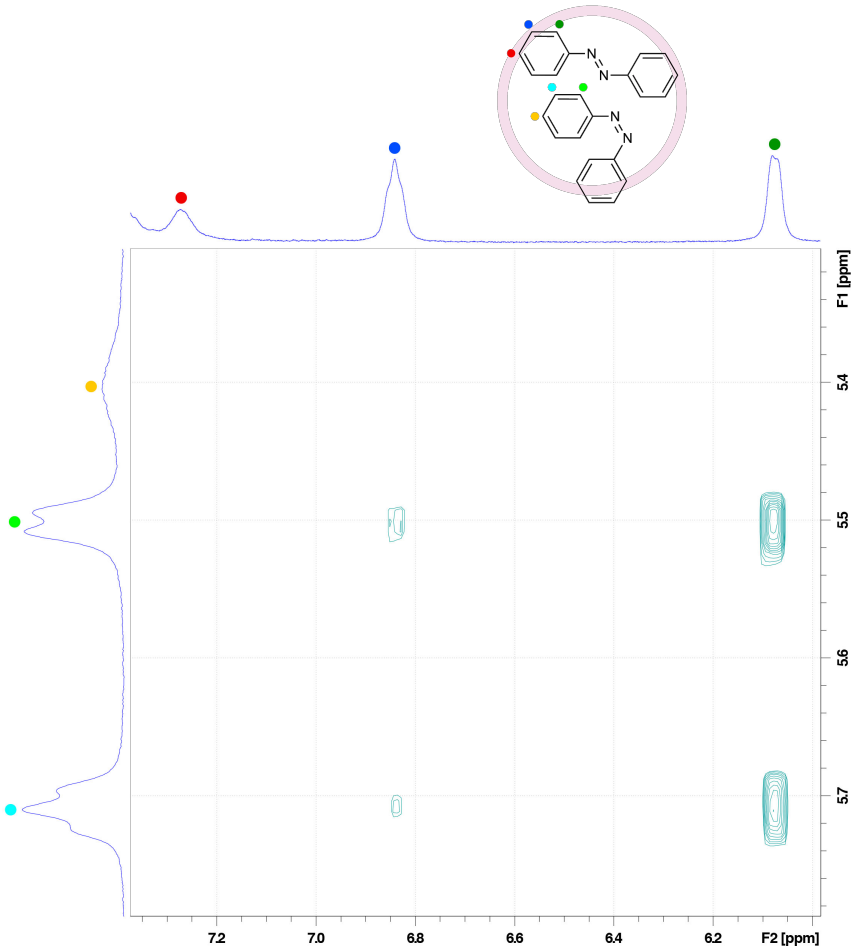

Fig. S21. Partial ^{1}H-^{1}H NOESY NMR spectrum of $\mathbf{2}_2\subset\mathbf{1}$ subjected to partial isomerization and consisting of a ~1:1 mixture of *trans*-**2** and *cis*-**2** (500 MHz, D_2O, 298 K) (the corresponding full-range spectrum is shown in Fig. S20). The three signals in the partial ^{1}H NMR spectrum shown on top can be attributed to the protons of *trans*-**2**. The three signals in the partial ^{1}H NMR spectrum shown on the left can be attributed to the protons of *cis*-**2**. nOe correlations between *trans*-**2**'s protons and *cis*-**2**'s protons reveal through-space interactions between the two isomers of **2**, confirming that they can coexist within the same cage. Note the strong correlation between *trans*-**2**'s *ortho* protons and *cis*-**2**'s *ortho* and *meta* protons. There is also a weak correlation between *trans*-**2**'s *meta* protons and *cis*-**2**'s *ortho* and *meta* protons. The *para* protons of neither *trans*-**2** nor *cis*-**2** show any correlations with other protons of **2**.

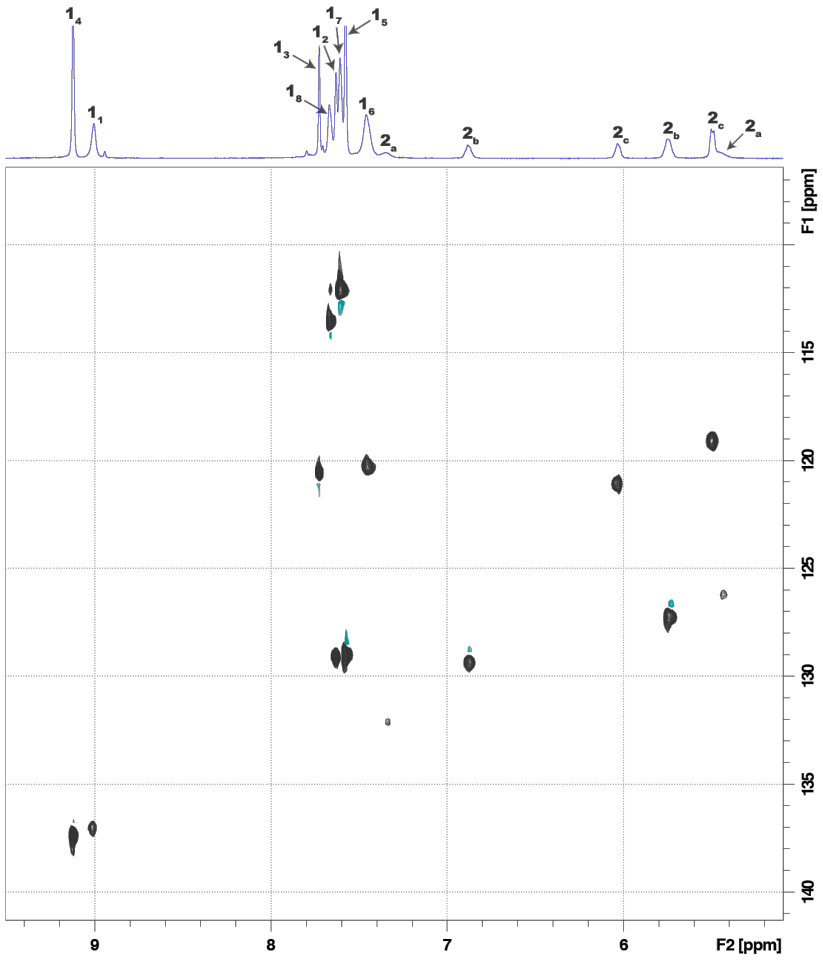

Fig. S22. Partial ^{1}H-^{13}C HSQC NMR spectrum of $\mathbf{2}_2\subset\mathbf{1}$ following exposure to UV light (λ = 365 nm) (500 MHz, D_2O, 298 K).

7. Characterization of inclusion complex (*trans*-**3**)$_2\subset$**1**

Inclusion complex (*trans*-**3**)$_2\subset$**1** was obtained in ~35% yield (i.e., treating **1** with excess of *trans*-**3** resulted in filling of ~35% of the cages).

^{1}H NMR (500 MHz, D_2O, 298 K): δ = 9.10 (s, 8H, $\mathbf{1}_4$), ~9.00 (br, 4H, $\mathbf{1}_1$), 7.68 (br, 20H, $\mathbf{1}_{3+6+7+8}$), 7.54 (s, 16H, $\mathbf{1}_{2+5}$), 7.51 (br, 1H, $\mathbf{3}_a$), 7.29 (br, 2H, $\mathbf{3}_b$), 6.24 (br, 2H, $\mathbf{3}_c$), 6.19 (br, 2H, $\mathbf{3}_{b'}$), 6.11 (br, 1H, $\mathbf{3}_f$), 5.87 (br, 2H, $\mathbf{3}_{c'}$), 5.33 (m, 2H, $\mathbf{3}_{g+h}$), 4.50 (br, 2H, $\mathbf{3}_e$), 3.12–3.08 (m, 24H, $\mathbf{1}_{CH2}$), 2.78–2.64 (m, 72H, $\mathbf{1}_{CH3}$). **^{13}C NMR** (125 MHz, D_2O, 298 K): δ = 160.34 ($\mathbf{3}_{a'}$), 150.63 ($\mathbf{3}_d$), 144.38 ($\mathbf{3}_{d'}$), 137.95 ($\mathbf{1}_9$), 137.60 ($\mathbf{1}_{10}$), 137.45 ($\mathbf{1}_4$), 137.05 ($\mathbf{1}_1$), 132.61 ($\mathbf{3}_f$), 131.61 ($\mathbf{3}_a$) 130.00 ($\mathbf{3}_b$), 128.81 ($\mathbf{1}_{2+5}$), 122.78 ($\mathbf{3}_{b'}$), 120.96 ($\mathbf{3}_c$), 120.70 ($\mathbf{1}_3$), 120.45 ($\mathbf{1}_6$), 117.81 ($\mathbf{3}_{g/h}$), 114.79 ($\mathbf{1}_8$), 113.77 ($\mathbf{3}_{c'}$), 112.62 ($\mathbf{1}_7$), 68.65 ($\mathbf{3}_e$), 62.48 ($\mathbf{1}_{CH2}$), 50.23 ($\mathbf{1}_{CH3}$), 49.98 ($\mathbf{1}_{CH3}$). **^{1}H-DOSY NMR** (D_2O, 298 K): D = 0.19 (± 0.01) × 10^{-5} cm^2/s. **Elemental analysis**: calcd: C, 38.07; H, 4.62; N, 20.66; found: 38.06; H, 4.76; N, 20.50.

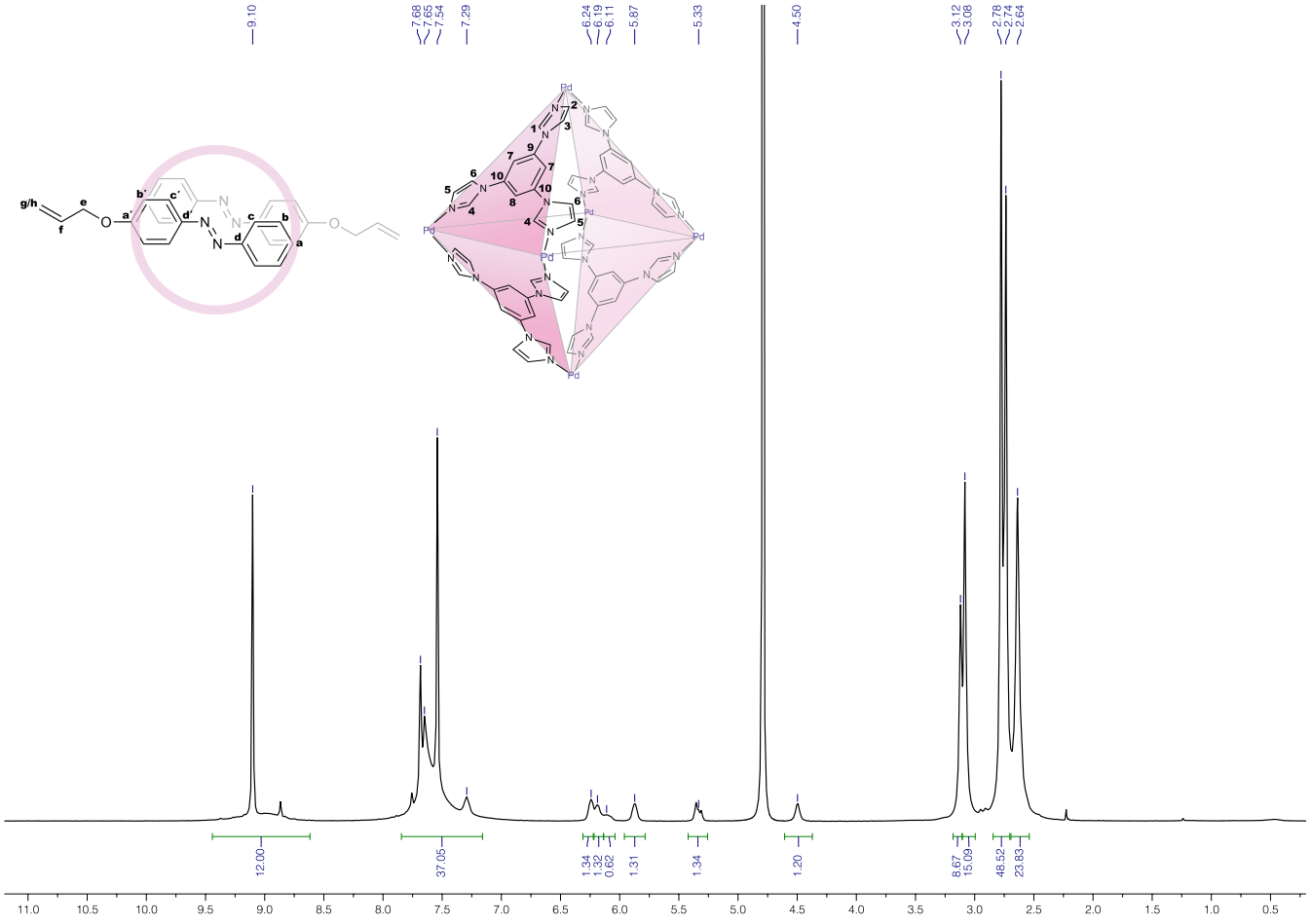

Fig. S23. ^{1}H NMR spectrum of (*trans*-**3**)$_2$⊂**1** (500 MHz, D_2O, 298 K). For signal assignment, see p. 22.

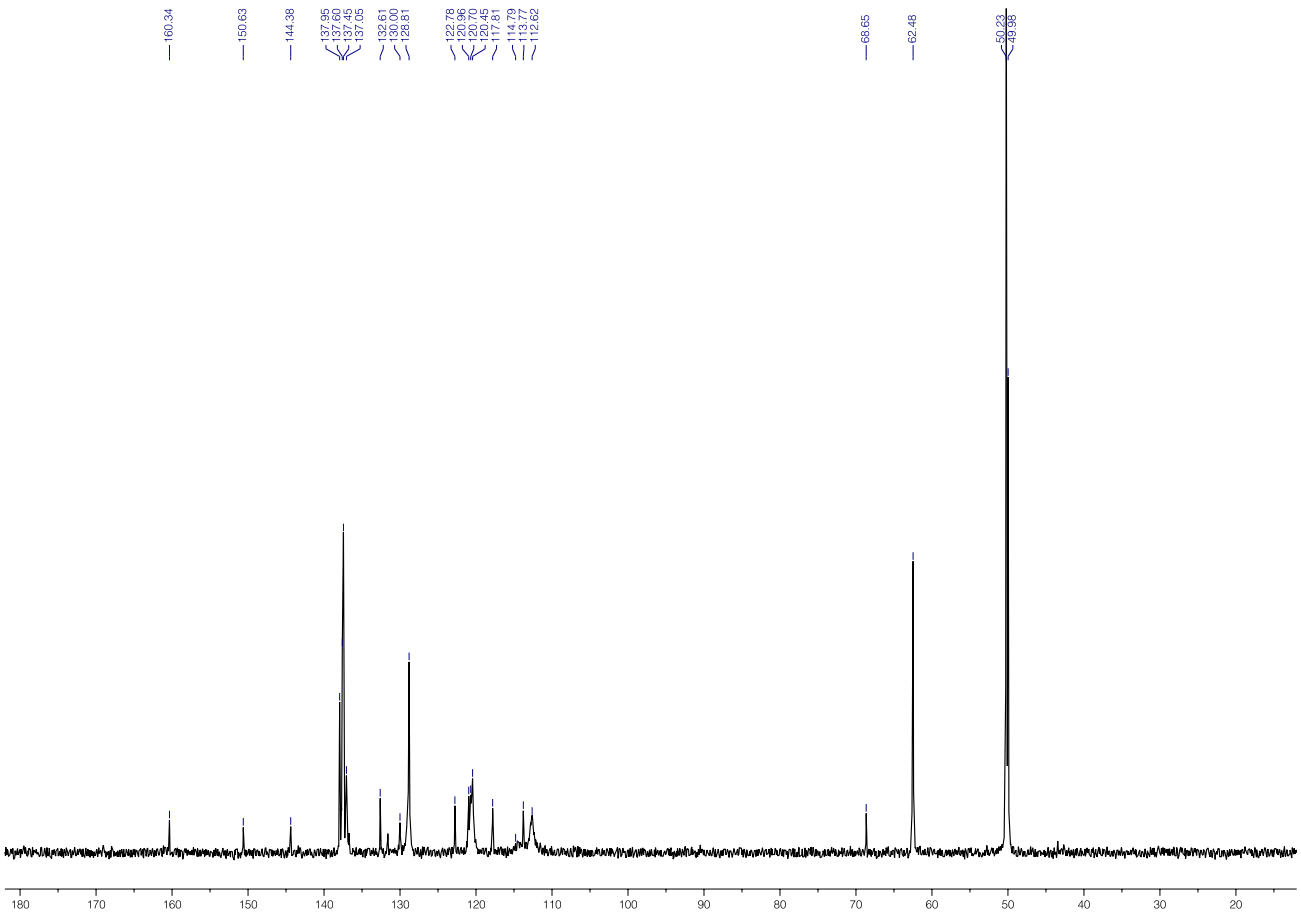

Fig. S24. ^{13}C NMR spectrum of (*trans*-**3**)$_2$⊂**1** (125 MHz, D_2O, 298 K).

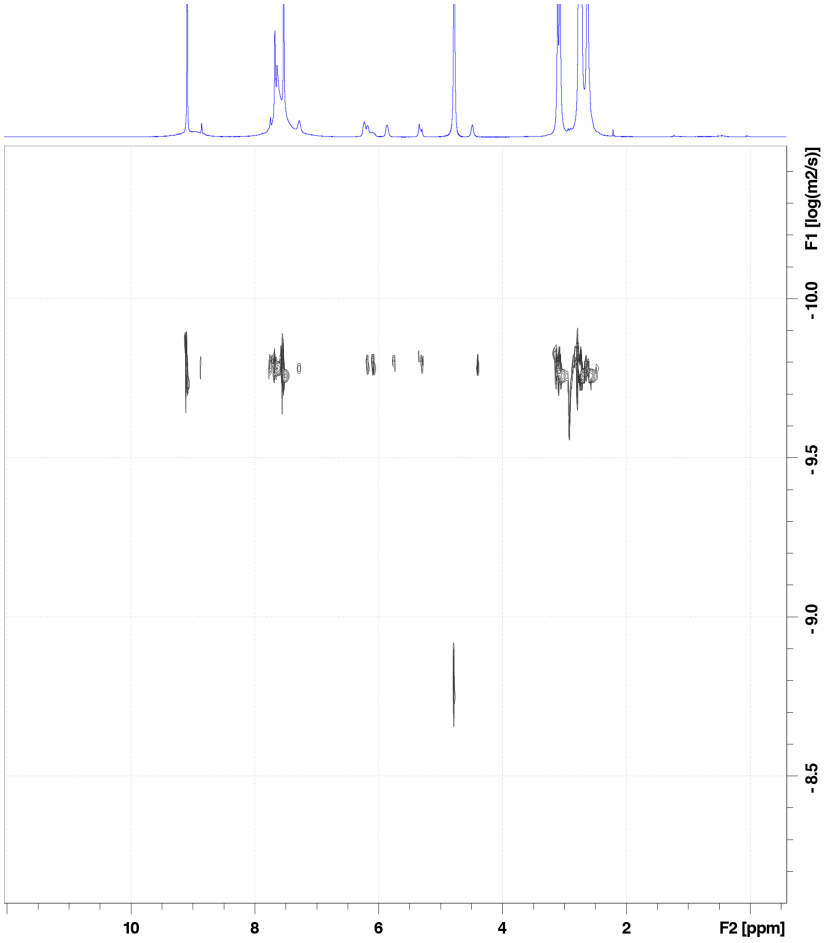

Fig. S25. ^{1}H DOSY NMR spectrum of (*trans*-**3**)$_2$⊂**1** (400 MHz, D_2O, 298 K).

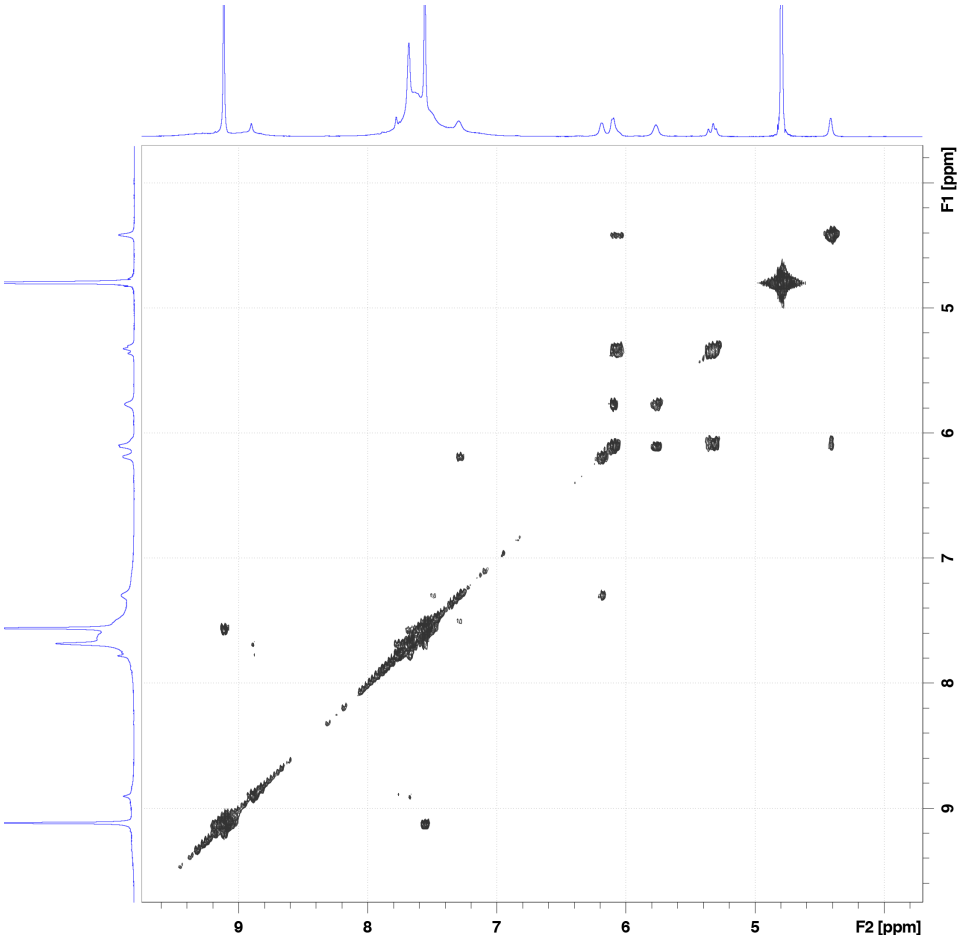

Fig. S26. ^{1}H-^{1}H COSY NMR spectrum of (*trans*-**3**)$_2$⊂**1** (500 MHz, D_2O, 298 K).

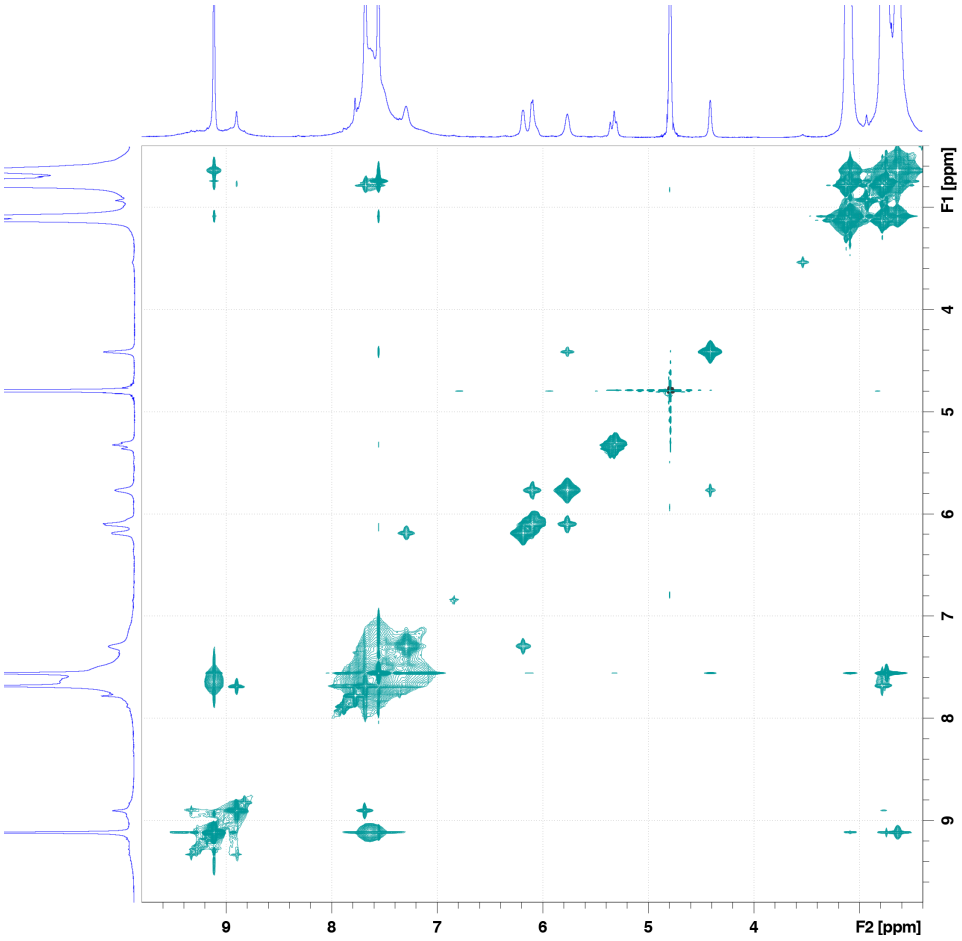

Fig. S27. ^{1}H-^{1}H NOESY NMR spectrum of (*trans*-**3**)$_2$⊂**1** (500 MHz, D_2O, 298 K).

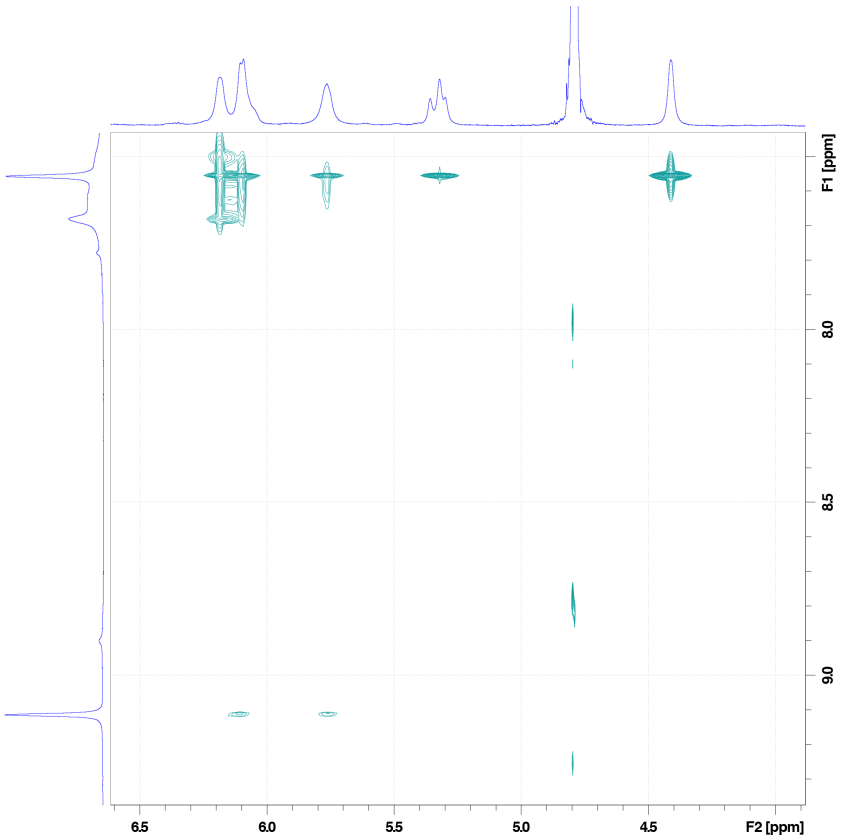

Fig. S28. Partial ^{1}H-^{1}H NOESY NMR spectrum of (*trans*-**3**)$_2$⊂**1** showing nOe correlations between the host and the guests (500 MHz, D_2O, 298 K) (the corresponding full-range spectrum is shown in Fig. S27).

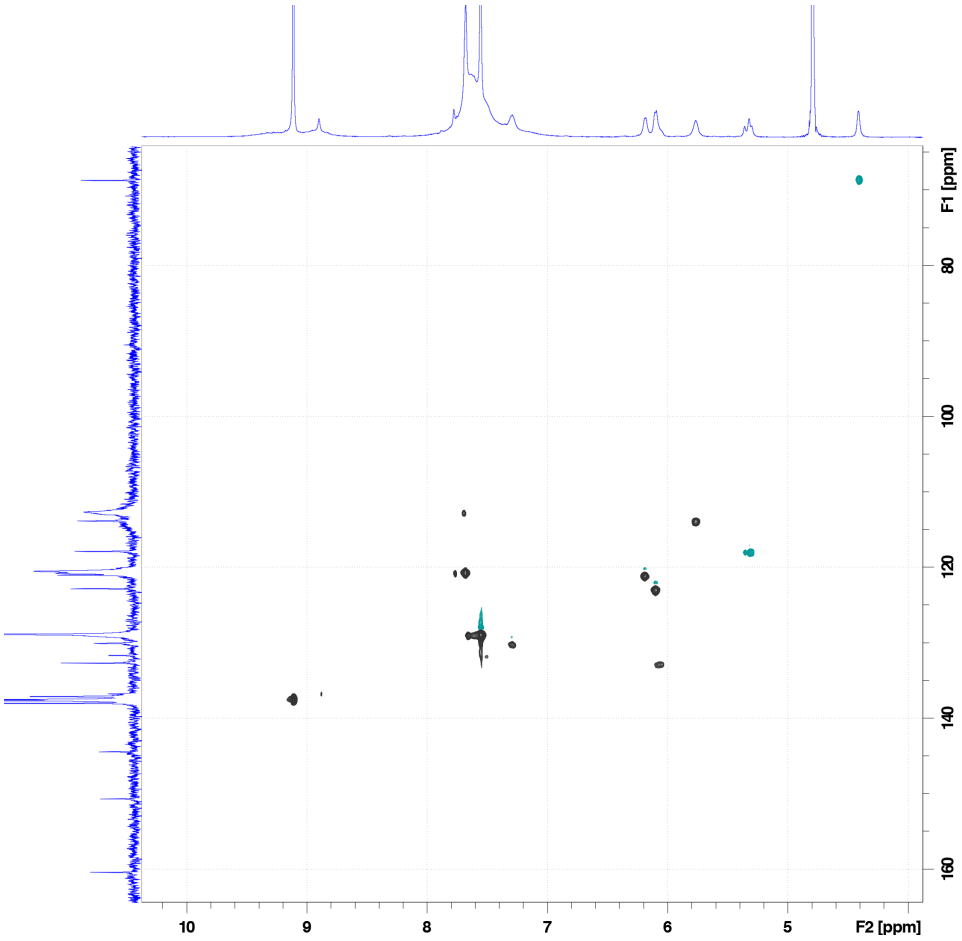

Fig. S29. ^{1}H-^{13}C HSQC NMR spectrum of (*trans*-**3**)$_2$⊂**1** (500 MHz, D_2O, 298 K).

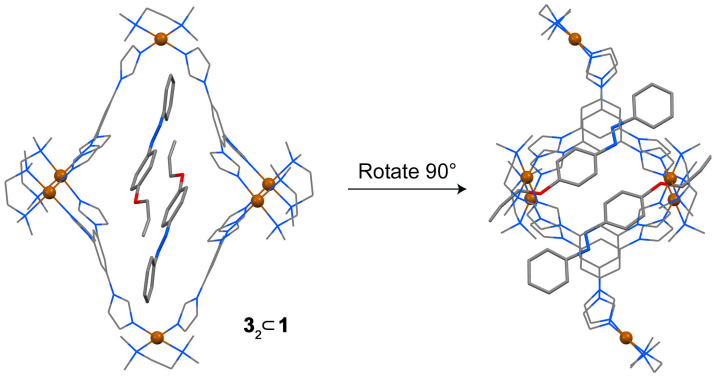

Fig. S30. Two views of the X-ray crystal structure of (*trans*-**3**)$_2$⊂**1** where **3** = *p*-allyloxyazobenzene as a model *para*-functionalized azobenzene. See also Fig. S31.

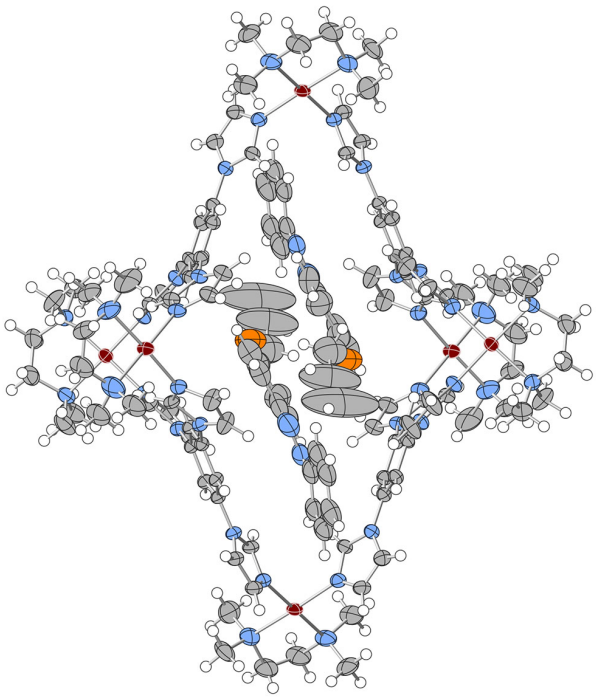

Fig. S31. ORTEP representation of the X-ray structure of inclusion complex (*trans*-**3**)$_2$⊂**1** (thermal ellipsoids at a 50% probability level). Anions and solvent molecules were eliminated for clarity. Pd, brown; C gray; N, blue; O, orange, H, white.

Analysis of intermolecular interactions within inclusion complex (*trans*-**3**)$_2$⊂**1**

Analysis was performed with PLATON on the cif file deposited in CCDC (accession number 1569281).

Host-guest interactions

Two benzene rings of cage **1** participate in π-π stacking interactions: Ring10 (C22-C27); Ring11 (C37-C42). Two benzene rings of encapsulated azobenzenes **3** participate in π-π stacking interactions: Ring12 (C49-C54); Ring13 (C55-C60).

The table below lists distances between the center of gravity of a given ring to the plane of the neighboring ring (in blue); distances between the center of gravity of the neighboring ring to the plane of the given ring (in red); and dihedral angles between the planes of the two rings (in green).

	Ring12	Ring13
Ring10	3.36 Å / 3.07 Å 17.3°	3.33 Å / 3.54 Å 14.0°
Ring11	3.72 Å / 2.82 Å 23.8°	

In addition, the following edge-to-face interactions are present:

C50 to the imidazole ring (N9N10C28C29C30), distance = 3.42 Å
C50 to the imidazole ring (N13N14C28C29C30), distance = 3.45 Å

Guest-guest interactions

The distance between the center of gravity of azobenzene's Ring13 to the plane of the benzene ring of the symmetry-generated neighboring azobenzene is 3.27 Å. The dihedral angle between the planes of the benzene rings is 0° (symmetry relation 2-x,1-y,z).

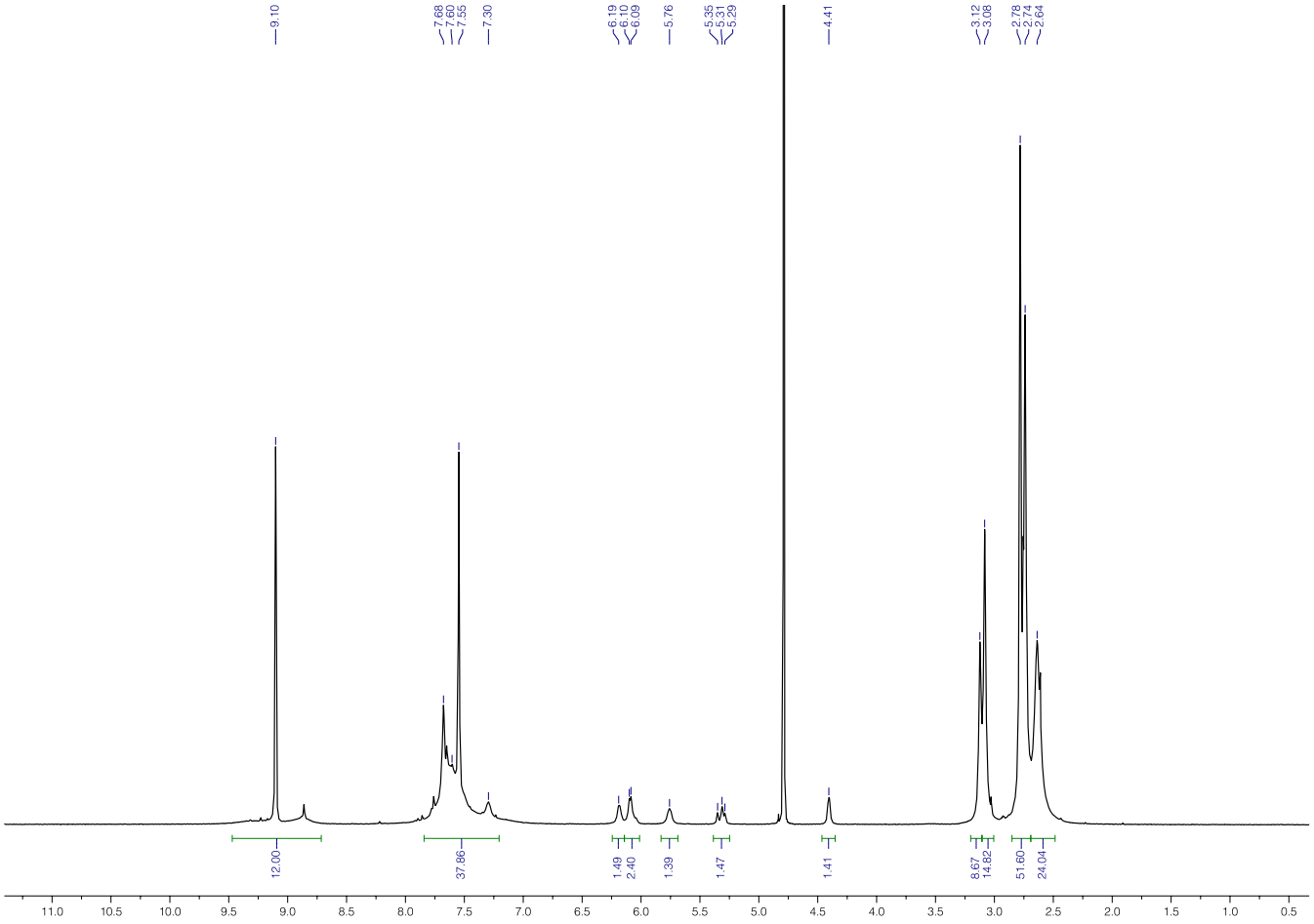

Fig. S32. ^{1}H NMR spectrum obtained by dissolving crystalline (*trans*-**3**)$_2$⊂**1** in water (500 MHz, D_2O, 298 K). Integration reveals that 36% (as opposed to the expected 100%) of the cages are filled, compared to 33% in the sample obtained by saturating a solution of **1** with *trans*-**3** (Fig. S23). Upon placing (*trans*-**3**)$_2$⊂**1** in water, a hazy suspension was obtained. Upon standing, a yellow solid (*trans*-**3**) precipitated. The resulting yellow supernatant was analyzed by NMR.

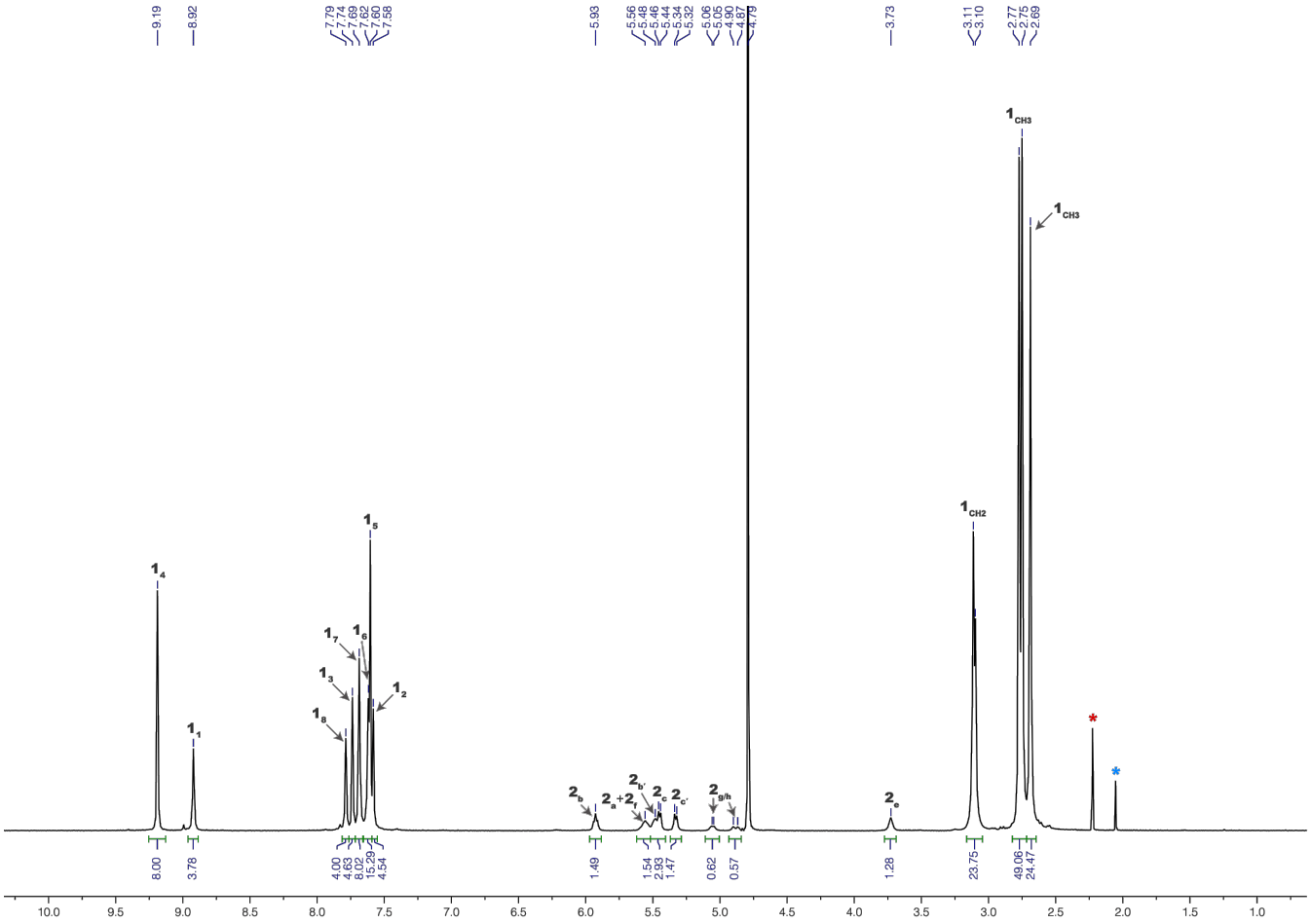

Fig. S33. ^{1}H NMR spectrum of (*trans*-**3**)$_2$⊂**1** after exposure to UV light (500 MHz, D_2O, 298 K). Blue asterisk denotes acetone. Black asterisk denotes acetonitrile.

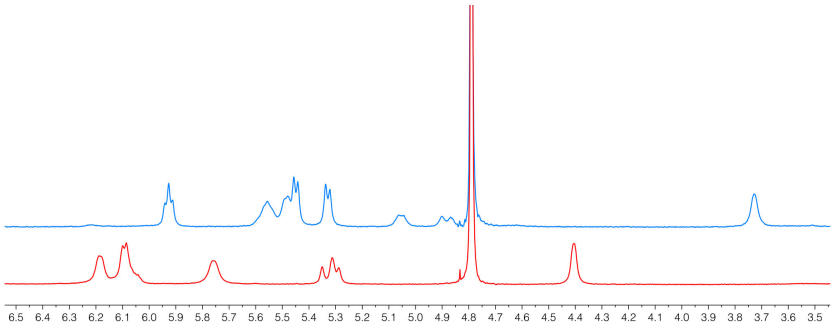

Fig. S34. Comparison of partial ^{1}H NMR spectra of (*trans*-**3**)$_2$⊂**1** before (blue) and after (red) exposure to UV light (extracted from Fig. S23 and S33, respectively).

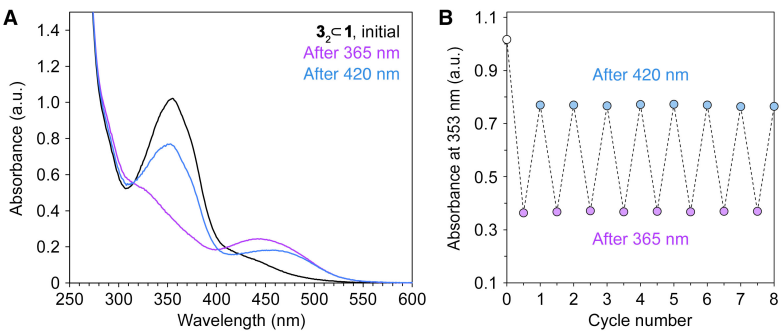

Fig. S35. *(A)* Changes in the UV/Vis absorption spectrum of (*trans*-**3**)$_2$⊂**1** following exposure to UV light (4 min) and then to blue light (4 min). (*B*) Eight cycles of reversible photoisomerization of **3** within (*trans*-**3**)$_2$⊂**1** followed by UV/Vis absorption spectroscopy.

8. Characterization of inclusion complex *cis*-**4**⊂**1**

Inclusion complex *cis*-**4**⊂**1** was obtained in ~100% yield (i.e., all the cages were filled when treated with excess of *cis*-**4**).

^{1}H NMR (500 MHz, D_2O, 298 K): δ = 9.22 (s, 8H, $\mathbf{1}_4$), 8.89 (s, 4H, $\mathbf{1}_1$), 7.82 (s, 4H, $\mathbf{1}_8$), 7.79 (s, 4H, $\mathbf{1}_3$), 7.75 (s, 8H, $\mathbf{1}_6$), 7.73 (s, 8H, $\mathbf{1}_7$), 7.64 (s, 8H, $\mathbf{1}_5$), 7.61 (s, 4H, $\mathbf{1}_2$), 5.48 (br, 2H, *cis*-$\mathbf{4}_a$), 5.20 (d, ^3J = 7.2 Hz, 4H, *cis*-$\mathbf{4}_b$), 3.10 (m, 24H, $\mathbf{1}_{CH2}$), 2.77–2.71 (m, 72H, $\mathbf{1}_{CH3}$), 2.53 (s, 12H, *cis*-$\mathbf{4}_{CH3}$). **^{13}C NMR** (125 MHz, D_2O, 298 K): δ = 148.56 (*cis*-$\mathbf{4}_c$), 138.47 ($\mathbf{1}_9$), 137.36 ($\mathbf{1}_{10+4}$), 137.02 ($\mathbf{1}_1$), 131.81 (*cis*-$\mathbf{4}_d$), 128.92 ($\mathbf{1}_5$), 128.76 ($\mathbf{1}_2$), 127.87 (*cis*-$\mathbf{4}_a$), 120.58 ($\mathbf{1}_3$), 120.51 ($\mathbf{1}_6$), 112.45 ($\mathbf{1}_8$), 111.96 ($\mathbf{1}_7$), 102.73 (*cis*-$\mathbf{4}_b$), 62.57 ($\mathbf{1}_{CH2}$), 53.75 (*cis*-$\mathbf{4}_{CH3}$), 50.34 ($\mathbf{1}_{CH3}$), 50.18 ($\mathbf{1}_{CH3}$), 50.05 ($\mathbf{1}_{CH3}$). **^{1}H-DOSY NMR** (D_2O, 298 K): D = 0.19 (± 0.01) × 10^{-5} cm^2/s. **Elemental analysis**: calcd: C, 38.57; H, 4.68; N, 20.08; found: 38.46; H, 4.78; N, 20.15.

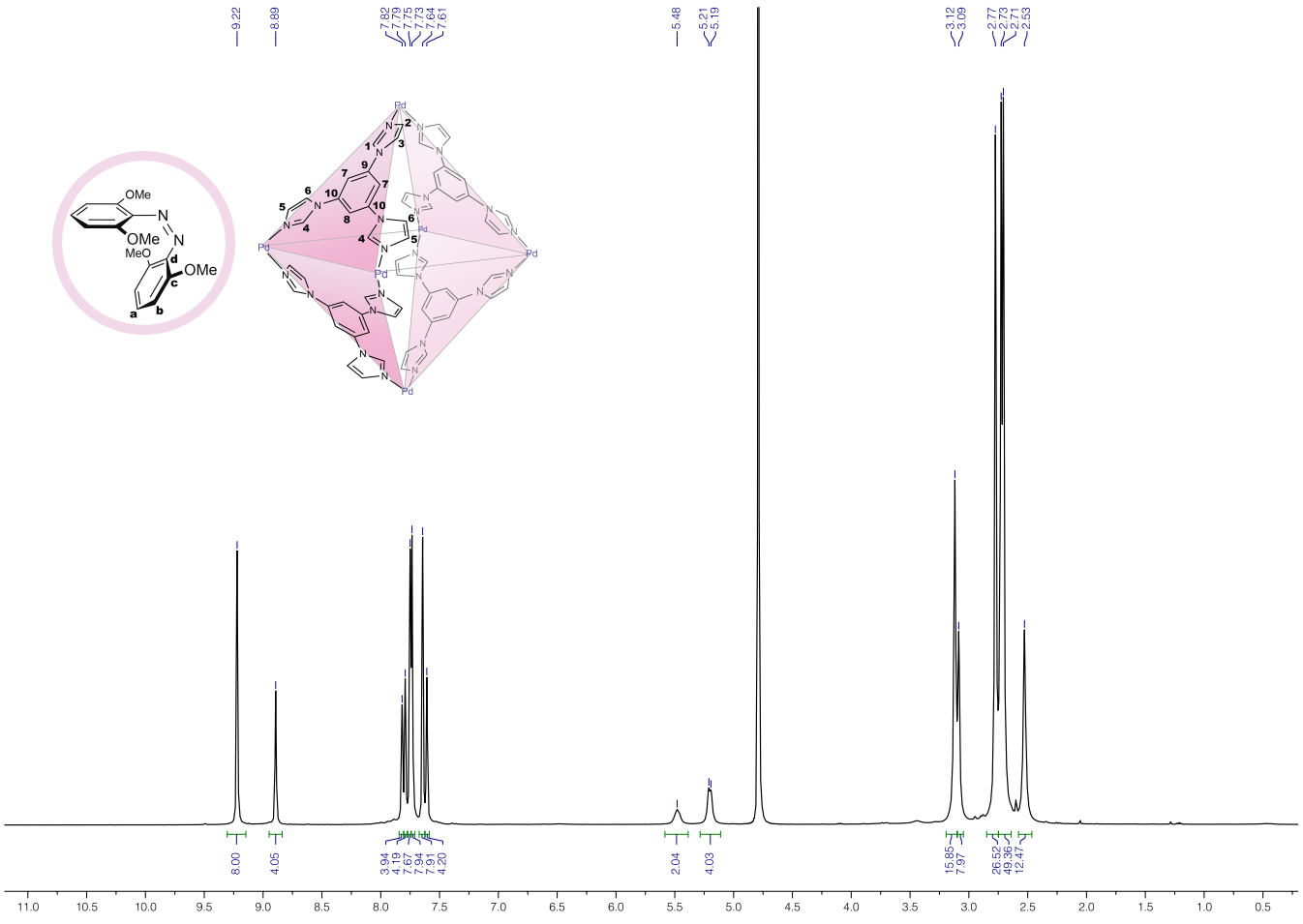

Fig. S36. ^{1}H NMR spectrum of *cis*-**4**⊂**1** (500 MHz, D_2O, 298 K). For signal assignment, see p. 34, above.

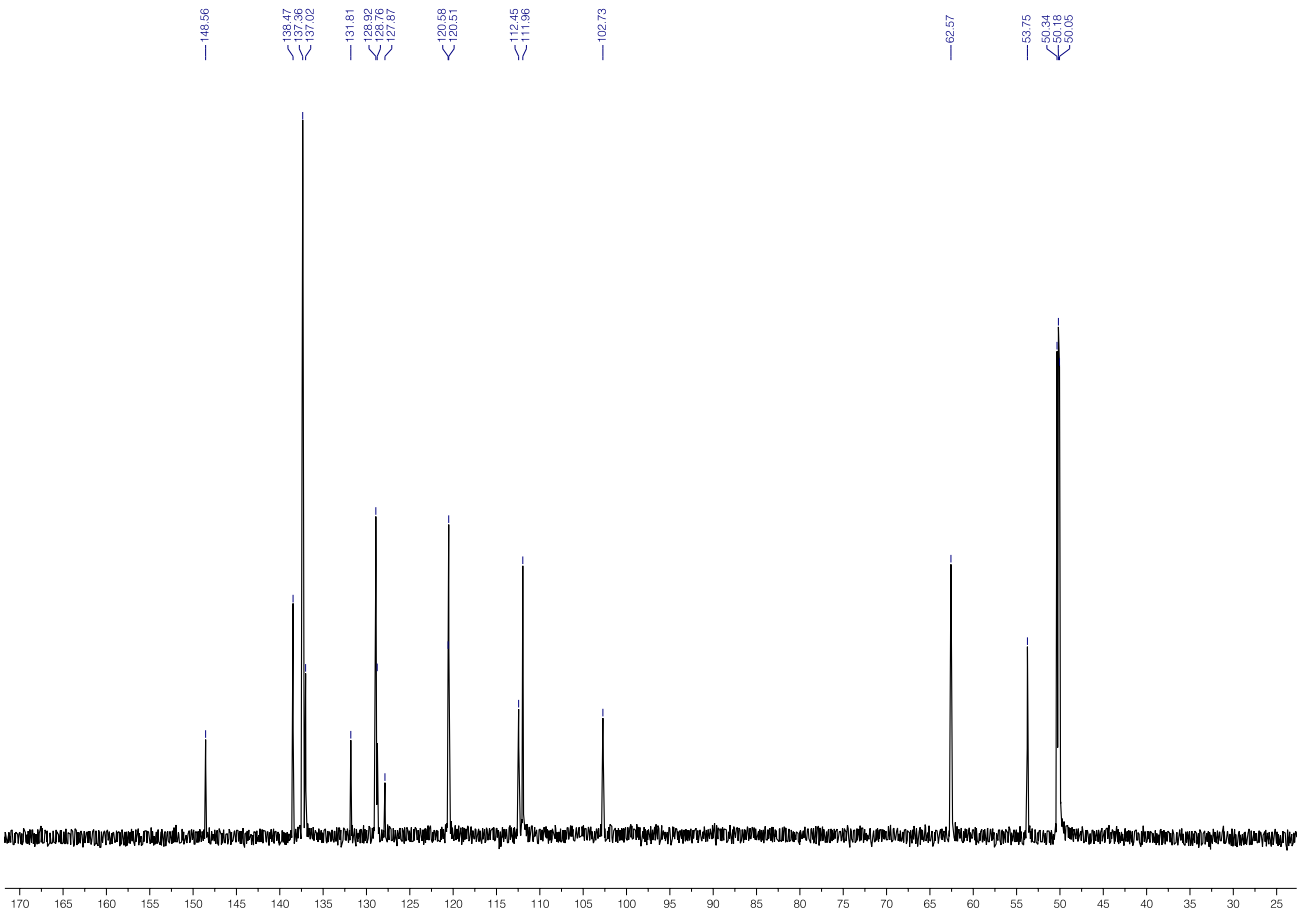

Fig. S37. ^{13}C NMR spectrum of *cis*-**4⊂1** (125 MHz, D_2O, 298 K).

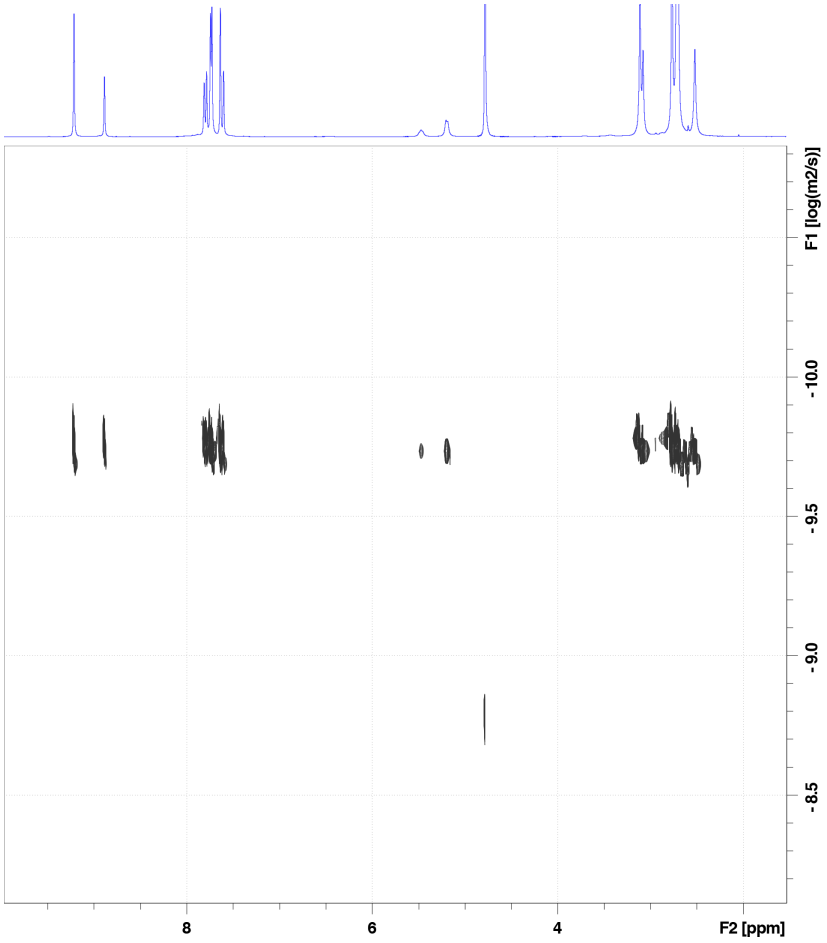

Fig. S38. ^{1}H DOSY NMR spectrum of *cis*-**4⊂1** (400 MHz, D_2O, 298 K).

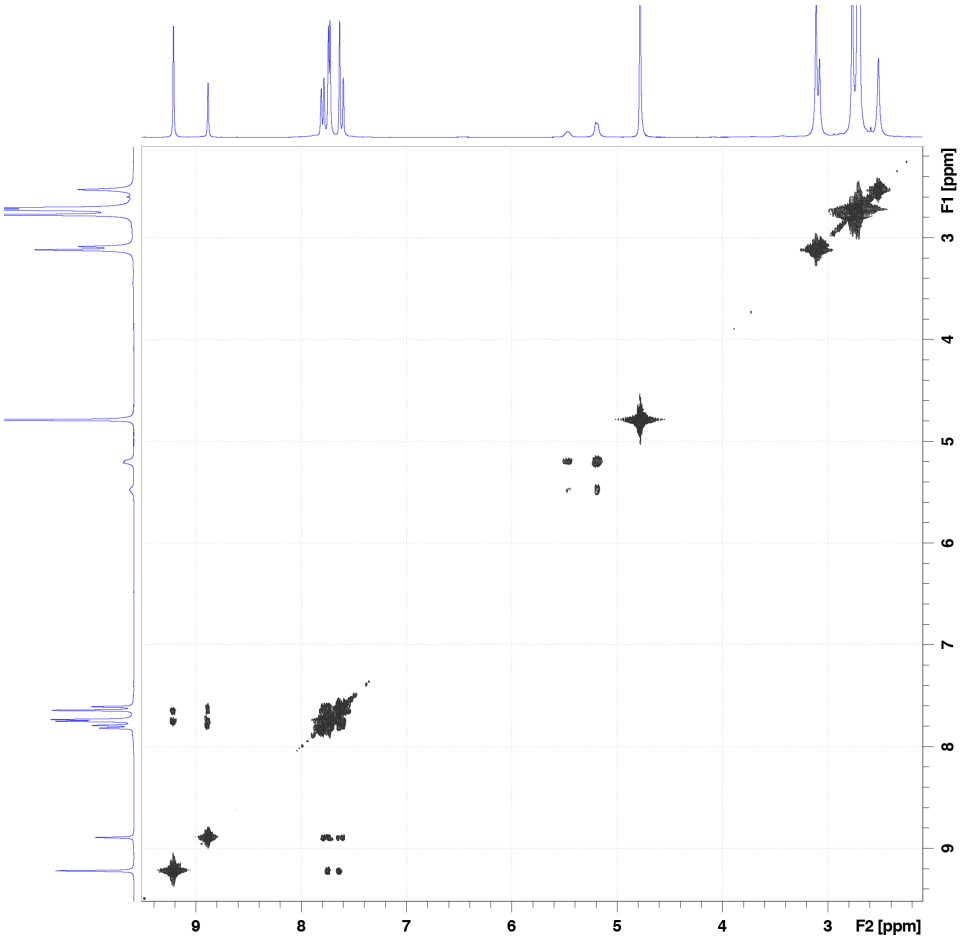

Fig. S39. ^{1}H-^{1}H COSY NMR spectrum of *cis*-**4**⊂**1** (500 MHz, D_2O, 298 K).

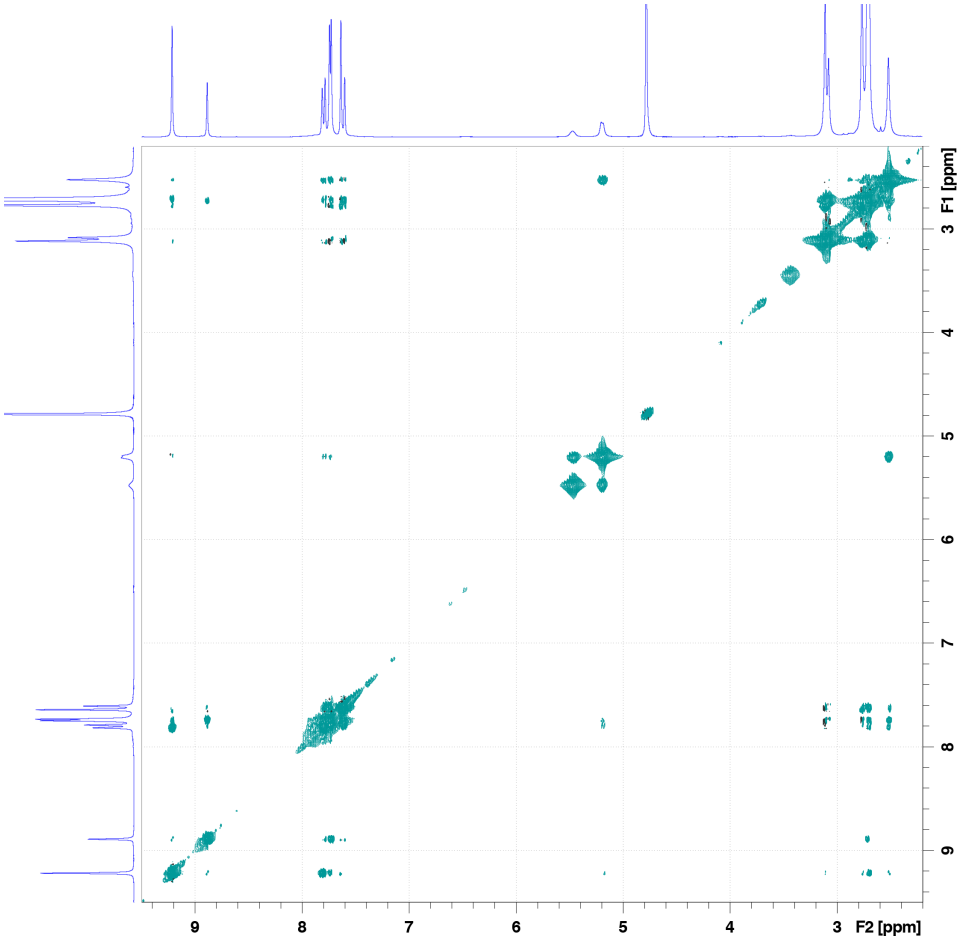

Fig. S40. ^{1}H-^{1}H NOESY NMR spectrum of *cis*-**4⊂1** (500 MHz, D_2O, 298 K).

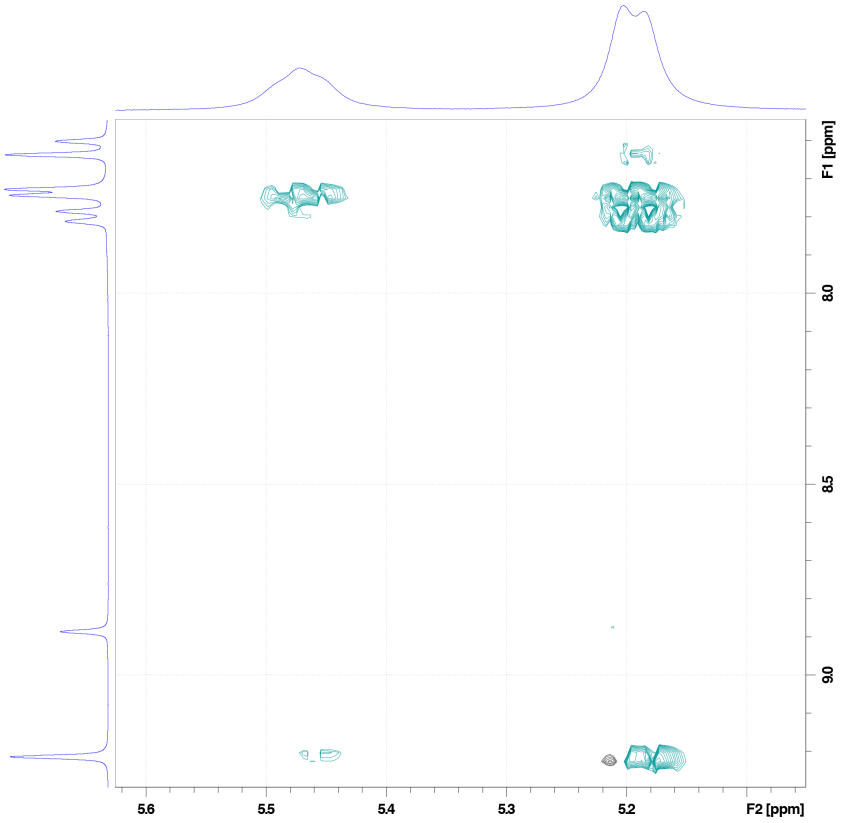

Fig. S41. Partial ^{1}H-^{1}H NOESY NMR spectrum of *cis*-**4**⊂**1** showing nOe correlations between the host and the guests (500 MHz, D_2O, 298 K) (the corresponding full-range spectrum is shown in Fig. S40).

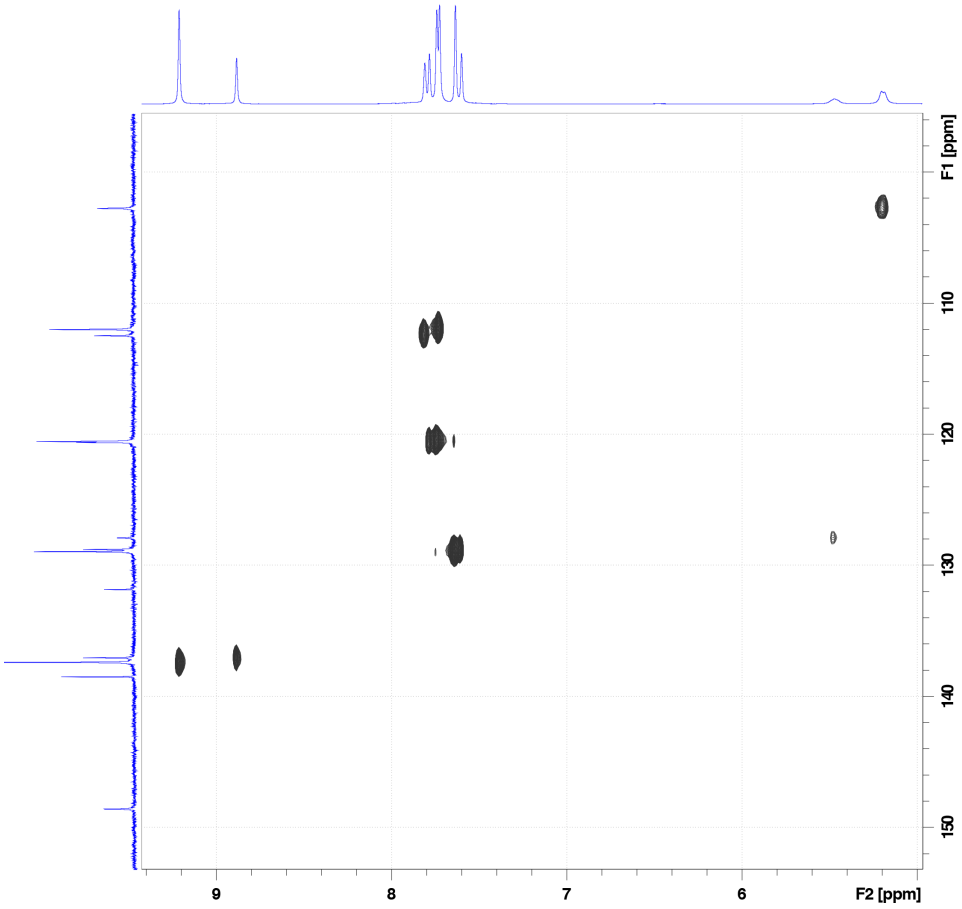

Fig. S42. ^{1}H-^{13}C HSQC NMR spectrum of *cis*-**4⊂1** (500 MHz, D_2O, 298 K).

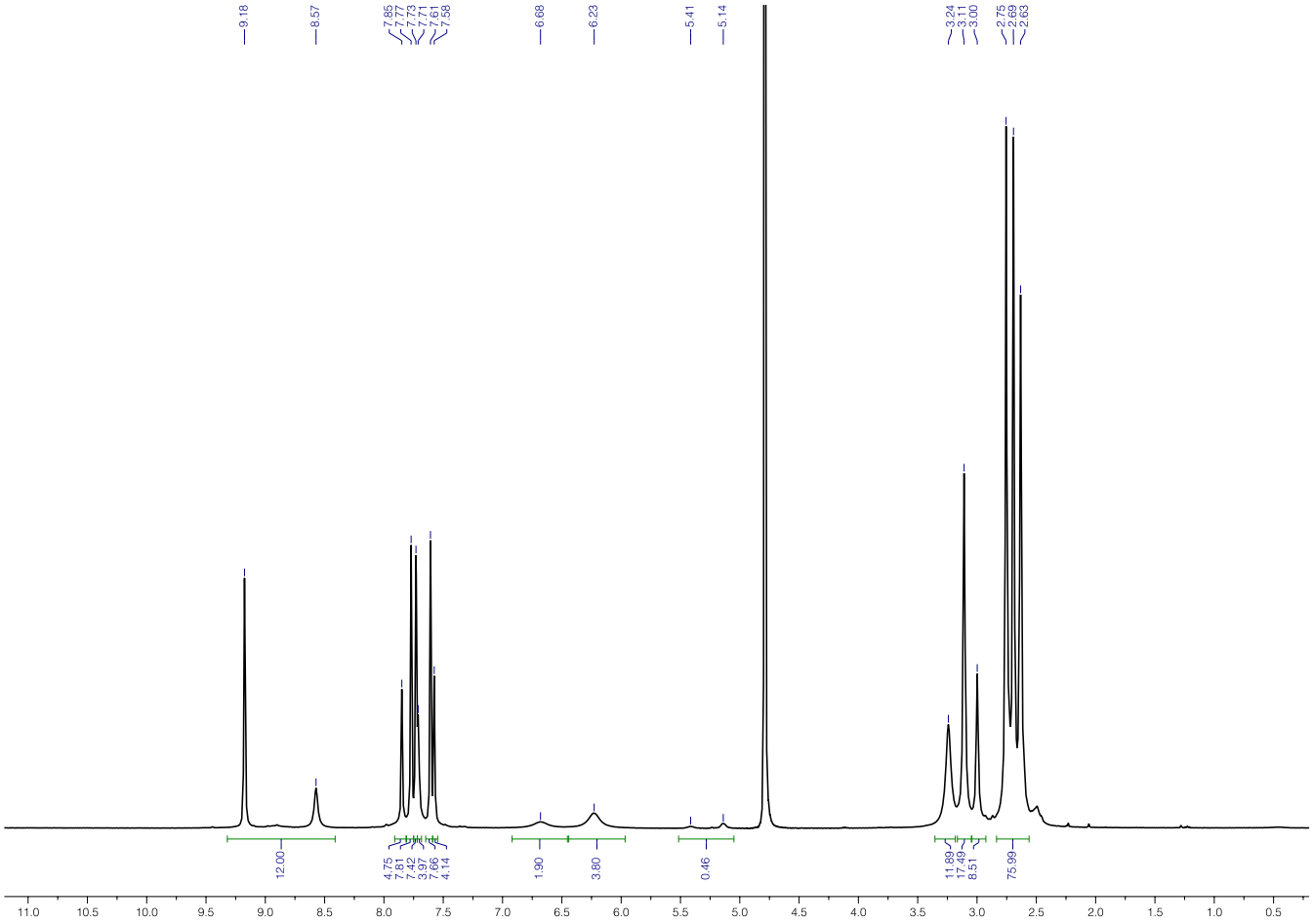

Fig. S43. ^{1}H NMR spectrum of *cis*-**4⊂1** (400 MHz, D_2O, 298 K) after exposure to blue light.

9. Characterization of inclusion complex *trans*-**4**⊂**1**

Inclusion complex *trans*-**4**⊂**1** was obtained in ~100% yield (i.e., all the cages were filled when treated with excess of *trans*-**4**).

^{1}H NMR (500 MHz, D_2O, 323 K): δ = 9.42 (s, 8H, $\mathbf{1}_4$), 8.94 (s, 4H, $\mathbf{1}_1$), 8.18 (s, 4H, $\mathbf{1}_3$), 8.09 (s, 8H, $\mathbf{1}_7$), 8.03 (s, 8H, $\mathbf{1}_6$), 7.94 (s, 8H, $\mathbf{1}_5$), 7.93 (s, 8H, $\mathbf{1}_{2+8}$), 7.03 (br, 2H, *trans*-$\mathbf{4}_a$), 6.59 (br, 4H, *trans*-$\mathbf{4}_b$), 3.59 (s, 12H, *trans*-$\mathbf{4}_{CH3}$), 3.45 (s, 16H, $\mathbf{1}_{CH2}$), 3.36 (s, 8H, $\mathbf{1}_{CH2}$), 3.11 (s, 24H, $\mathbf{1}_{CH3}$), 3.04 (s, 24H, $\mathbf{1}_{CH3}$), 3.00 (s, 24H, $\mathbf{1}_{CH3}$). **^{13}C NMR** (125 MHz, D_2O, 323 K): δ = 151.85 (*trans*-$\mathbf{4}_c$), 137.93 ($\mathbf{1}_9$), 137.73 ($\mathbf{1}_{4+10}$), 137.03 ($\mathbf{1}_1$), 131.98 (*trans*-$\mathbf{4}_a$), 131.60 (*trans*-$\mathbf{4}_d$), 128.80 ($\mathbf{1}_{2+5}$), 120.54 ($\mathbf{1}_6$), 120.28 ($\mathbf{1}_3$), 114.06 ($\mathbf{1}_8$), 112.43 ($\mathbf{1}_7$), 104.61 (*trans*-$\mathbf{4}_b$), 62.58 ($\mathbf{1}_{CH2}$), 62.49 ($\mathbf{1}_{CH2}$), 55.75 (*trans*-$\mathbf{4}_{CH3}$), 50.28 ($\mathbf{1}_{CH3}$), 50.16 ($\mathbf{1}_{CH3}$), 50.02 ($\mathbf{1}_{CH3}$).

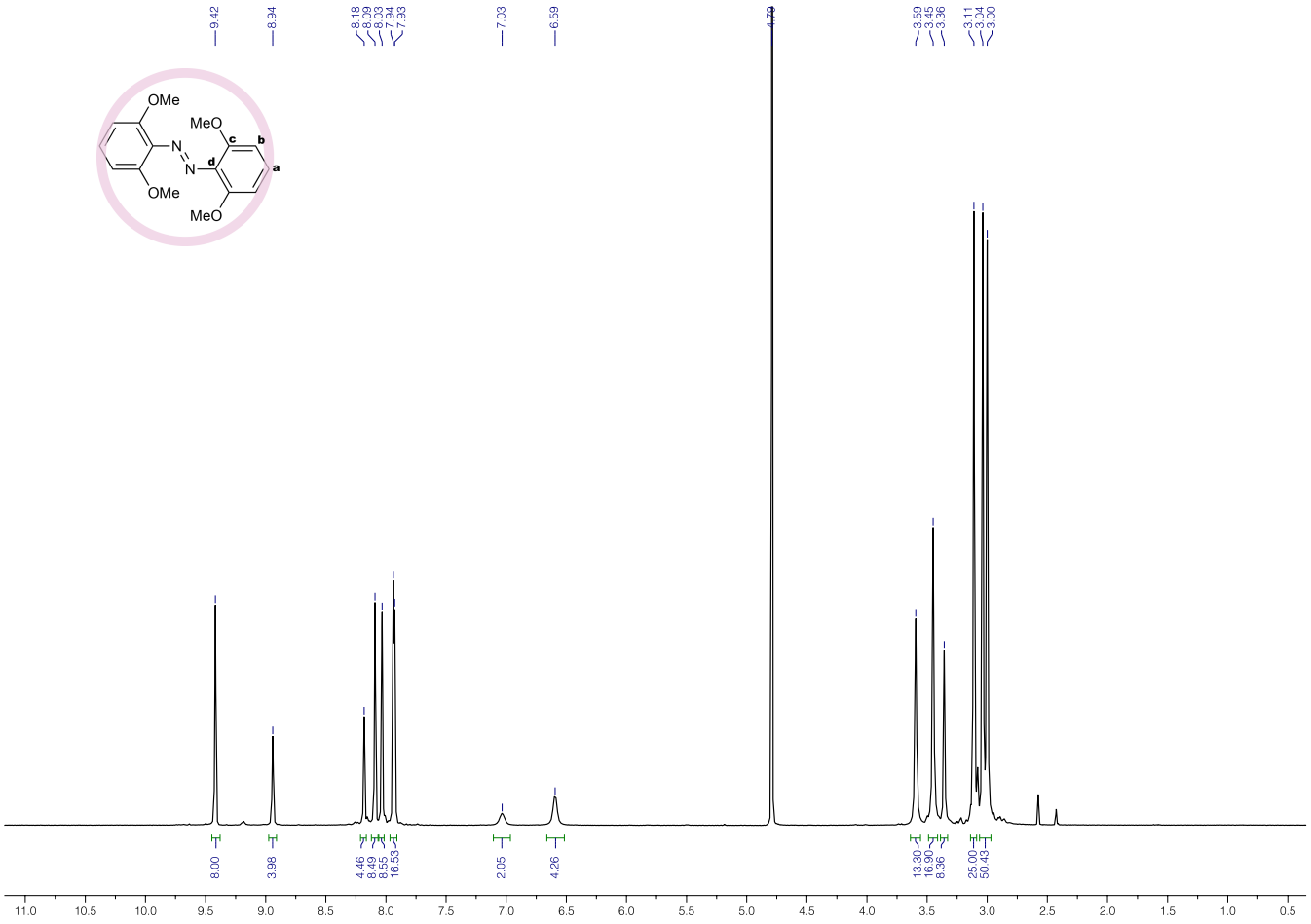

Fig. S44. ^{1}H NMR spectrum of *trans*-**4**⊂**1** (500 MHz, D_2O, 323 K). For signal assignment, see p. 42, above.

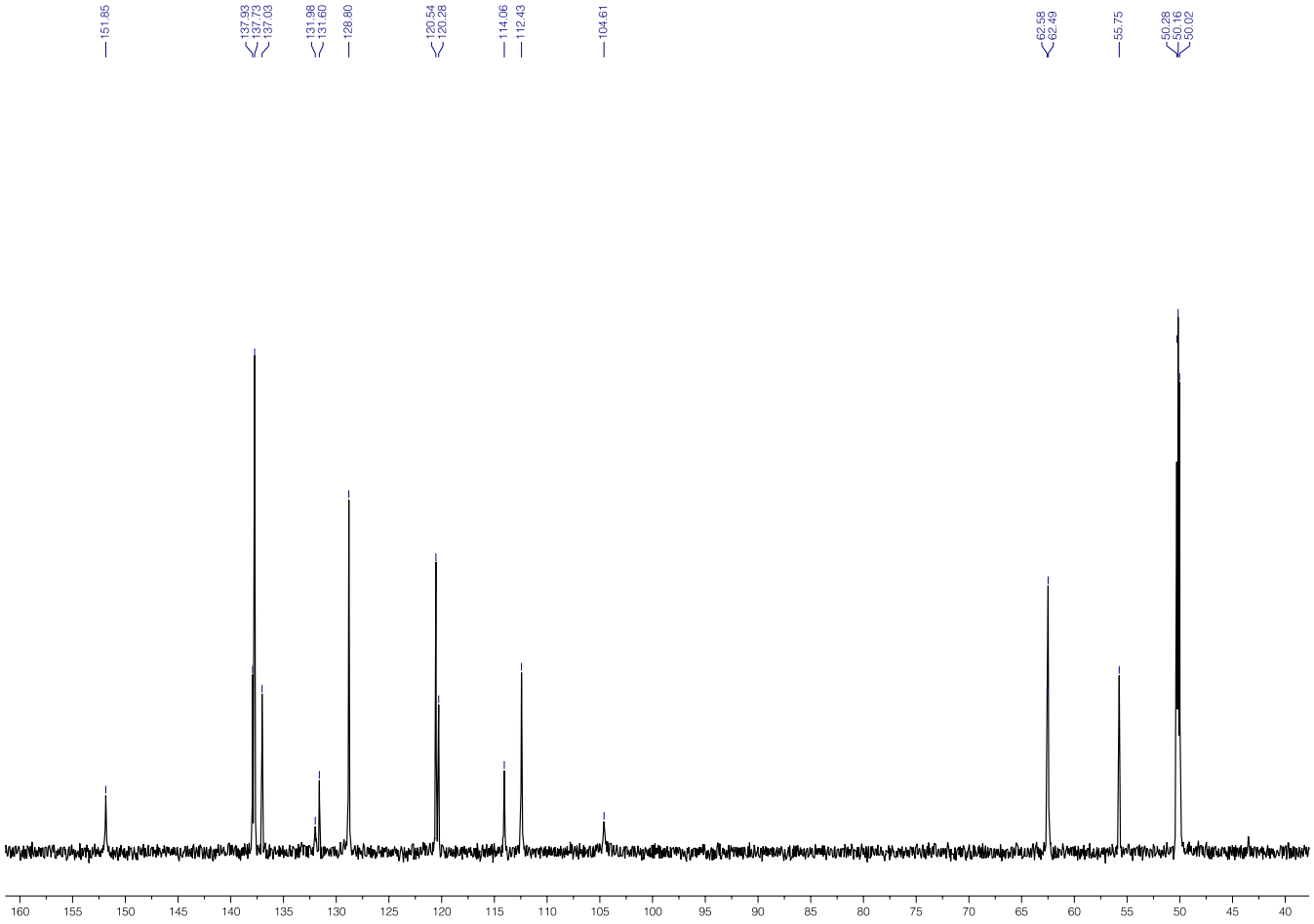

Fig. S45. ^{13}C NMR spectrum of *trans*-**4⊂1** (125 MHz, D_2O, 323 K).

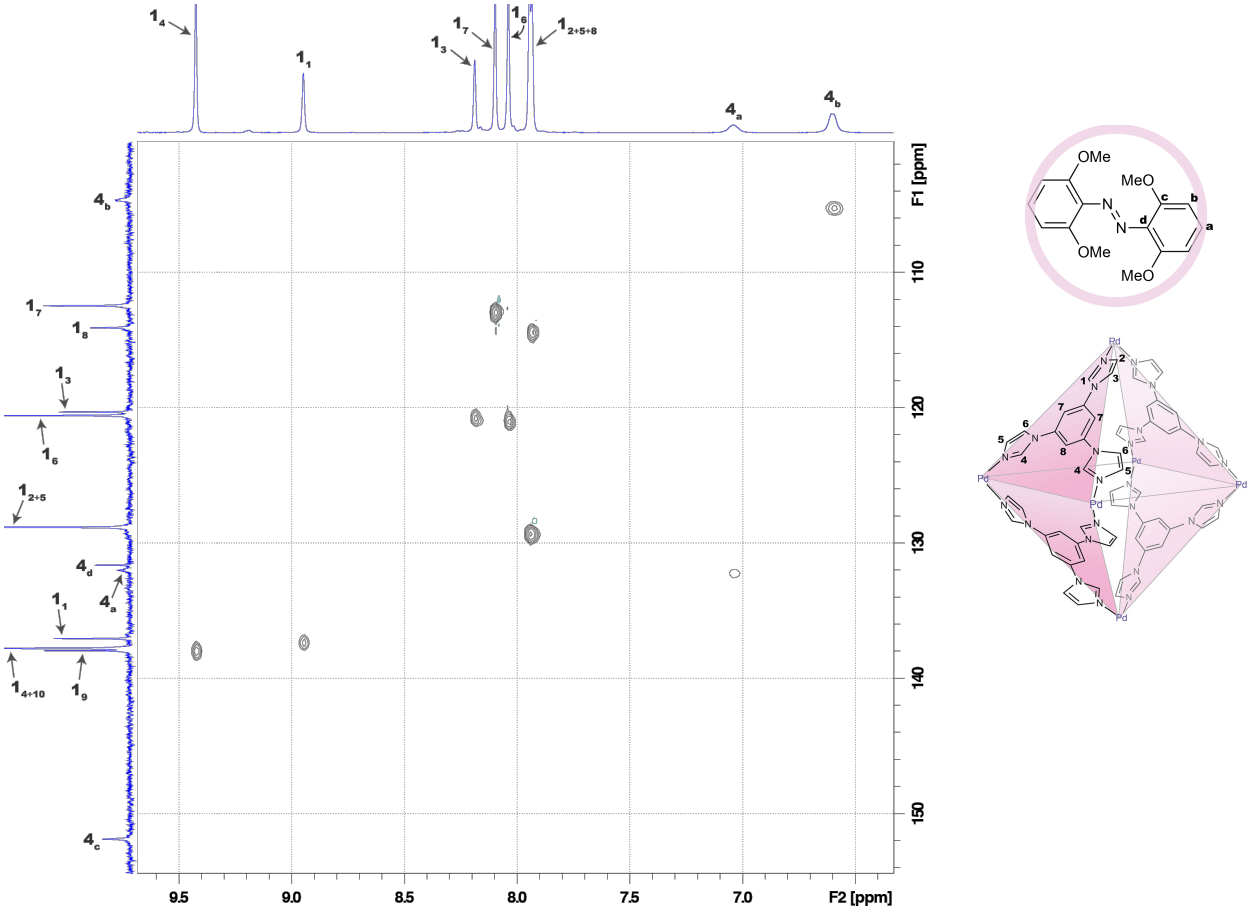

Fig. S46. Partial ^{1}H-^{13}C HSQC NMR spectrum of *trans*-**4⊂1** (125 MHz, D_2O, 323 K).

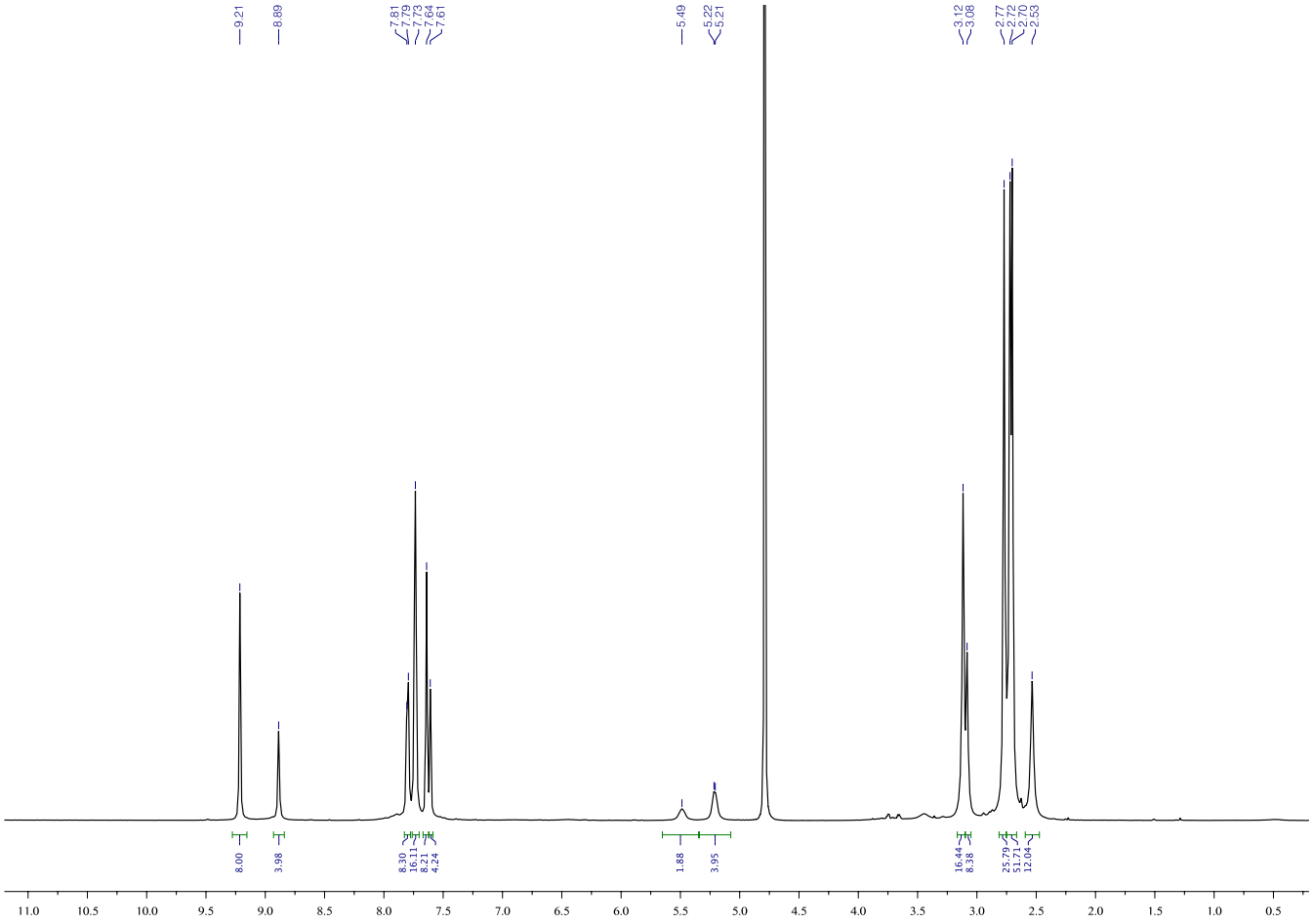

Fig. S47. ^{1}H NMR spectrum of *trans*-**4**⊂**1** (500 MHz, D_2O, 298 K) after exposure to yellow light.

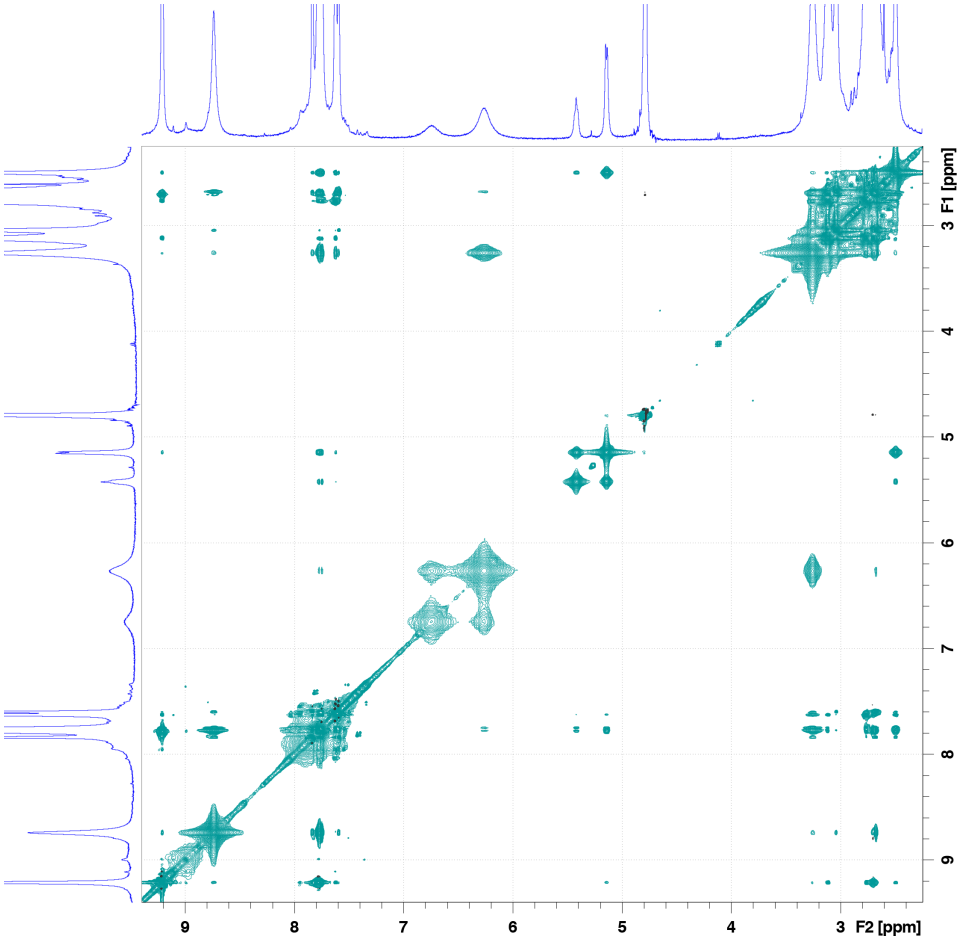

Fig. S48. ^{1}H-^{1}H NOESY NMR spectrum of **4⊂1** subjected to partial isomerization and containing a ~1:1 mixture of *trans*-**4** and *cis*-**4** (500 MHz, D_2O, 298 K).

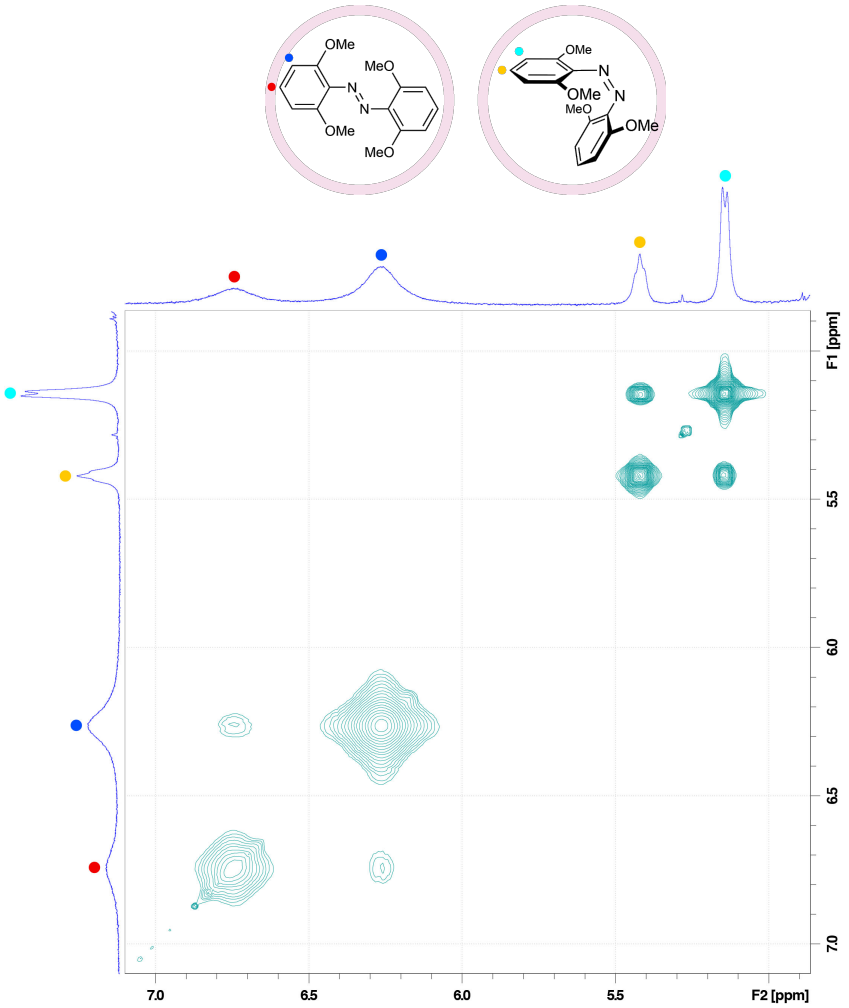

Fig. S49. Partial ^{1}H-^{1}H NOESY NMR spectrum of **4⊂1** subjected to partial isomerization and consisting of a ~1:1 mixture of *trans*-**4** and *cis*-**4** (500 MHz, D_2O, 298 K) (the corresponding full-range spectrum is shown in Fig. S48). The signals centered at ~6.75 ppm and at ~6.27 ppm correspond to *para* and *meta* protons of *trans*-**4**, respectively. The signals centered at ~5.42 ppm and at ~5.15 ppm correspond to *para* and *meta* protons of *cis*-**4**, respectively. The absence of nOe correlations between *trans*-**4**'s and *cis*-**4**'s protons indicates that host **1** is incapable of simultaneously accommodating *cis*-**4** and *trans*-**4**, which suggests that all inclusion complexes involving **4** are of 1:1 stoichiometry.

10. Characterization of inclusion complex (*trans*-**5**)$_2$⊂**1**

Inclusion complex **5**$_2$⊂**1** was obtained in ~100% yield (i.e., all the cages were filled when treated with excess of *trans*-**5**).

^{1}H NMR (500 MHz, D_2O, 298 K): δ = 9.31 (s, 8H, **1**$_4$), 8.93 (s, 4H, **1**$_1$), 7.77 (s, 8H, **1**$_{3+8}$), 7.62 (s, 12H, **1**$_{2+7}$), 7.48 (s, 8H, **1**$_5$), 7.19 (br, 10H, **1**$_6$+**5**$_a$), 6.32 (t, ^3J = 9.3 Hz, 8H, **5**$_b$), 3.10–3.06 (m, 24H, **1**$_{CH2}$), 2.77–2.57 (m, 72H, **1**$_{CH3}$). **^{13}C NMR** (125 MHz, D_2O, 298 K): δ = 154.80 (**5**$_c$, dd, $^1J_{CF}$ = 261.4 Hz, $^3J_{CF}$ = 4.0 Hz), 138.24 (**1**$_9$), 137.49 (**1**$_{10}$), 137.32 (**1**$_4$), 136.61 (**1**$_1$), 132.85 (**5**$_a$, t, $^3J_{CF}$ = 10.1 Hz), 129.27 (**5**$_d$, t, $^2J_{CF}$ = 8.7 Hz), 129.12 (**1**$_2$), 128.97 (**1**$_5$), 120.42 (**1**$_3$), 119.50 (**1**$_6$), 112.25 (**5**$_b$, dd, $^2J_{CF}$ = 19.1 Hz, $^4J_{CF}$ = 2.8 Hz), 111.20 (**1**$_8$), 110.92 (**1**$_7$), 62.53 (**1**$_{CH2}$), 50.22 (**1**$_{CH3}$), 50.05 (**1**$_{CH3}$). **^{1}H-DOSY NMR** (D_2O, 298 K): D = 0.19 (± 0.01) × 10^{-5} cm^2/s. **Elemental analysis**: calcd: C, 39.02; H, 4.26; N, 19.72; found: 39.01; H, 4.34; N, 19.73.

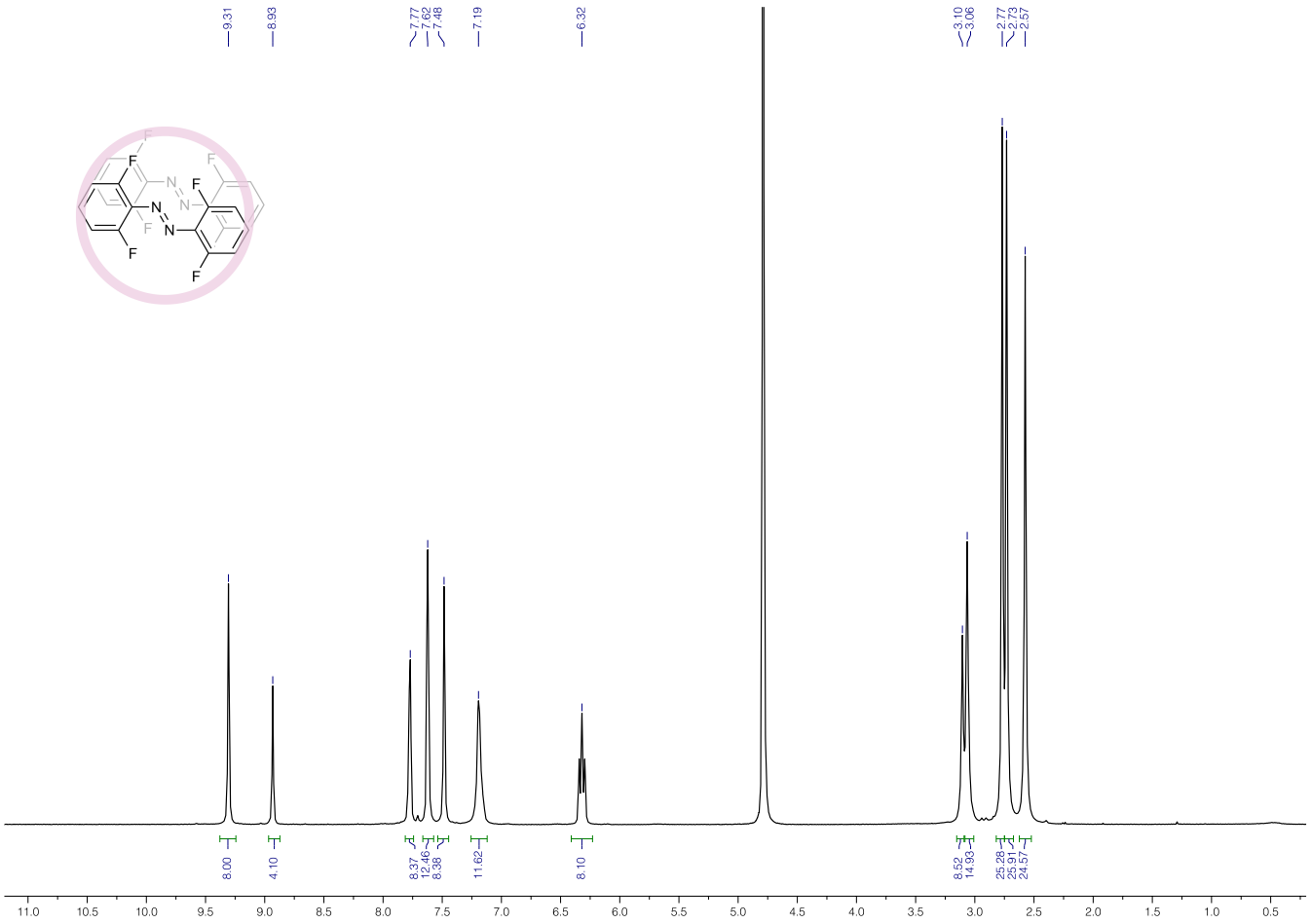

Fig. S50. ^{1}H NMR spectrum of **5**$_2$⊂**1** (500 MHz, D_2O, 298 K).

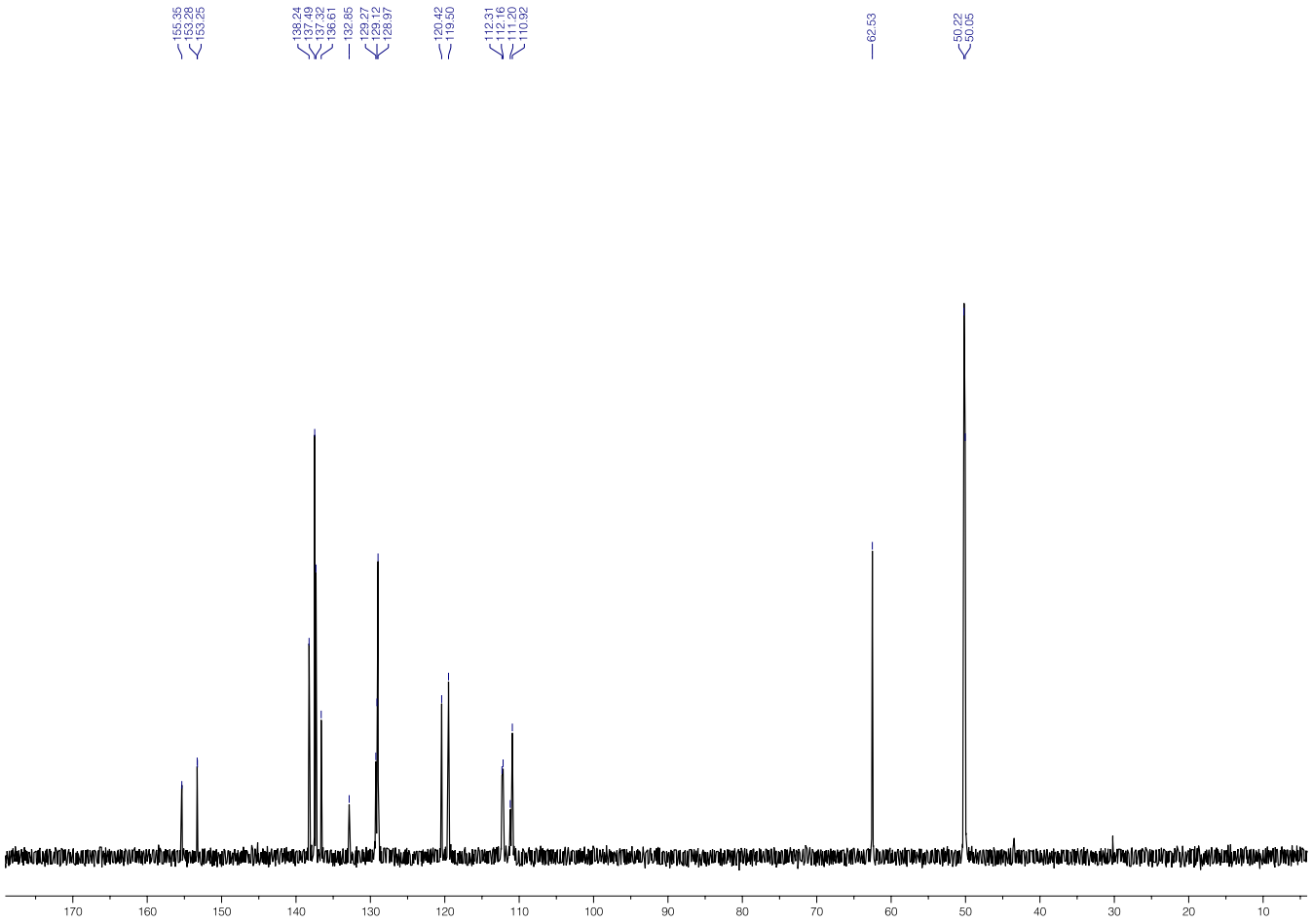

Fig. S51. ^{13}C NMR spectrum of $\mathbf{5}_2\subset\mathbf{1}$ (125 MHz, D_2O, 298 K).

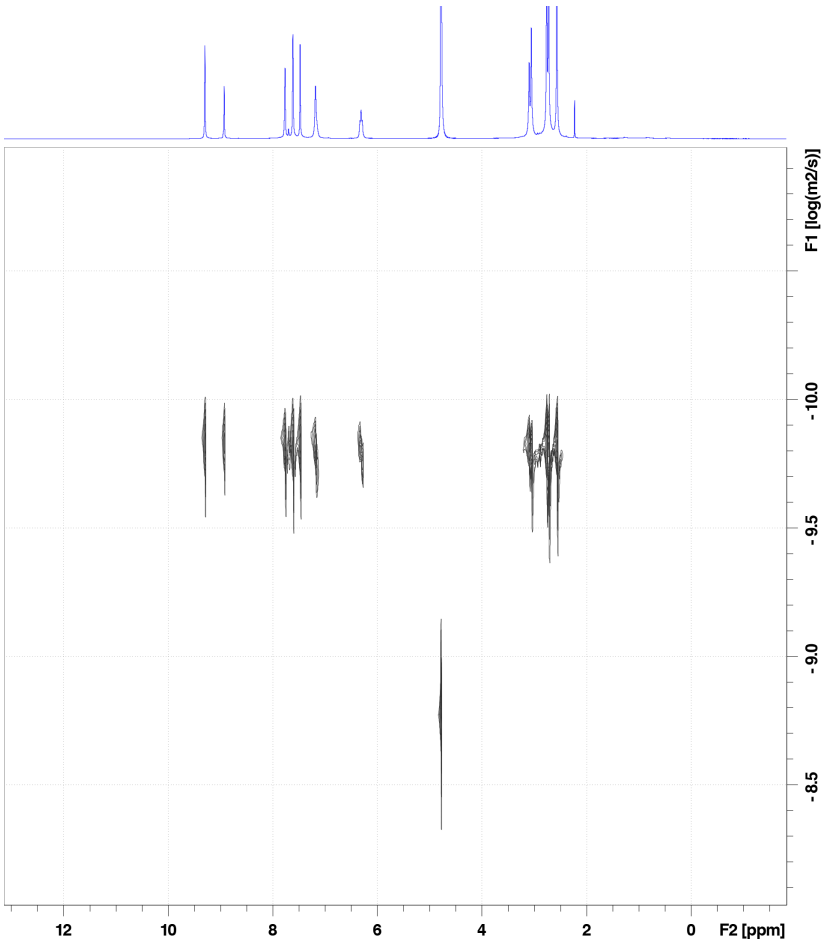

Fig. S52. ^{1}H DOSY NMR spectrum of $\mathbf{5}_2\subset\mathbf{1}$ (400 MHz, D_2O, 298 K).

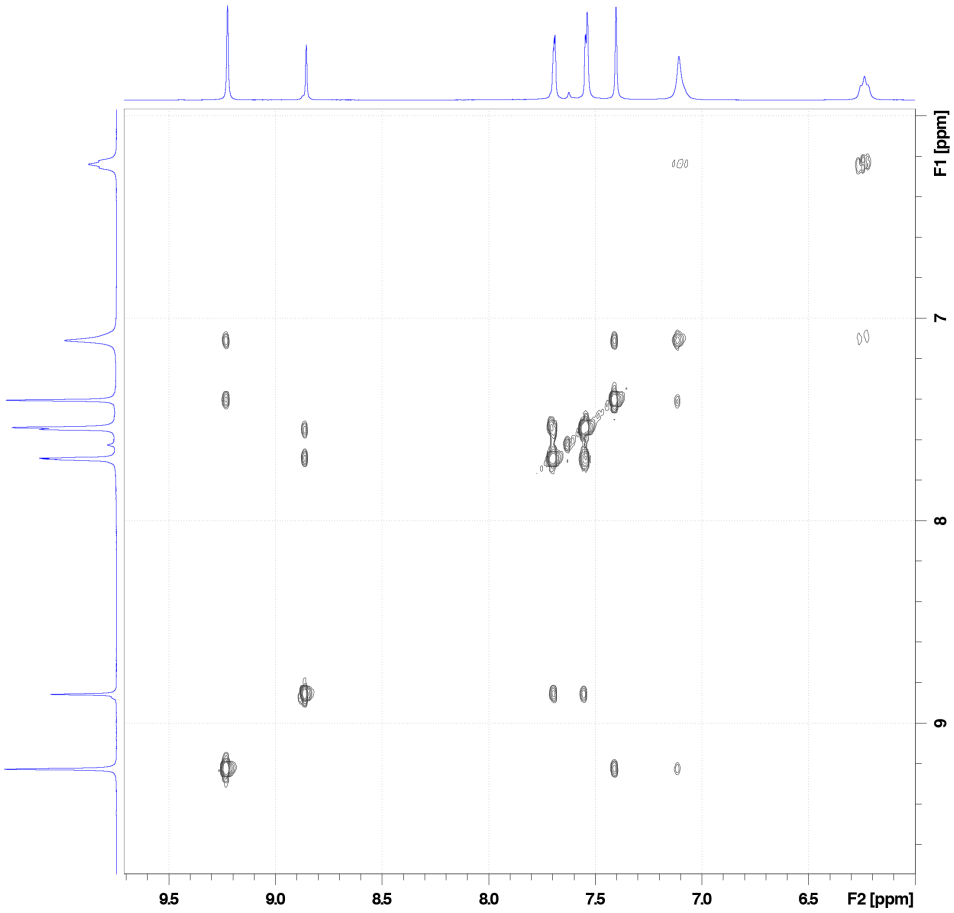

Fig. S53. ^{1}H-^{1}H COSY NMR spectrum of $\mathbf{5}_2\subset\mathbf{1}$ (500 MHz, D_2O, 298 K).

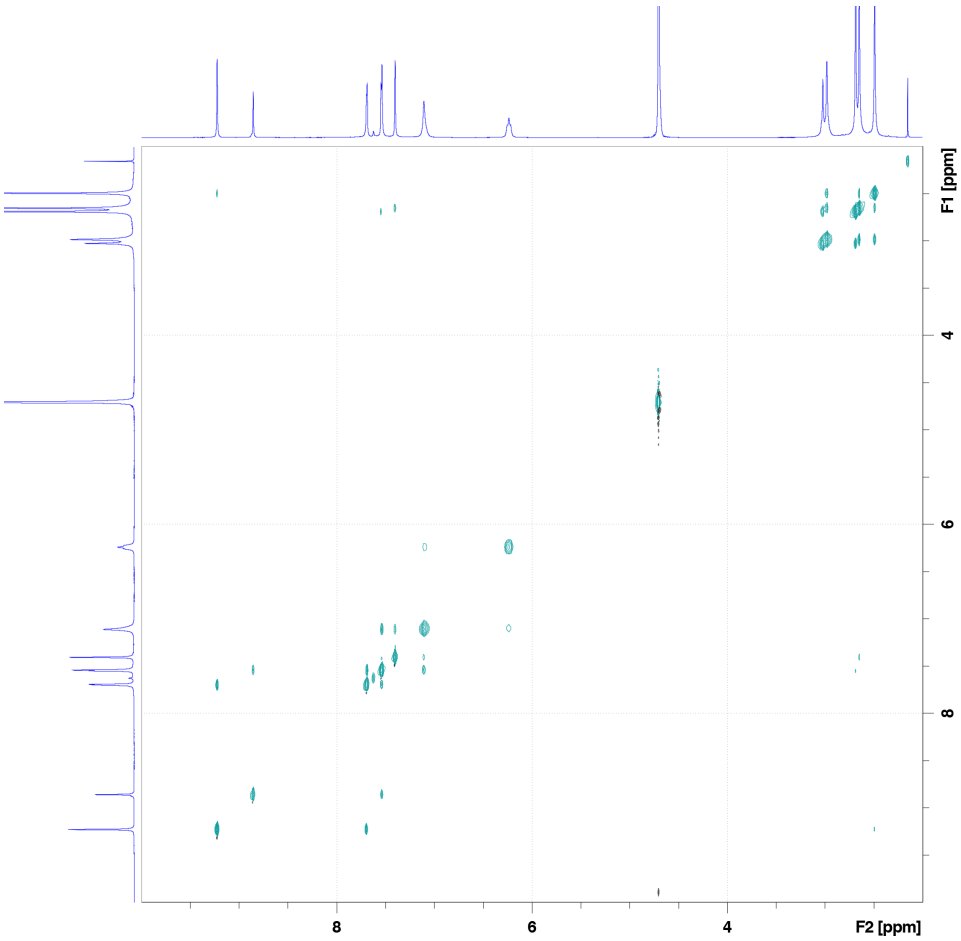

Fig. S54. ^{1}H-^{1}H NOESY NMR spectrum of $\mathbf{5}_2\subset\mathbf{1}$ (500 MHz, D_2O, 298 K).

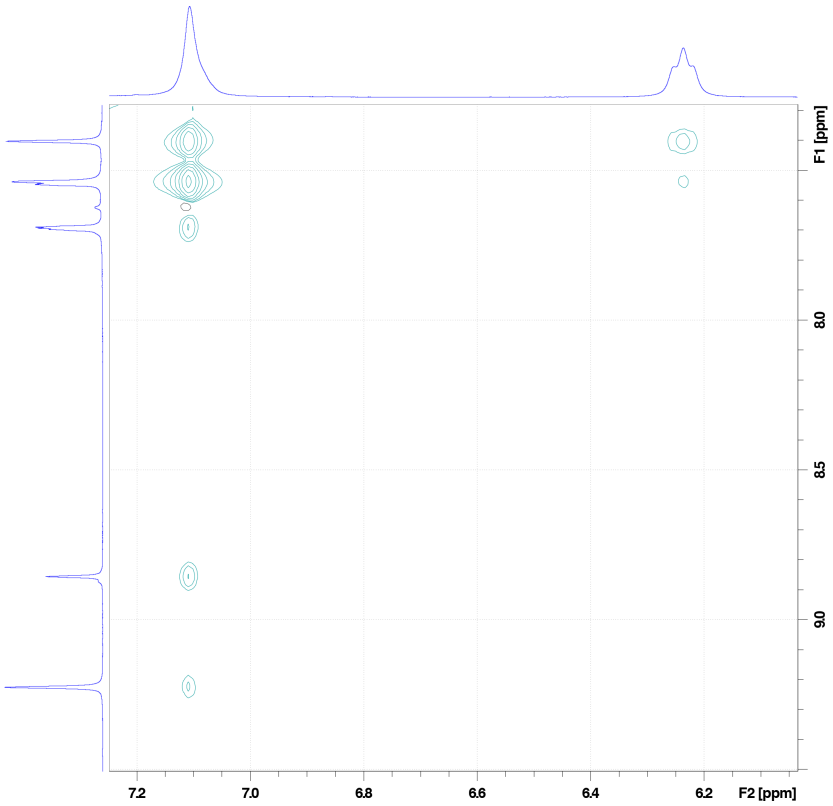

Fig. S55. Partial ^{1}H-^{1}H NOESY NMR spectrum of $\mathbf{5}_2\subset\mathbf{1}$ showing nOe correlations between the host and the guests (500 MHz, D_2O, 298 K) (the corresponding full-range spectrum is shown in Fig. S54).

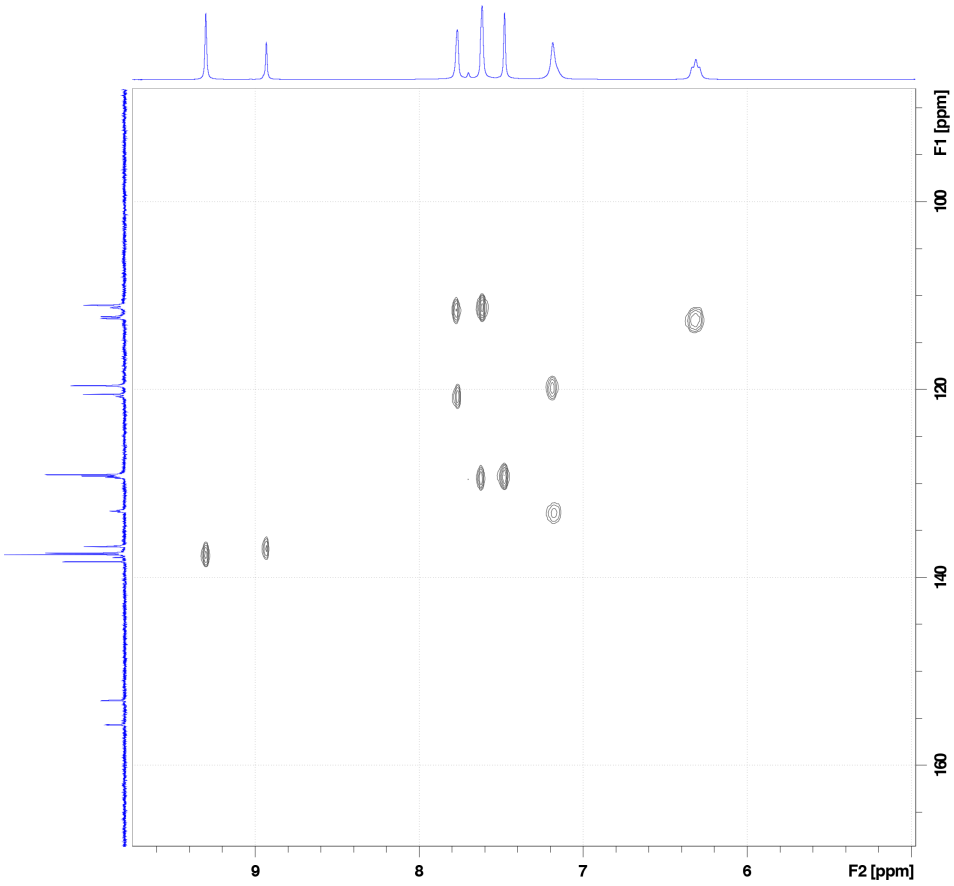

Fig. S56. ^{1}H-^{13}C HSQC NMR spectrum of $\mathbf{5}_2\subset\mathbf{1}$ (400 MHz, D_2O, 298 K).

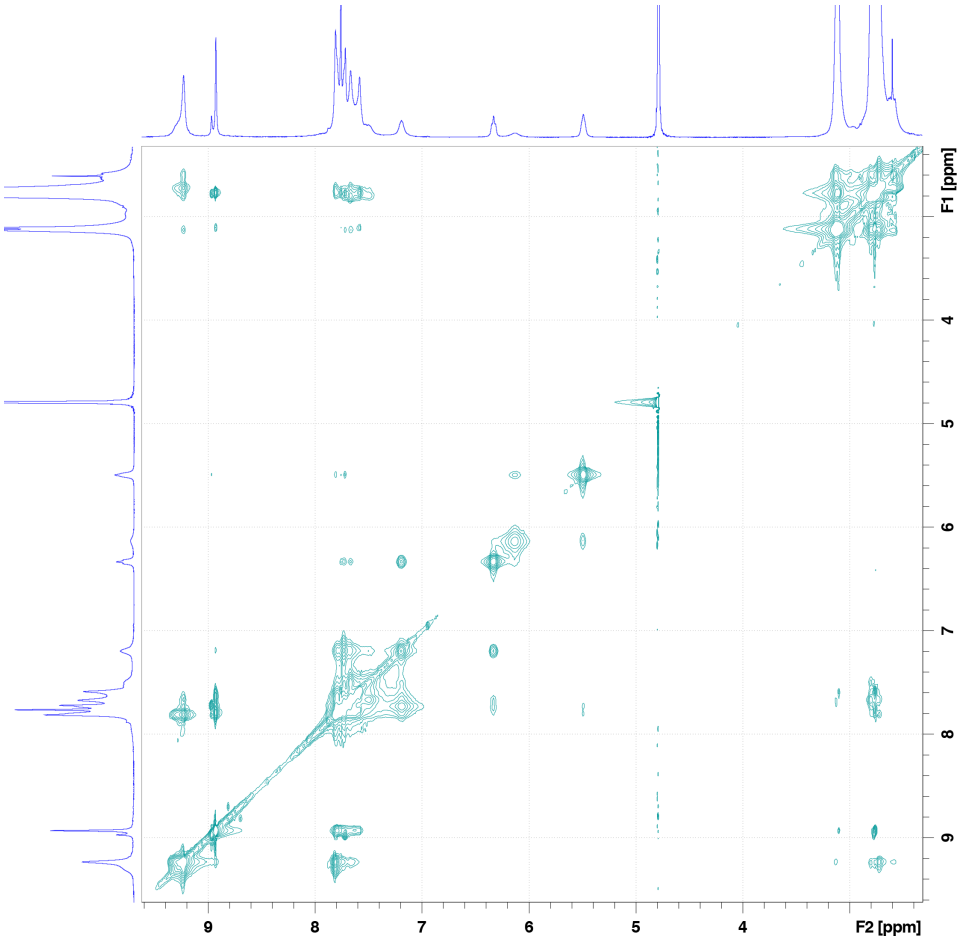

Fig. S57. ^{1}H-^{1}H NOESY NMR spectrum of $\mathbf{5}_2\subset\mathbf{1}$ subjected to partial isomerization and consisting of a ~1:1 mixture of *trans*-**5** and *cis*-**5** (500 MHz, D_2O, 298 K).

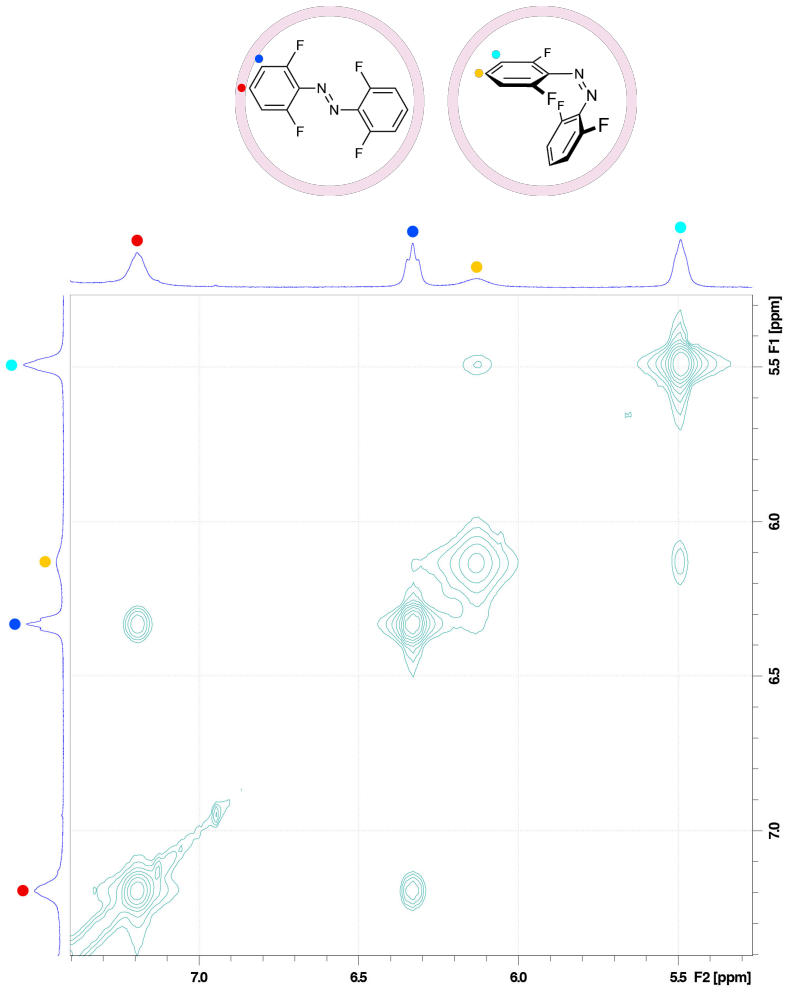

Fig. S58. Partial ^{1}H-^{1}H NOESY NMR spectrum of $\mathbf{5}_2\subset\mathbf{1}$ subjected to partial isomerization and consisting of a ~1:1 mixture of *trans*-**5** and *cis*-**5** (500 MHz, D_2O, 298 K) (the corresponding full-range spectrum is shown in Fig. S57). The signals at ~6.35 ppm and ~7.2 ppm correspond to *meta* and *para* protons of *trans*-**5**, respectively. The signals at ~5.5 ppm and ~6.15 ppm correspond to *meta* and *para* protons of *cis*-**5**, respectively. The absence of nOe correlations between *trans*-**5**'s and *cis*-**5**'s protons indicates that they do not stably coexist in the same cage molecule.

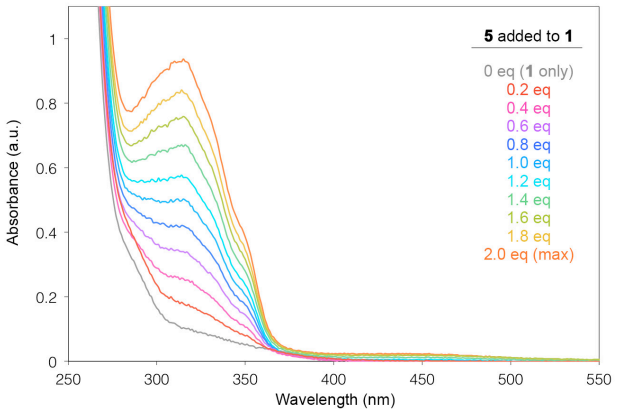

Fig. S59. Changes in the UV/Vis spectra of **1** in the presence of increasing amounts of **5**.

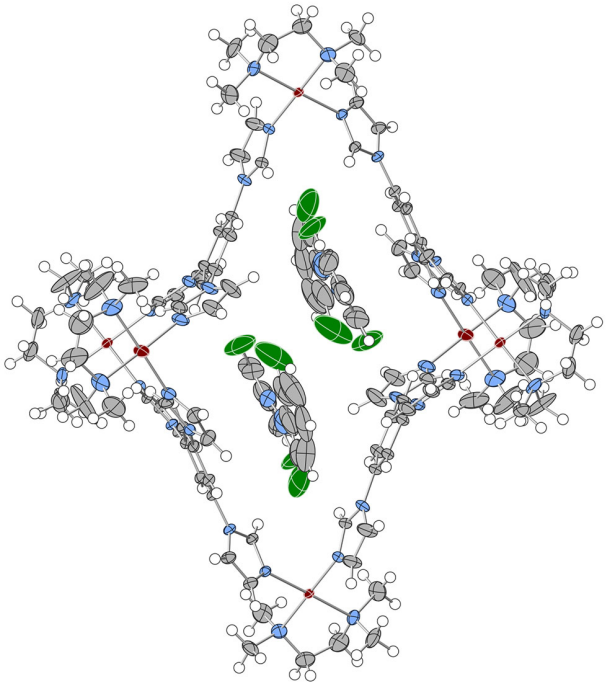

Fig. S60. ORTEP representation of the X-ray structure of the inclusion complex (*trans*-**5**)$_2$⊂**1** (thermal ellipsoids at a 50% probability level). Anions and solvent molecules were eliminated for clarity. Pd, brown; C gray; N, blue; F, green, H, white.

Dissolving crystalline (*trans*-**5**)$_2$⊂**1** in water was not followed by precipitation of *trans*-**5** (in contrast to (*trans*-**2**)$_2$⊂**1** and (*trans*-**3**)$_2$⊂**1**; see Figs. S16 and S32, respectively).

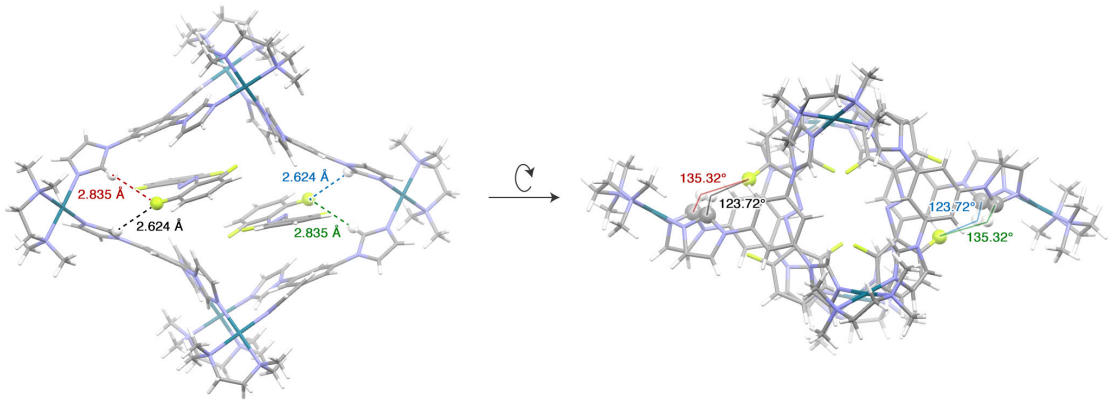

Fig. S61. H···F distances and C-H···F angles in the crystal structure of (*trans*-**5**)$_2$⊂**1**. The average H···F distance in (*trans*-**5**)$_2$⊂**1** is 2.73 Å, whereas the average C-H···F angle is 129.5°, which constitutes a moderately strong C-H···F hydrogen bond (5).

Analysis of intermolecular interactions within inclusion complex (*trans*-**3**)$_2$⊂**1**

Analysis was performed with PLATON on the cif file deposited in CCDC (accession number 1569281).

Host-guest interactions

Two benzene rings of cage **1** participate in π-π stacking interactions: Ring10 (C22-C27); Ring11 (C37-C42). Two benzene rings of encapsulated azobenzenes **3** participate in π-π stacking interactions: Ring12 (C49-C54); Ring13 (C55-C60).

The table below lists distances between the center of gravity of a given ring to the plane of the neighboring ring (in blue); distances between the center of gravity of the neighboring ring to the plane of the given ring (in red); and dihedral angles between the planes of the two rings (in green).

	Ring12	Ring13
Ring10	3.34 Å / 4.22 Å 50.1°	3.83 Å / 3.87 Å 35.5°
Ring11	3.33 Å / 3.60 Å 5.9°	3.25 Å / 3.63 Å 12.4°

In addition, the following edge-to-face interactions are present:

C60-F1 to the imidazole ring (N7N8C19C20C21), distance = 4.30 Å
C60-F1 to the imidazole ring (N13N14C46C47C48), distance = 4.82 Å

Guest-guest interactions

The distance between the center of gravity of azobenzene's Ring13 to the plane the symmetry-generated neighboring azobenzene's Ring12 is 3.74 Å. The distance between the center of gravity of azobenzene's Ring12 to the plane of the neighboring azobenzene's Ring13 is 2.63 Å. The dihedral angle between the planes of the benzene rings is 17.5° (symmetry relation 1-x,-y,-z).

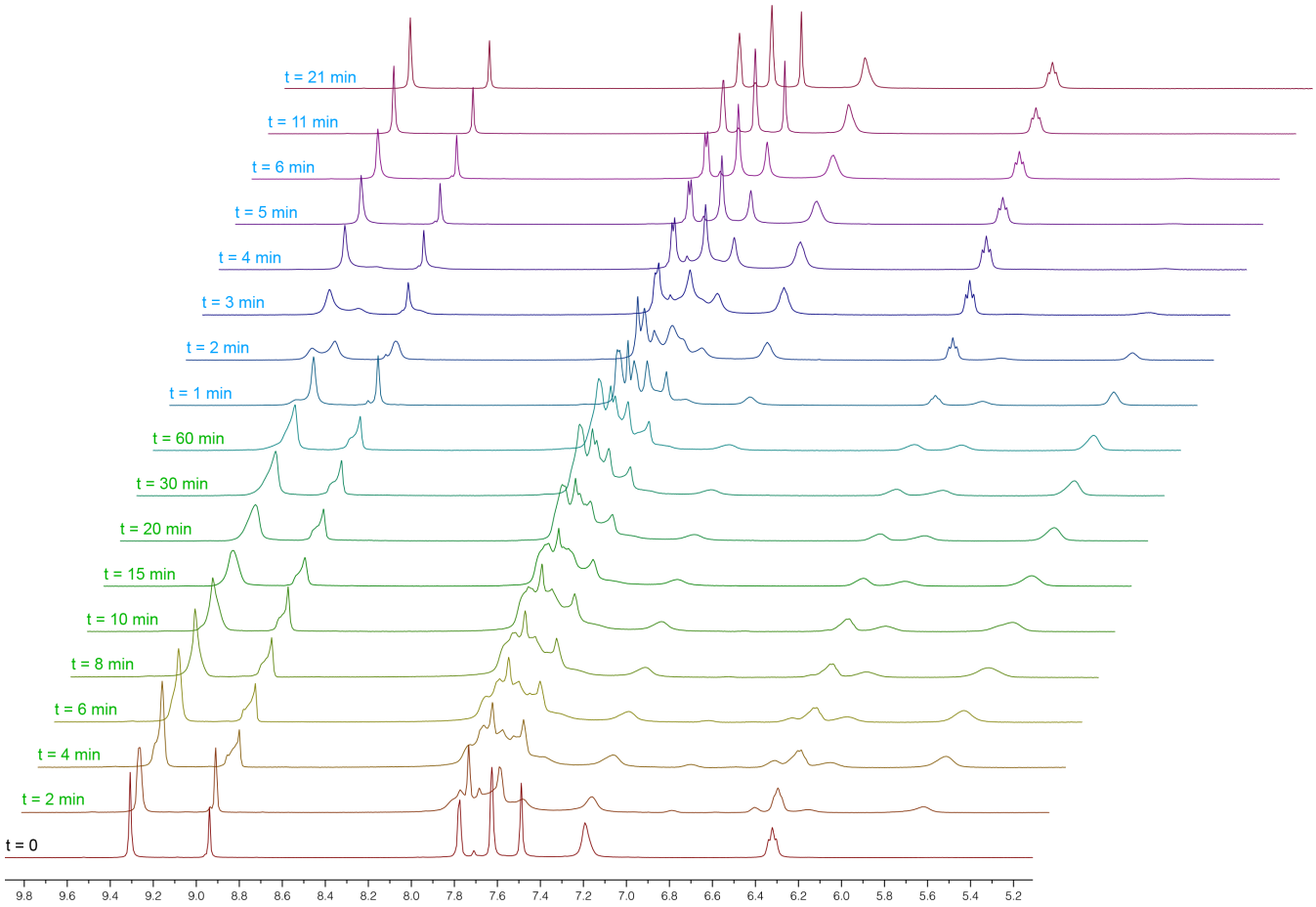

Fig. S62. A series of ^{1}H NMR spectra (500 MHz, D_2O, 298 K) of (*trans*-**5**)$_2$⊂**1** at a concentration of ~15 mg/mL, following exposure to green light (λ = 520 nm) inside the NMR spectrometer (using an optical fiber) for different periods (indicated in green font) for up to 60 min and after a subsequent exposure to blue light (blue font) for up to 21 min, during which a complete back-isomerization was achieved.

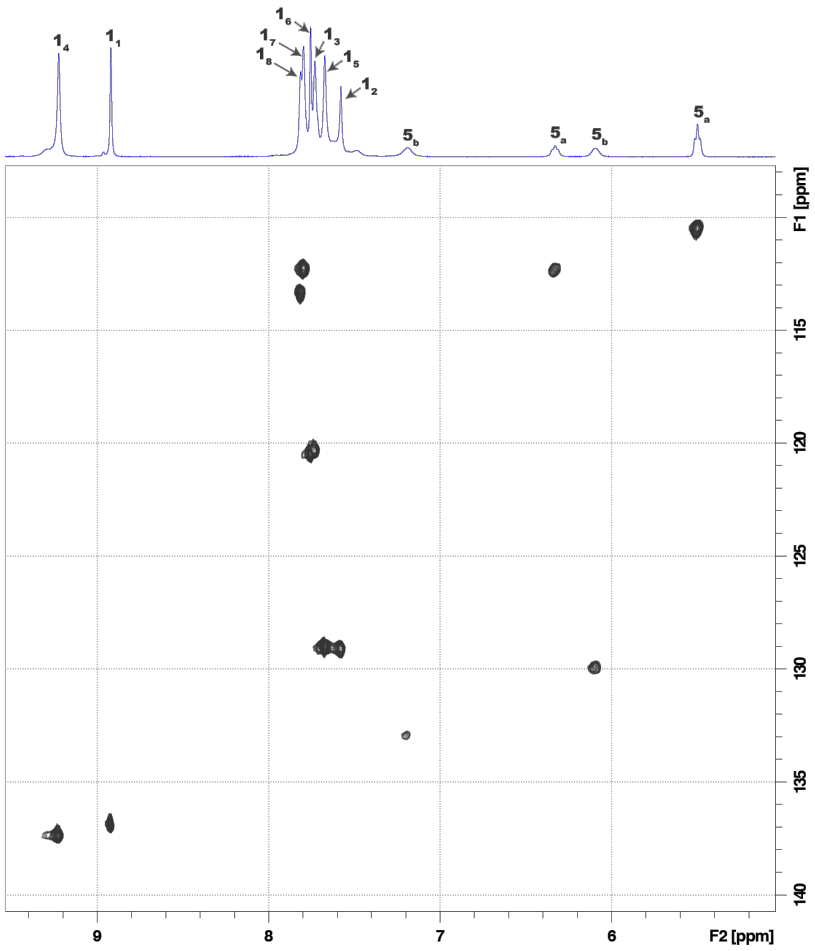

Fig. S63. ^{1}H-^{13}C HSQC NMR spectrum of $\mathbf{5}_2\subset\mathbf{1}$ following exposure to green light (λ = 520 nm) (500 MHz, D_2O, 298 K).

11. Analysis of guest-induced distortion of cage **1**

To determine the degree of structural deformation of cage **1** (6) induced by azobenzenes **2**, **3**, and **5**, we superimposed the X-ray structures of:

- **1** and $\mathbf{2}_2\subset\mathbf{1}$,
- **1** and $\mathbf{3}_2\subset\mathbf{1}$, and
- **1** and $\mathbf{5}_2\subset\mathbf{1}$ (Fig. S64, bottom panel).

In all cases, the cage undergoes pronounced structural changes upon binding azobenzenes. Root-mean-square displacements correspond to 1.230 for $\mathbf{2}_2\subset\mathbf{1}$ vs. **1**, 1.389 for $\mathbf{3}_2\subset\mathbf{1}$ vs. **1**, and 1.348 for $\mathbf{5}_2\subset\mathbf{1}$ vs. **1**. Maximal displacements were determined as 2.076 Å for $\mathbf{2}_2\subset\mathbf{1}$ vs. **1**, 2.002 Å for $\mathbf{3}_2\subset\mathbf{1}$ vs. **1**, and 2.408 Å for $\mathbf{5}_2\subset\mathbf{1}$ vs. **1**.

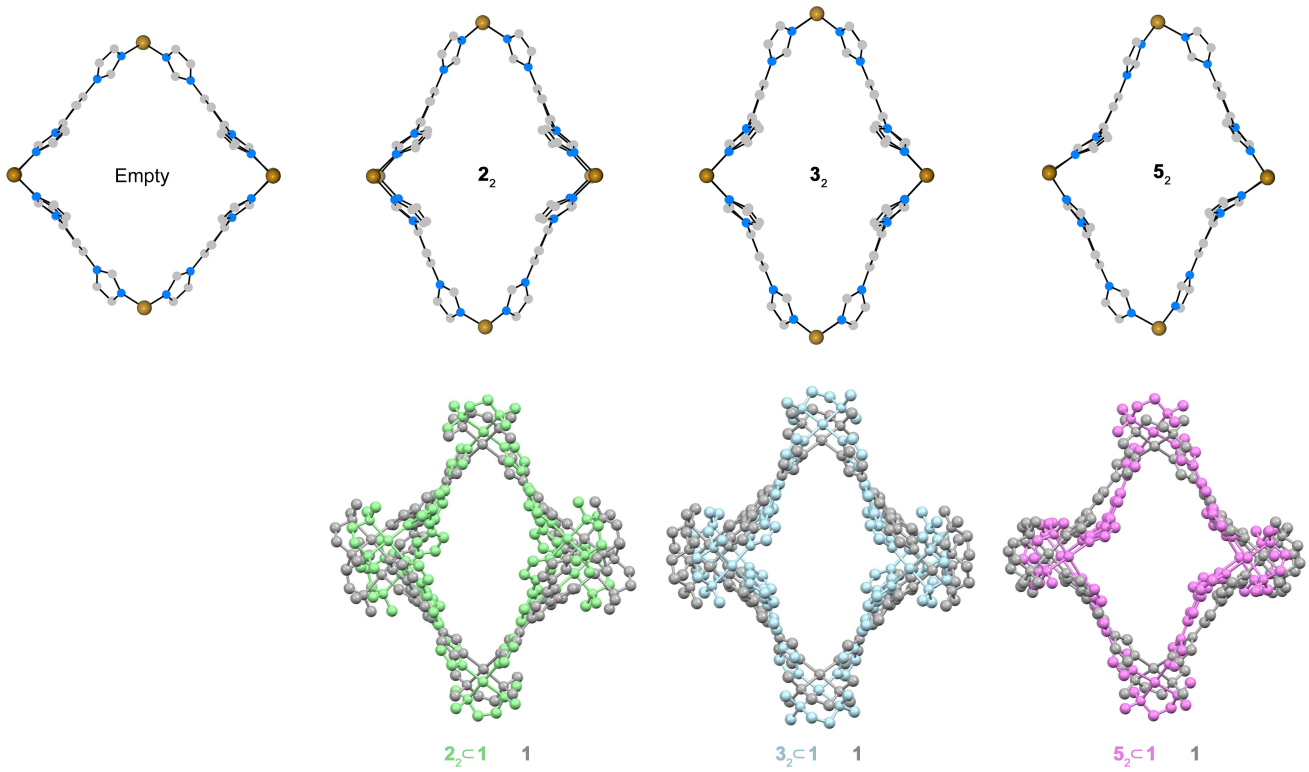

Fig. S64. Top panel: Comparison of the X-ray crystal structures of guest-free cage **1** with **1** encapsulating azobenzenes **2**, **3**, and **5** (hydrogen atoms and tmeda capping ligands were removed for clarity). Bottom panel: Superpositions of guest-free **1** with **1** encapsulating azobenzenes **2**, **3**, and **5** (hydrogen atoms removed for clarity).

12. Investigating light-induced expulsion of **5** from (*trans*-**5**)$_2$⊂**1**

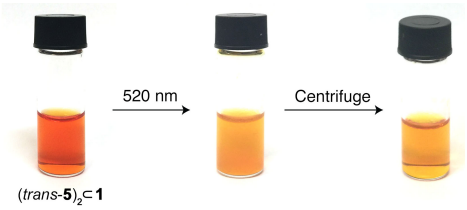

Fig. S65. Photographs of **5**$_2$⊂**1** in water (c ≈ 10 mM) before (left) and after (center) exposure to green light and after centrifuging and collecting the supernatant (right).

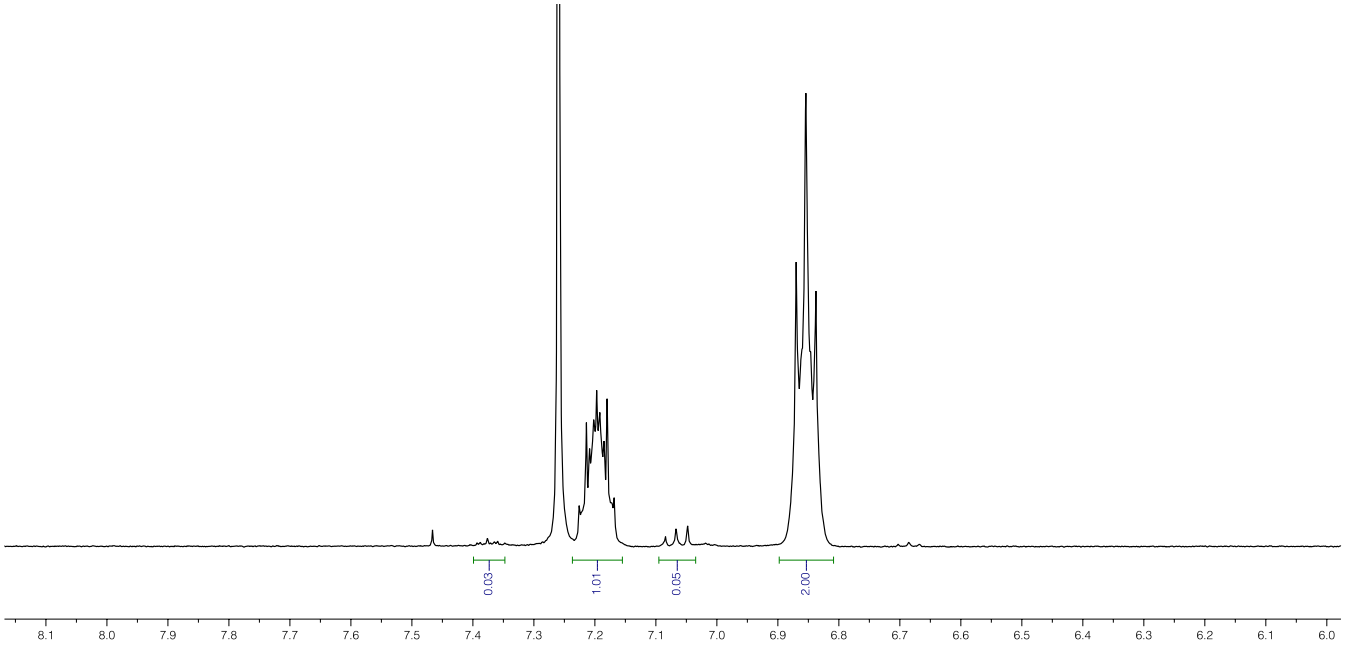

Fig. S66. ^{1}H NMR spectrum of the precipitate obtained by exposing (*trans*-**5**)$_2$⊂**1** to green light (500 MHz, $CDCl_3$, 298 K). The spectrum shows the presence of *cis*-**5** with less than 3% of the *trans* isomer.

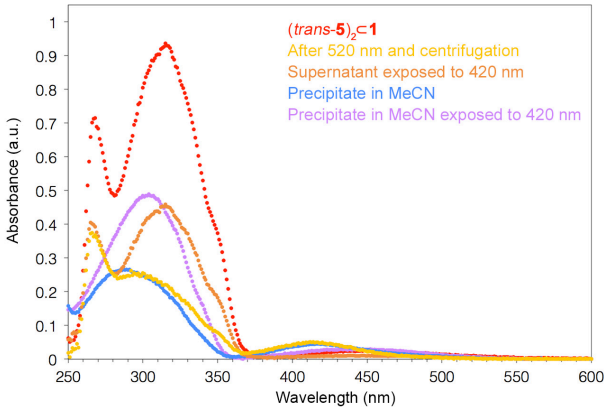

Fig. S67. Following expulsion of **1** from (*trans*-**5**)$_2$⊂**1** by UV/Vis spectroscopy.
Red: UV/Vis absorption spectra of (*trans*-**5**)$_2$⊂**1** in water;
Yellow: Solution obtained by exposing (*trans*-**5**)$_2$⊂**1** to 520 nm light followed by removing the precipitate by centrifugation; Orange: Supernatant shown in yellow exposed to 420 nm light;
Blue: MeCN solution of precipitate collected by centrifuging (*trans*-**5**)$_2$⊂**1** following its exposure to 520 nm light;
Purple: Solution shown in blue exposed to 420 nm light.

- The spectra shown in red, yellow, and orange are shown after subtracting spectra of pure **1** at the same concentration.
- The samples shown in red, orange, and purple contain predominantly *trans*-**5**; the samples shown in yellow and blue contain predominantly *cis*-**5**.

Absorbance at λ_{max} of the orange spectrum is roughly half that of the red spectrum, which indicates that ~50% of **5** is expelled from the cage using 520 nm light. This conclusion is further supported by i) similar values of absorbance at λ_{max} of the orange and the purple spectra, ii) similar values of absorbance at λ_{max} of the yellow and the blue spectra. The experiments were carried out on a c = 5 mM solution of **5**$_2$⊂**1**. Prior to recording UV/Vis spectra, the samples were diluted 100-fold.

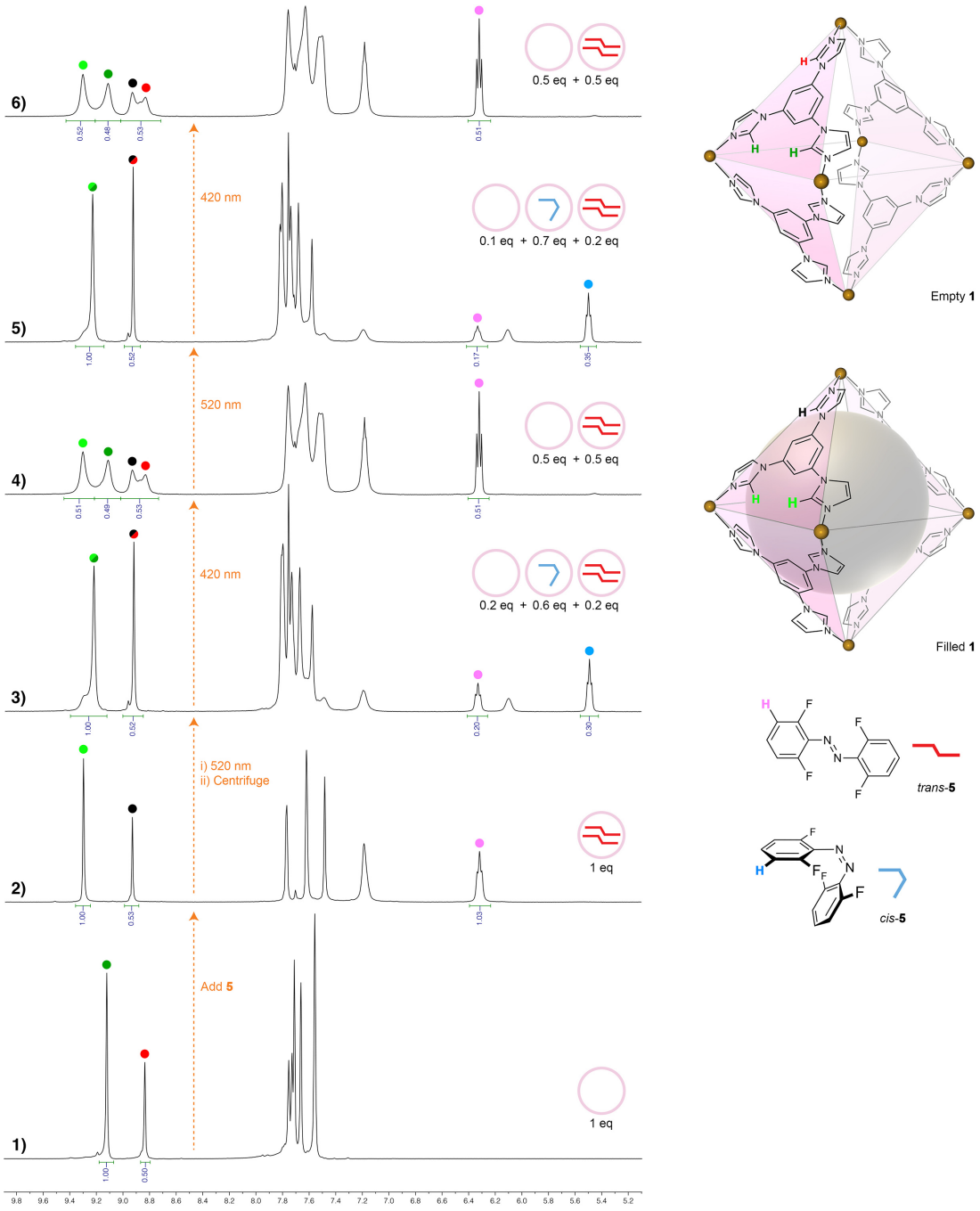

Fig. S68. From the bottom: **1)** ^{1}H NMR spectrum (500 MHz, D_2O, 298 K) of cage **1**. **2)** NMR spectrum of (*trans*-**5**)$_2$⊂**1**. The signal at ~7.2 ppm corresponds to the *para* protons of *trans*-**5** overlapping with one of the protons of **1**. **3)** NMR spectrum of (*trans*-**5**)$_2$⊂**1** exposed to green light, followed by removal of the precipitate. The signal at ~6.1 ppm corresponds to the *para* protons of *cis*-**5**. **4)** NMR spectrum of (*trans*-**5**)$_2$⊂**1** exposed to green light, followed by removal of the precipitate and subsequent exposure to blue light. Note that the signals due to azobenzene protons are identical to those in spectrum 2) except that the signal intensity decreased by half. Also note the presence of two sets of the imidazole signals with relative intensities 2:2:1:1. The positions of these signals match those of the empty cage (spectrum 1) and the completely filled cage (spectrum 2; compare with Fig. 3C in the main text). Overall, these results suggest the coexistence of two populations of cages: empty **1** and **1** encapsulating

dimer of *trans*-**5**. **5)** NMR spectrum of sample 4) exposed to green light. Note that this time, no precipitation was observed, in agreement with reaction equation, (*trans*-**5**)$_2$⊂**1** + **1** → 2 *cis*-**5**⊂**1**. The spectrum is very similar to that of 3). **6)** NMR spectrum of sample 5) exposed to blue light. The spectrum is very similar to that of 4).

To obtain additional insight into the binding of *cis*-**5** by **1**, we compared the NMR spectrum of a solution obtained by exposing (*trans*-**5**)$_2$⊂**1** to green light with the one recorded after a direct encapsulation of *cis*-**5** (Fig. S69). The *cis* isomer of **5** was obtained by the light-induced expulsion of *cis*-**5** from **5**$_2$⊂**1**. Interestingly, *cis*-**5** obtained this way contained a significantly smaller fraction of the *trans* isomer (<3%) compared to the sample obtained slowly evaporating the solvent (CH_2Cl_2) from the solution of **5** under intense green light irradiation (~10% *trans*). Inclusion complex (*cis*-**5**)⊂**1** was obtained by stirring excess of solid *cis*-**5** with an aqueous (D_2O) solution of cage **1** for 24 hr at room temperature in the dark. NMR spectra revealed that the resulting mixture (following removal of excess of solid *cis*-**5**) comprised ~64% of (*cis*-**5**)⊂**1**, ~30% of free **1**, and ~6% of (*trans*-**5**)$_2$⊂**1** (spectrum 2 in Fig. S69). The relatively large fraction of unoccupied cage can be attributed to the lower affinity of **1** to *cis*-**5** vs. *trans*-**5** dimer. The unexpectedly large fraction of *trans*-**5** in the final solution (~16% vs. <3% in the solid) can be due to *cis*→*trans* isomerization of **5** induced by the cage, which can again be explained by the relatively high affinity to **1** to *trans*-**5**.

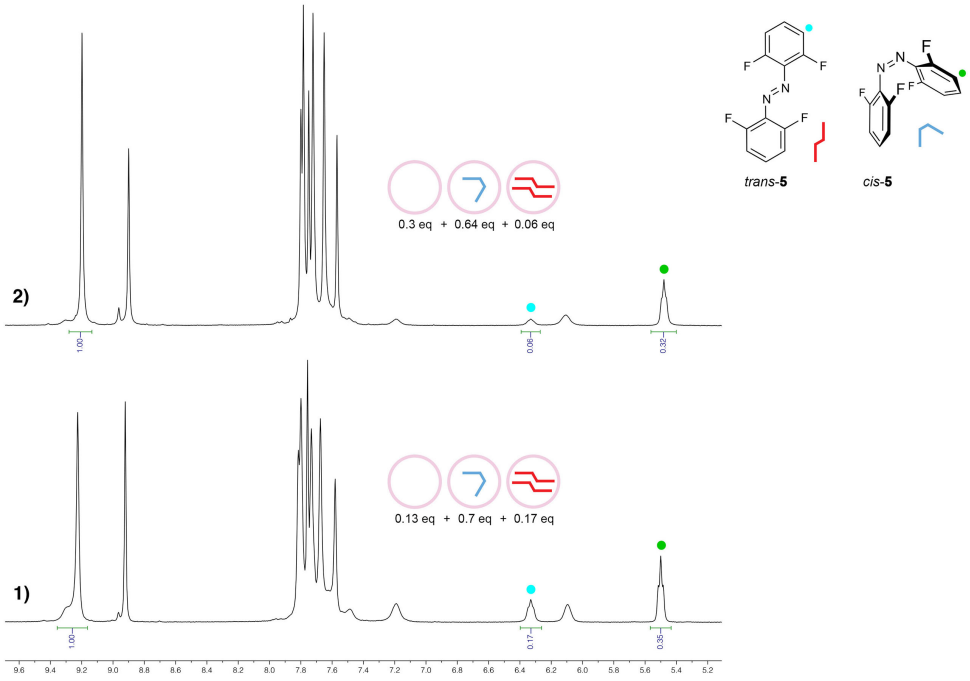

Fig. S69. From the bottom: **1)** ^{1}H NMR spectrum (500 MHz, D_2O, 298 K) of a solution obtained by exposing (*trans*-**5**)$_2$⊂**1** to green light (replotted from **3** in Fig. S68). **2)** ^{1}H NMR spectrum (500 MHz, D_2O, 298 K) of a solution prepared by encapsulating *cis*-**5**.

13. Fabrication of light-sensitive agarose gel

One gram of agarose (CAS # 9012-36-6, biotechnology grade, Amresco product # 0710) was added to an Erlenmeyer flask containing 50 mL of distilled water. The mixture was heated in a microwave oven until water started to boil and for an additional 3 min. Then, heating was discontinued and the flask was removed from the oven. The resulting colorless, homogeneous solution was poured while hot between two glass slides separated by a 1 mm spacer. After having been cooled to room temperature, a 5×4×0.1 cm piece of solidified agarose gel was placed in a Petri dish containing 2 mL of a 12 mM solution of (*trans*-**5**)$_2$⊂**1** in distilled water for 2 h. Finally, the gel was briefly rinsed with water.

14. Solid-state photoswitching of **2**$_2$⊂**1** and **5**$_2$⊂**1**

To investigate the possibility of photoswitching of encapsulated azobenzenes in the solid state, we prepared thin films of **2**$_2$⊂**1** and **5**$_2$⊂**1** on glass slides by evaporating water from the respective solutions. UV/Vis spectra were recorded and the samples were exposed to UV (365 nm; **2**$_2$⊂**1**) or green (520 nm; **5**$_2$⊂**1**) light until no further changes in the spectra could be seen. Next, the samples were exposed to blue light (420 nm) and the sequence was repeated for several cycles.

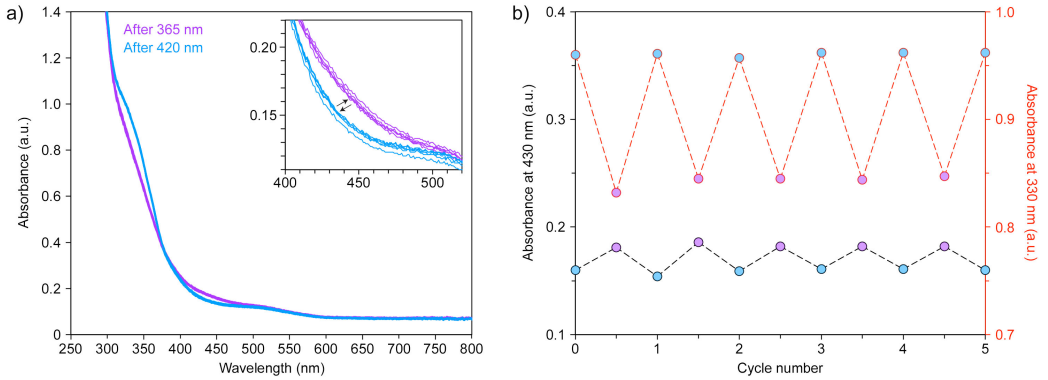

Fig. S70. Effect of irradiating **2**$_2$⊂**1** in the solid state. *Left*: Switching the optical response by alternating exposure to UV (10 min) and blue light (10 min). *Right*: Changes in the absorbance at 330 nm and 430 nm induced by alternating exposure to UV and blue light.

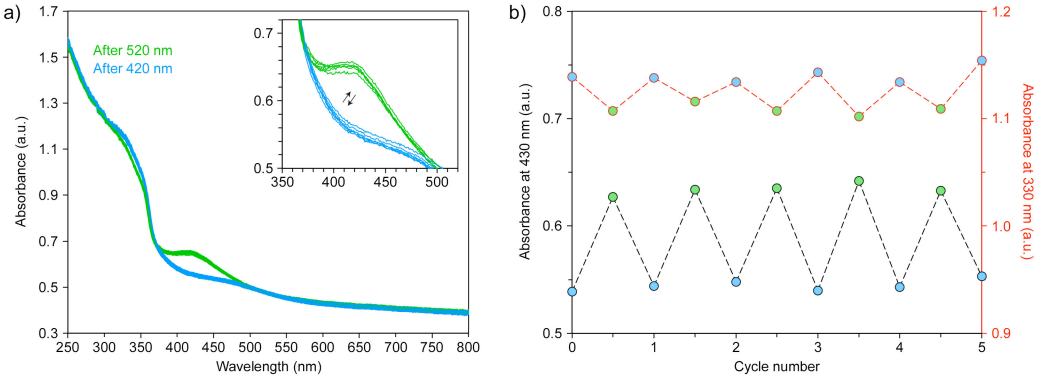

Fig. S71. Effect of irradiating **5**$_2$⊂**1** in the solid state. *Left*: Switching the optical response by alternating exposure to green light (4 min) and blue light (6 min).

15. Infrared (IR) analysis of the inclusion complexes

In addition to X-ray crystallography, NMR, and elemental analysis, we attempted to characterize the inclusion complexes by IR absorption spectroscopy. However, the IR absorption of **1** and the inclusion complexes were overwhelmed by the response due to the cage and the differences between the spectra were small.

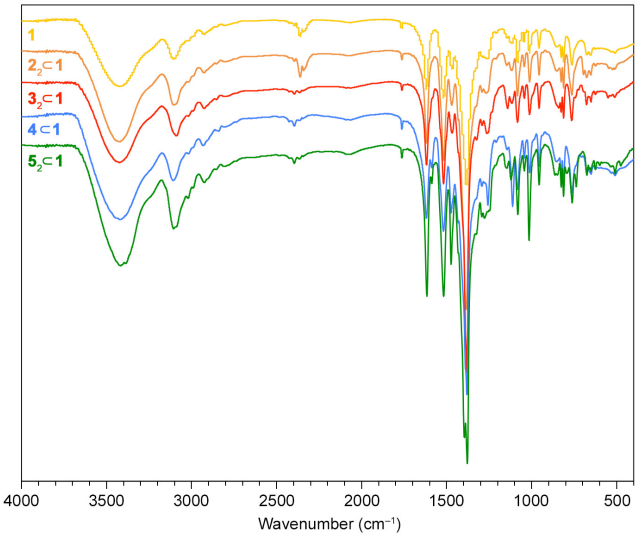

Fig. S72. IR absorption spectra of cage **1** and inclusion complexes $\mathbf{2}_2\subset\mathbf{1}$, $\mathbf{3}_2\subset\mathbf{1}$, $\mathbf{4}\subset\mathbf{1}$, and $\mathbf{5}_2\subset\mathbf{1}$.

- **1** (KBr, ν, cm^{-1}): 3421 (O–H), 3103 (C–H), 2927 (C–H), 1618 (C=N), 1518 (C=C), 1383, 1082, 1011, 956, 825, 811, 762.
- (*trans*-**2**)$_2\subset$**1** (KBr, ν, cm^{-1}): 3431 (O–H), 3105 (C–H), 2927 (C–H), 1618 (C=N), 1519 (C=C), 1385, 1083, 1011, 956, 826, 812, 763.
- (*trans*-**3**)$_2\subset$**1** (KBr, ν, cm^{-1}): 3424 (O–H), 3088 (C–H), 2925 (C–H), 1618 (C=N), 1581 (N=N), 1518 (C=C), 1468 (C=C), 1380, 1259 (C–N), 1141, 1116, 1081, 1043, 1012, 956, 826, 812, 764.
- *cis*-**4**$\subset$**1** (KBr, ν, cm^{-1}): 3420 (O–H), 3107 (C–H), 2931 (C–H), 1618 (C=N), 1587 (N=N), 1518 (C=C), 1473 (C=C), 1380, 1257 (C–N), 1111, 1082, 1011, 956, 826, 761.
- (*trans*-**5**)$_2\subset$**1** (KBr, ν, cm^{-1}): 3416 (O–H), 3105 (C–H), 2925 (C–H), 1616 (C=N), 1587 (N=N), 1517 (C=C), 1473 (C=C), 1378, 1277 (C–N), 1121, 1081, 1015, 956, 826, 812, 761, 737.

16. Impact of encapsulation on the photoisomerization of azobenzenes

We were interested in how encapsulating azobenzenes affects the composition of the photostationary states. Figures S72-S75 show the effect of photoirradiation of non-encapsulated azobenzenes **2**-**5** in organic solvents. Comparison with **2**-**5** in the presence of cage **1** is discussed in the figure captions. It should be emphasized, however, that the comparison is not trivial because the encapsulation entails the change of the environment from an organic solvent to water.

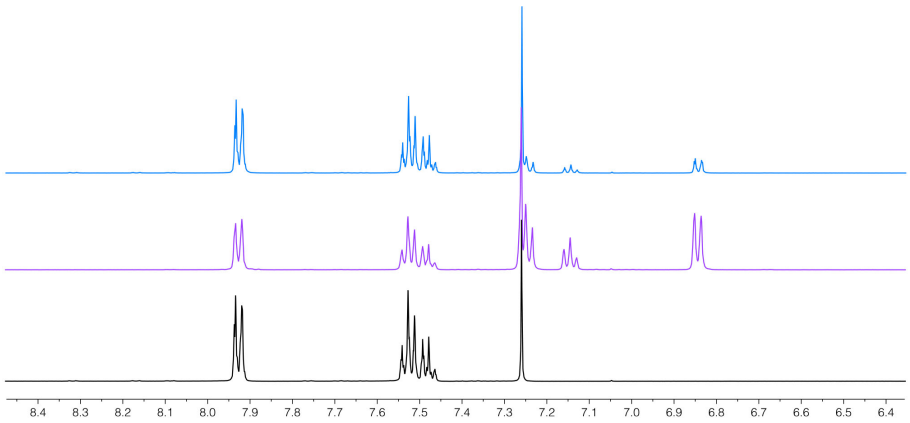

Fig. S73. Partial ^{1}H NMR spectra of **2** in $CDCl_3$ (500 MHz, 298 K): initial (black, 100% *trans*), after 2 hr of exposure to a 365 nm light (purple, 47% *trans*), and after the subsequent exposure (10 min) to a 420 nm light (blue, 83% *trans*). The poor photostationary state induced by UV light is due to the relatively poor overlap between **2**'s absorption and the UV source's emission. Changing the solvent to CD_3CN, CD_3OD, or DMSO-d_6 afforded even lower amounts of *cis*-**2**.

The presence of **1** had a profound beneficial effect of the *trans*→*cis* conversion efficiency: $\mathbf{2}_2\subset\mathbf{1}$ in the presence of 0.4 eq of free **1** (the lowest amount rendering $\mathbf{2}_2\subset\mathbf{1}$ stable in water) exposed to UV afforded ~60% of *cis*-**2**. The amount of cis-2 was increased to ~72% upon adding an additional 1 eq of **1** (overall 1.4 eq of free **1**) and to ~85% upon adding additional 3 eq of **1** (overall 3.4 eq of free **1**). Subsequent exposure of $\mathbf{2}_2\subset\mathbf{1}$ (without extra **1**) to blue light resulted in 11% of the residual *cis*-**2**.

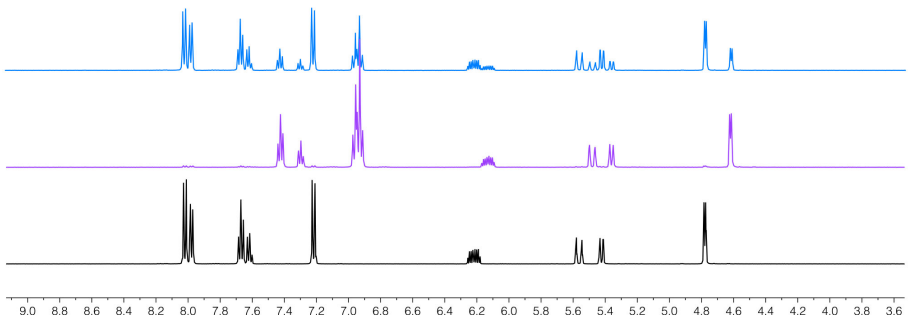

Fig. S74. Partial ^{1}H NMR spectra of **3** in CD_3CN (500 MHz, 298 K): initial (black, 100% *trans*), after 40 min of exposure to a 365 nm light (purple, 4% *trans*), and after the subsequent exposure (25 min) to a 420 nm light (blue, 69% *trans*).

Similarly, $\mathbf{3}_2\subset\mathbf{1}$ in the presence of ~2 eq of free **1** (the lowest amount rendering $\mathbf{3}_2\subset\mathbf{1}$ stable in water) isomerized efficiently when exposed to UV light—in fact, no residual *trans* isomer could be detected (Fig. S34).

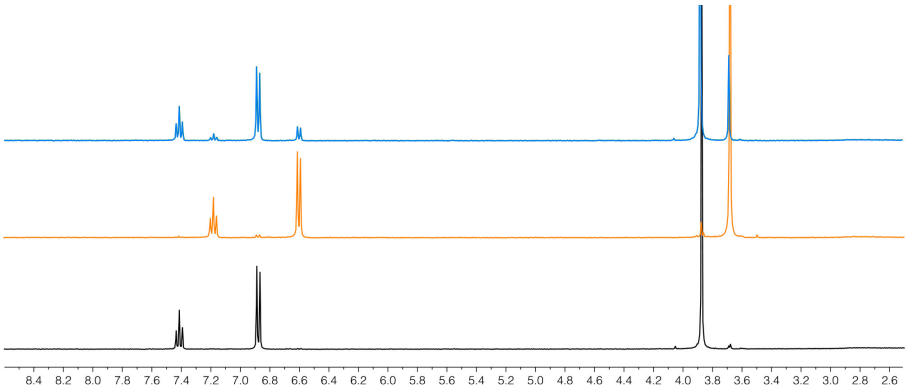

Fig. S75. Partial ^{1}H NMR spectra of **4** in CD_3CN (500 MHz, 298 K): initial (black, 100% *trans*), after 20 min of exposure to a 580 nm light (orange, 4% *trans*), and after the subsequent exposure (20 min) to a 420 nm light (blue, 85% *trans*).

When the photoisomerization was carried out in the presence of **1** in water, the equilibrium was further shifted towards the more stable isomer, with ~93% *trans* under blue light and no detectable *trans* under yellow light (Fig. S43 and S47, respectively).

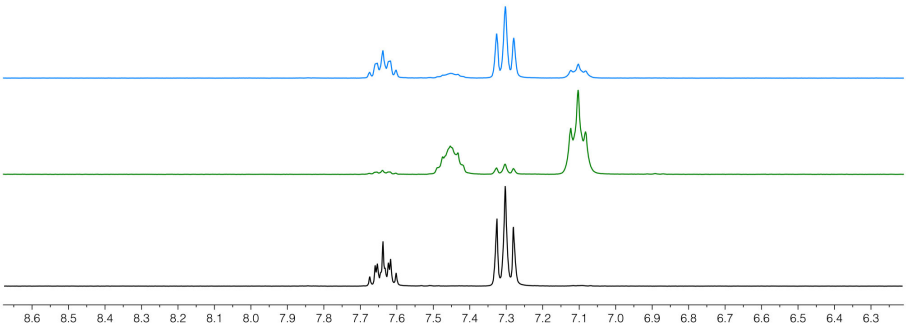

Fig. S76. Partial ^{1}H NMR spectra of **5** in CD_3CN (500 MHz, 298 K): initial (black, 100% *trans*), after 10 min of exposure to a 520 nm light (green, 9% *trans*), and after the subsequent exposure (20 min) to a 420 nm light (blue, 79% *trans*).

Exposing an aqueous solution of $\mathbf{5}_2\subset\mathbf{1}$ to green light decreased the amount of *trans*-**5** to only ~19% (Fig. S68 and Fig. 3 in the main text), with most of *cis*-**5** precipitating out. Subsequent exposure to blue light regenerated the solution of (*trans*-**5**)$_2\subset$**1** with less than 1% of the *cis* isomer. Interestingly, in the presence of one extra equivalent of **1**, the amount of the residual *trans*-**5** under green light irradiation amount to as much as ~33% (spectrum 5 in Fig. S68). This result can be attributed to the relatively high affinity of **1** towards *trans*- vs. *cis*-**5** (see also the discussion preceding Fig. S69). Subsequent exposure to blue light afforded (*trans*-**5**)$_2\subset$**1** with <1% of *cis*-**5** (spectrum 6 in Fig. S68).

17. X-ray data collection and structure refinement

Single crystals of inclusion complexes (*trans*-**2**)$_2\subset$**1**, (*trans*-**3**)$_2\subset$**1**, and (*trans*-**5**)$_2\subset$**1** were obtained by slow evaporation of water from the respective aqueous solutions. Single crystals of *cis*-**5** were obtained by slow evaporation of water from the aqueous solution of *cis*-**5**$\subset$**1**. The diffraction data of (*trans*-**2**)$_2\subset$**1**, (*trans*-**3**)$_2\subset$**1**, and *cis*-**5** were collected on a Rigaku XtaLAB^{PRO} diffractometer using Cu-Kα radiation (1.54184 Å) and processed with CrysAlis^{PRO}. The diffraction data of (*trans*-**5**)$_2\subset$**1** were collected on a Bruker APEX-II Kappa

CCD diffractometer using Mo-Kα radiation (0.7107 Å) and processed with SAINT. Data collection was performed under a stream of nitrogen at 100 K. The structures were solved by direct methods using SHELXT (7). All non-hydrogen atoms were further refined by SHELXL with anisotropic displacement coefficients (8). Hydrogen atoms were assigned isotropic displacement coefficients, U(H) = 1.2U(C) or 1.5U (C-methyl), and their coordinates were allowed to ride on their respective carbons. Crystallographic data and refinement parameters are summarized in Table S1.

Species	(*trans*-**2**)$_2$⊂**1**	(*trans*-**3**)$_2$⊂**1**	(*trans*-**5**)$_2$⊂**1**	*cis*-**5**
CCDC No.	1551435	1569281	1551438	1569282
Formula*	$C_{480}H_{656}N_{198}O_{187}Pd_{24}$	$C_{126}H_{172}N_{52}O_{96}Pd_6$	$C_{120}H_{156}F_8N_{49}O_{27}Pd_6$	$C_{12}H_6F_4N_2$
Formula weight*	14745.59	4587.96	3507.33	254.19
Crystal system	Monoclinic	Triclinic	Triclinic	Orthorhombic
Space group	$P2_1/c$	$P\bar{1}$	$P\bar{1}$	$Pna2_1$
Crystal size (mm)	0.376×0.083×0.077	0.128×0.066×0.060	0.250×0.140×0.100	0.100×0.100×0.100
Crystal color and shape	Orange needle	Orange prism	Orange prism	Orange block
Temperature (K)	100	100	100	100
Wavelength (Å)	1.54178	1.54178	0.71073	1.54178
a (Å)	18.28560(10)	18.0192(1)	15.3303(5)	13.8743(2)
b (Å)	34.5838(2)	18.8066(1)	16.1494(5)	11.5126(2)
c (Å)	30.6461(2)	20.4806(1)	20.0076(7)	6.5526(1)
α (°)	90	116.3318(5)	69.631(2)	90
β (°)	100.7740(10)	96.4839(4)	81.977(2)	90
γ (°)	90	111.9048(4)	83.372(2)	90
Volume (Å^3)	19038.5(2)	5438.18(5)	4586.3(3)	1046.64(3)
Z	1	1	1	4
ρ_{calcd},(g cm^{-1})	1.286	1.401	1.270	1.613
μ (mm^{-1})	5.145	4.796	0.652	1.307
No. of reflections (unique)	120635 (34814)	276289(22146)	136893 (23880)	7899(2114)
R_{int}	0.0548	0.0517	0.0537	0.0416
Completeness to θ (%)	99.9	99.5	99.9	99.2
Data / restraints / parameters	34814 / 136 / 2089	22146 / 194 / 1148	23880 / 79 / 901	2114 / 1 / 163
Goodness-of-fit on F^2	1.047	1.016	1.246	1.126
Final R_1 and wR_2 indices [$I > 2\sigma(I)$]	0.0932, 0.2557	0.0772, 0.2129	0.0545, 0.1552	0.0482, 0.1354
R_1 and wR_2 indices (all data)	0.0994, 0.2608	0.0783, 0.2139	0.0703, 0.1626	0.0496, 0.1368

Table S1. Crystallographic data.
*Formula and weight derived from the crystal structure.

18. Supplementary references

1. Samanta D, Mukherjee S, Patil YP, & Mukherjee PS (2012) Self-assembled Pd_6 open cage with triimidazole walls and the use of its confined nanospace for catalytic Knoevenagel- and Diels-Alder reactions in aqueous medium. *Chemistry* 18:12322–12329.
2. Ledin PA*, et al.* (2014) Star-shaped molecules with polyhedral oligomeric silsesquioxane core and azobenzene dye arms. *Langmuir* 30:8856–8865.
3. Hansen MJ, Lerch MM, Szymanski W, & Feringa B (2016) Direct and versatile synthesis of red-shifted azobenzenes. *Angew Chem Int Ed* 55:13514–13518.
4. Bléger D, Schwarz J, Brouwer AM, & Hecht S (2012) *o*-Fluoroazobenzenes as readily synthesized photoswitches offering nearly quantitative two-way isomerization with visible light. *J Am Chem Soc* 134:20597–20600.
5. Thalladi VR*, et al.* (1998) C-H···F interactions in the crystal structures of some fluorobenzenes. *J Am Chem Soc* 120:8702–8710.
6. Samanta D*, et al.* (2018) Reversible chromism of spiropyran in the cavity of a flexible coordination cage. *Nat Commun* 9:641.
7. Sheldrick GM (2015) SHELXT - Integrated space-group and crystal-structure determination. *Acta Crystallogr A* 71:3–8.
8. Sheldrick GM (2008) A short history of SHELX. *Acta Crystallogr A* 64:112–122.